Regulation of Nicotinic Acetylcholine Receptor Stability at the Mouse Neuromuscular Junction

by

Marcelo Pires de Oliveira

A dissertation submitted in partial fulfillment
of the requirements for the degree of
Doctor of Philosophy
(Molecular, Cellular and Developmental Biology)
in The University of Michigan
2014

Doctoral Committee:

Professor Mohammed Akaaboune, Chair
Professor Richard I. Hume
Assistant Professor Orie T. Shafer
Professor Edward L. Stuenkel

“Quoniam angelis suis mandabit de te, ut custodiant te in omnibus viis tuis.”
Ps 90:11

© Marcelo Pires de Oliveira

2014

Acknowledgements

I would like to thank my family, specially my parents, Osmar and Matilde, and my brother Márcio, for their unfailing support and love.

With thanks to Dr. Mohammed Akaaboune for his orientation, mentoring and guidance, for patience and example and for managing a great learning environment.

To all past and present members of the Akaaboune lab lab: in particular, Dr. Chakib Mouslim and Derek Moen, who are co-authors of chapters in this thesis, and Dr. Mohamed Aittaleb, for his persistent help, support and character. Most specially, I would like to thank Dr. Isabel Martinez-Pena y Valenzuela, co-author of chapter II and first author on chapter III, without whom none of this work would have been possible, and who in addition to crucial intellectual and technical support, is the heart of the our lab.

To all my friends, whose support was invaluable for this thesis, especially my friends in MCDB, partaker of these joys and difficulties. In particular, I thank Katherine Lelito, Dr. Sukanya Punthambaker, Mohammad Samie and Qi Zhang for their friendship, which I will treasure forever.

To the members of my thesis committee, Dr. Richard Hume, Dr. Orie Shafer and Dr. Edward Stuenkel for their advice, help suggestions for my projects, as well as for the great experiences they have provided in the classroom.

To all the faculty and staff of the MCDB department, especially Dr. Anuj Kumar, Dr. Laura Olsen, Mary Carr, Diane Murphy, and Gregg Sobocinski for their help throughout the years.

Finally, through the intercession of the Most Blessed Virgin Mary, I would like to thank God, to whom all rightful gratitude is given.

Table of Contents

List of Figures

Abstract

The effectiveness of synaptic transmission at most mammalian synapses depends largely on the maintenance of a high density of postsynaptic receptors. In a mature synapse, this density is highly dynamic and can be regulated by several factors including synaptic activity, post-translational modifications of receptors, and scaffold proteins. In my thesis work, I focused on the regulation of AChR clustering, which is the hallmark of a neuromuscular junction, a well characterized cholinergic synapse between the motor neuron and the skeletal muscle. Among several pathways, I first focused on the role of α-syntrophin (α-syn), a member of the dystrophin glycoprotein complex (DGC), in the development and modulation of nAChR dynamics of the mouse NMJ. Using α-syn knock-out mice, I showed that α-syn is not required for synapse formation, but it is essential for synapse maturation. Particularly, I demonstrated that during the maturation of synapses, the integrity of the postsynaptic apparatus is altered, the turnover rate of AChRs increases significantly, and the number/density of AChRs is impaired. The synaptic alterations observed in this mouse mutant were explained by the loss of tyrosine phosphorylated α-dystrobrevin (α-dbn). Interestingly, when GFP-α-dbn1 was electroporated into sternomastoid muscles of α-syn mutant, most of synaptic abnormalities were partially restored. In the second part of my thesis work, I investigated the role of serine/threonine kinases, particularly PKC and PKA on the regulation of nAChR trafficking. We found that PKC accelerates nAChR removal and inhibits recycling at the NMJ, while PKA has the opposite effect. Finally, I begin to address the role of the Wnt/β-catenin pathway in the adult NMJ, and we show that β-catenin interacts with the DGC in mature synapses, via rapsyn. Taken together, these results provide new

insights into the cellular and molecular underlying signaling of the regulation of nAChR trafficking and dynamics.

Chapter I

Introduction

Communication between neurons is crucial for transmission and processing of information in the central nervous system (CNS), as well as control of functional effectors by nerves. Most synapses in the nervous systems of mammals are chemical synapses, characterized by a specialized presynaptic terminal juxtaposed to a highly distinct postsynaptic density. From the presynaptic terminal, the neuronal action potential triggers the release of neurotransmitter-packed vesicles; these molecules then diffuse through the few micrometers-wide synaptic space. In the postsynaptic membrane, in most mammalian CNS synapses, there is a markedly high density of postsynaptic receptors. These postsynaptic receptors usually trigger ionic currents directly (ionotropic receptors) or modulate ion channels indirectly (metabotropic receptors) to modulate the excitability or the activity of the postsynaptic cell. Therefore, the concentration of receptors at the postsynaptic density is crucial for the modulation of synaptic strength. In fact, in the past decades, an extensive body of research has shown that posttranslational modifications and regulation of intracellular trafficking of receptors can modulate the postsynaptic density of receptors, in turn leading to those forms of synaptic plasticity most relevant for memory consolidation, long-term potentiation (LTP) and depression (LTD) (Huganir and Nicoll, 2013).

Due to the difficulties in accessibility and small size (≈ 1 μm) of central synapses, the peripheral neuromuscular junction (NMJ) has been widely used as a model synapse. Since NMJs and central synapses share many similarities, understanding the behavior of receptors at the NMJ may also give insights into changes at the less accessible central synapses. The

NMJ is an excitatory synapse in which maintenance of a high density of ionotropic nicotinic acetylcholine receptors (nAChRs) is crucial for maintaining appropriate physiological function. It has remarkable features that make it an excellent model to investigate the dynamics of synaptic receptors in living animals: 1) the high density of synaptic nAChRs facilitates detection; 2) the availability of a marker (α-bungarotoxin; BTX) that binds specifically and quasi-irreversibly to muscle nAChRs and that can be labeled with different fluorescent and/or biochemical tags; 3) its easy accessibility for manipulation and its simple morphology for examination; and 4) the possibility of viewing the same individual synapses over days or perhaps even months, a pre-requisite for understanding the basics of long term changes in neuronal circuitry function. In addition to its relevance as a model synapse, neuromuscular transmission is also required for life, and deleteriously affected in many pathological conditions, such as trauma, degenerative diseases (lateral amyotrophic sclerosis, multiple sclerosis etc.), dystrophies and myasthenias. In all those disease states, the postsynaptic apparatus, most specifically receptor density is affected (Akaaboune et al., 1999; Grady et al., 1999; Durbeej and Campbell, 2002; Dupuis and Loeffler, 2009; Gilhus, 2012).

Together, our knowledge about these pathologies highlights the relevance of: a) maintaining a high density of postsynaptic nAChRs for proper NMJ function, b) the nAChR trafficking pathways, such as internalization and, more recently, recycling (Bruneau et al., 2005), in the maintenance of this density and c) the role of receptor-associated proteins in nAChR stability (Gilhus, 2012). Accordingly, this introduction will further discuss the nAChR intracellular trafficking pathways and the role of receptor-associated proteins in the regulation of receptor dynamics. Further, in this work, we will explore the role of the dystrophin-associated protein α-syntrophin in the development and regulation of nAChR dynamics in the mouse NMJ. Then, we will characterize the effect of PKA and PKC on the regulation of nAChR removal from synaptic sites as well as their recycling in adult NMJs.

Finally, we will show the results of our initial investigation into a possible role of the Wnt/β-catenin pathway in the adult NMJ. Together, these results advance our understanding of signaling mechanisms involved in the regulation of the crucial dynamics that maintain the density of postsynaptic receptors in the NMJ.

Dynamics of Nicotinic Acetylcholine Receptors and Receptor-Associated Proteins at the Vertebrate Neuromuscular Junction

Previously published in Current Alzheimer Research (Curr Alzheimer Res. 2013 Jul;10(6):631-41)

Marcelo Pires-Oliveira, Derek Moen and Mohammed Akaaboune (I was responsible for most of the literature review and writing of the manuscript)

Abstract

The mature neuromuscular junction (NMJ) is the best characterized cholinergic synapse. The maintenance of a high number and density of nicotinic acetylcholine receptors (nAChRs) at the postsynaptic membrane adjacent to the nerve terminal are crucial for NMJ function. This density is maintained by several factors, ranging from synaptic activity to postsynaptic scaffold proteins. Decreases in postsynaptic nAChR density are related to myasthenic syndromes in the peripheral NMJ, but are also associated in central synapses with neurodegenerative diseases such as Alzheimer's. In this review, we focus particularly on our increasing knowledge about the molecular dynamics of nAChR at the peripheral cholinergic NMJ and their regulation by the postsynaptic proteins of the dystrophin glycoprotein complex (DGC).

Introduction

The mature neuromuscular junction (NMJ) is characterized by a high postsynaptic density of nicotinic acetylcholine receptors (nAChRs) (Fambrough and Hartzell, 1972; Hartzell and Fambrough, 1972). Over the last decades, genetic, molecular and biochemical approaches have identified several molecules involved in the initial clustering of nAChRs (which have been extensively reviewed elsewhere) (Sanes and Lichtman, 2001; Wu et al., 2010) and in the stability of postsynaptic nAChRs. In the adult NMJ, the maintenance of a high density of receptors at the postsynaptic membrane is crucial for a normal, functioning synapse. Activity-dependent changes in receptor density are critical for both synaptic development and synaptic plasticity (Collingridge et al., 2004; Martinez-Pena y Valenzuela et al., 2010). In the central nervous system (CNS), the disassembly of the postsynaptic density is also a hallmark of many neurological diseases and pathological conditions. For example, the cholinergic system is consistently and dramatically affected in Alzheimer's disease (AD) (Picciotto and Zoli, 2002; Buckingham et al., 2009; Schliebs and Arendt, 2011). The expression of neuronal nAChRs subtypes, mainly α4β2 and α7, is markedly reduced in many brain regions of AD animal models and human patients (Buckingham et al., 2009). These changes are not due to transcriptional regulation of nAChR subunit genes, as mRNA remains unchanged (Buckingham et al., 2009), suggesting that AD-induced nAChR down-regulation resulted from defects in intracellular trafficking pathways or in their metabolic stability.

At cholinergic synapses in the CNS, the understanding of molecular dynamics of nAChRs and the underlying cellular and molecular mechanisms involved in their regulation is complicated by many factors, such as the large diversity of nAChR subunits, the prevalence of extrasynaptic clustered and unclustered nAChRs in neurons, and the crucial role of presynaptic nAChRs (Huh and Fuhrer, 2002; Lendvai and Vizi, 2008; McCann et al.,

2008). However, the accessibility of the NMJ provides obvious advantages in the study of nicotinic neurotransmission. Molecular signals involved in initial nAChR clustering and plasticity, postsynaptic receptor dynamics and the role of receptor-associated proteins on receptor stability all have been first studied at the NMJ, and were later found to be similar in neuronal-neuronal synapses (Huh and Fuhrer, 2002; Lai and Ip, 2003; Bruneau and Akaaboune, 2007; McCann et al., 2008; Shi et al., 2012). Therefore, this review will focus on these mechanisms that are presumed to be conserved between peripheral and CNS synapses. At mature synapses, the steady-state of synaptic receptors is maintained by the dynamic equilibrium between five main pathways: synthesis, lateral diffusion, internalization and degradation, and recycling (Figure 1.1). The regulation of each of these individual pathways in the NMJ will be discussed further.

Synthesis of nicotinic acetylcholine receptors in developing and mature synapses

During development, nAChRs are expressed throughout the muscle fiber. Even before muscle innervation, nAChRs cluster to the median region of muscle fibers, in a process called prepatterning (Harris, 1981; Lin et al., 2001; Yang et al., 2001). Several proteins expressed by the muscle have been implicated in initial receptor clustering, such as rapsyn, Dok7, lipoprotein receptor-related protein 4 (LRP4) and muscle-specific kinase (MuSK) (Sanes and Lichtman, 2001; Wu et al., 2010). More recently, expression of a constitutively active form of MuSK in muscle cells has been shown to be sufficient to prepattern receptor clusters and control where synapses can be formed (Kim and Burden, 2008). In the mature NMJ, the bulk of nAChR clusters in the postsynaptic membrane appears to come from subsynaptic nuclei, under the direct control of neuronal factors.

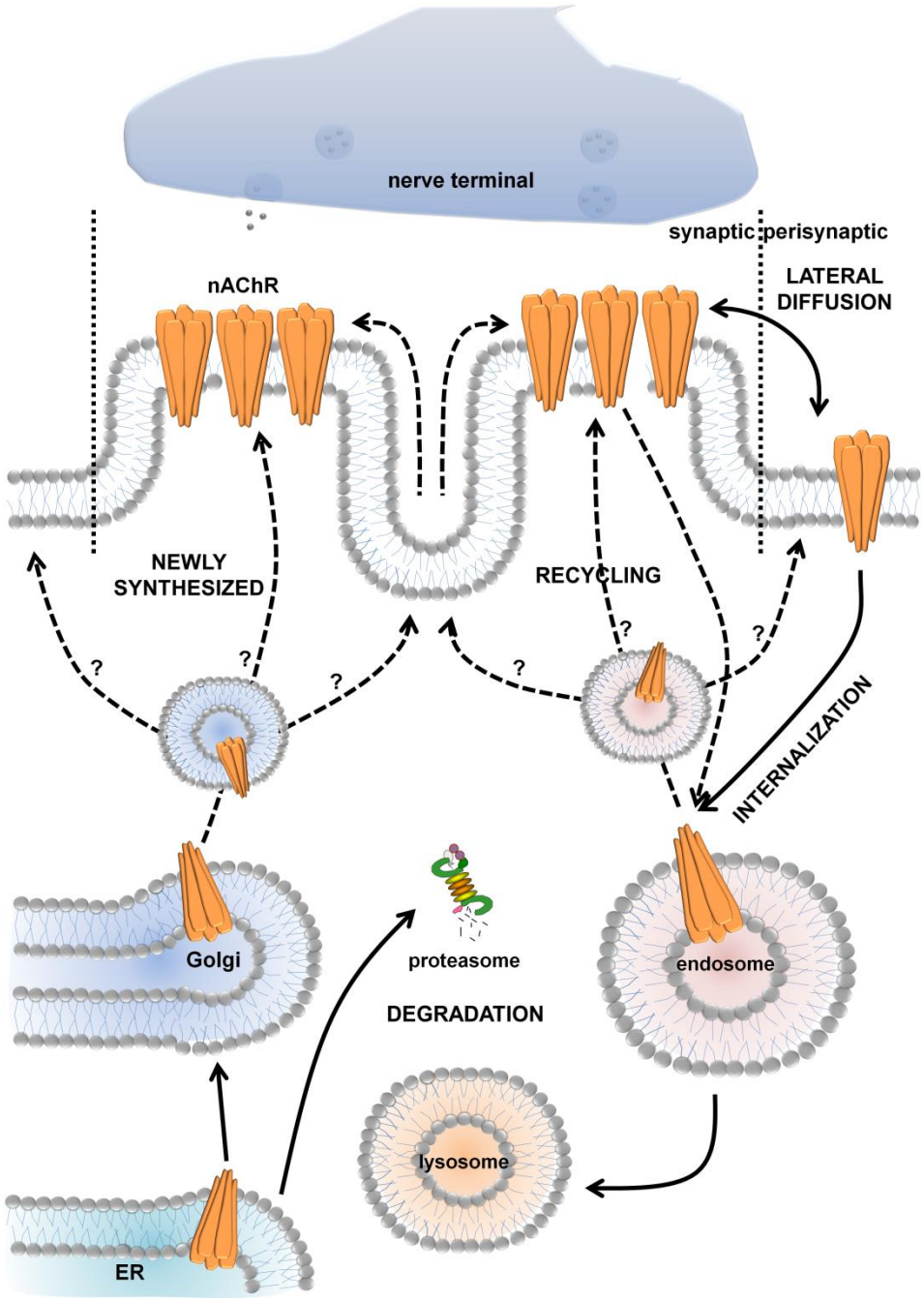

Figure 1.1. Dynamics of nicotinic acetylcholine receptors at the neuromuscular junction. Nicotinic acetylcholine receptors (nAChR) subunits are synthesized in the ER and exported to the muscle plasma membrane. From the ER, instead of being targeted to the cell surface, most nAChR subunits are degraded by the ER-associated ubiquitin-proteasome degradation pathway. In the postsynaptic membrane, there is significant lateral diffusion between the synaptic and perisynaptic membrane spaces. Lateral diffusion of nAChRs from the perisynapse into the NMJ contributes significantly to maintain the synaptic receptor density. Conversely, when receptors escape from the postsynaptic density into the perisynaptic space, there is significant internalization of nAChRs into endosomal compartments. Trafficking through the endosomal pathway, a fraction of internalized nAChRs is targeted for degradation. However, a significant portion of those nAChRs actually recycle back into the synaptic membrane, contributing to the maintenance of the synaptic nAChR pool. Most of these dynamics are tightly regulated in the NMJ by several stimuli, such as synaptic activity or association of dystrophin glycoprotein complex components (see text).

The molecular mechanisms by which neural activity induces gene expression in the subsynaptic nuclei encompass multiple simultaneous signaling pathways, but the two major factors involved are agrin and neuregulin-1 (NRG-1) released by the presynaptic terminal. Agrin binds the agrin receptor LRP4 in the sarcolemma, activating MuSK, which in turn activates the Rac/MKK7/JNK pathway, leading to expression of AChR subunits (Jones et al., 1996; Lacazette et al., 2003; Wiesner and Fuhrer, 2006).

The role of NRG-1 on regulation of nAChR synthesis is less clear. Based on work in cultured myotubes, it was long believed that NRG-1 could directly stimulate transcription of the nAChRε subunit gene, through the activation of mitogen-activated protein kinases (MAPK), ERK and JNK, which in turn activate the transcriptional regulator GA-binding protein (GABP) (Tansey et al., 1996; Altiok et al., 1997; Si et al., 1999). However, the role of NRG-1 *in vivo* remains highly controversial. It has been shown that mice deficient in NRG-1 or mice lacking in postsynaptic erbB2 and erbB4 NRG-1 receptors have normal synapses where receptors are normally clustered (Escher et al., 2005; Jaworski and Burden, 2006), suggesting that NRG-1 is not involved in regulation of AChR synthesis. Recently, a new role of NRG-1 in controlling the stabilization of recycled nAChRs has been uncovered (Schmidt et al., 2011) (see below). Based on these results and others, it appears that agrin is indeed the dominant signaling pathway through which motor neurons regulate nAChR synthesis in the subsynaptic compartment.

It is well established that electrical activity is important for nAChR expression at synaptic sites. In extrasynaptic regions, electrical activity is the predominant signal that ‘shuts off’ expression of synaptic proteins (Goldman et al., 1988; Sanes and Lichtman, 1999). Several molecular cues have been shown to be involved in the repression of synaptic components in the extrasynaptic regions. In the nuclei of these regions, the chromatin is typically condensed and transcriptionally inactive (Méjat et al., 2005). At the innervated

muscle, synaptic impulses (i.e., Ca^{2+} influx) activate Ca^{2+}-calmodulin-dependent kinase II (CaMKII) δ, which is highly concentrated at the NMJ and acts as a neural activity sensor. Activated CaMKIIδ tethers HDAC4 to the sarcolemma and prevents its translocation to the nucleus (Cohen et al., 2007). This relieves the repression of HDAC4 over two myogenin (MGN) repressors: the HDAC9 splice-variant MEF2-interacting transcription repressor (MITR)/histone deacetylase-related protein (HDRP) and Dach2 (Cohen et al., 2007, 2009; Tang et al., 2009). MITR recruits HDAC1 and HDAC3 to perform the catalytic activity involved in MGN suppression, since it lacks the catalytic domain required for histone deacetylase activity (Zhou et al., 2001; Méjat et al., 2005). Another transcription factor, Dach2, is thought to repress MGN at the MEF3 promoter site through its interaction with Six/Eya proteins (Li et al., 2003b; Tang and Goldman, 2006). Therefore, in the innervated muscle, MGN is highly repressed, as well as its target E-box promoter (5'-CANNTG-3') genes, including nAChRε, nACHRδ, and MuSK (Bessereau et al., 1994; Merlie et al., 1994; Méjat et al., 2005). Therefore, these synaptic proteins are mostly absent from the extrasynaptic sarcolemma. On the converse, denervation is sufficient to reverse this myogenic silencing program of synaptic genes in extrasynaptic nuclei: it induces nuclear accumulation of HDAC4 throughout the entire muscle fiber, decreases MITR, and increases MGN and ectopic nAChR synthesis throughout the whole muscle fiber (Adams et al., 1995a; Cohen et al., 2007).

Surface diffusion of nAChR

Early in muscle fiber development, nAChRs start to be expressed on the cell surface. While many nAChR molecules move freely throughout the sarcolemma, a few receptors presumably diffuse into and are trapped in spontaneous clusters, where newly synthesized nAChRs will then be inserted (Stya and Axelrod, 1983). The contribution of lateral diffusion

of surface nAChR into receptor clusters was initially demonstrated by Axelrod et al. (1976) using fluorescence recovery after photobleaching. They showed two populations of nAChRs on the surface of cultured myotubes that had distinguishable mobilities: largely immobilized nAChRs within clusters and highly mobile outside (Axelrod et al., 1976). Similar observations were obtained in adult muscle fibers, with densely packed, immobile junctional nAChRs and mobile extrajunctional ones (Stya and Axelrod, 1984). More recently, lateral diffusion of nAChRs was explored *in vivo* using the photo-unbinding method, which allows selective labeling of the nAChR populations within synaptic clusters with high spatial and temporal resolution. It is clear that nAChRs are in continuous movement between synaptic and non-synaptic regions and can constantly migrate from one region to another within the same synapse to maintain the steady-state postsynaptic receptor density overtime (Akaaboune et al., 2002).

It appears that the mobility of nAChRs is tightly regulated by intracellular scaffolding proteins (Axelrod et al., 1978). Recent studies using quantum dot-based single-molecule tracking techniques have shown that in myotubes deficient in rapsyn, where receptor clusters do not form (Gautam et al., 1995), the mobility of diffuse nAChRs is significantly increased, suggesting that association with rapsyn dramatically limits nAChR mobility (Piguet et al., 2011). However, it remains unknown whether other synaptic scaffold proteins are also limiting factors for nAChR mobility.

Internalization and degradation of nAChR from the postsynaptic membrane

At the NMJ, the steady-state density of postsynaptic nAChRs is established by rates of lateral diffusion, endocytosis and exocytosis (insertion of new and recycled receptors). It is well established that nAChRs migrate from the synapse into the perijunctional membrane,

where they are internalized through clathrin- and non-clathrin-dependent mechanisms (Berg and Hall, 1975; Chang and Huang, 1975; Akaaboune et al., 1999; Schmidt et al., 2011). The removal of receptors from synaptic sites and their internalization appear to be dependent on synaptic activity. For example, when neuromuscular transmission is functional, nAChR half-life is markedly long (10-14 days) (Akaaboune et al., 1999). However, when synaptic activity is blocked (surgically or pharmacologically), nAChR half-life decreases substantially to only a few hours (Akaaboune et al., 1999). Muscle depolarization appears to be critical for the stability of receptors. In denervated muscles or muscles treated with synaptic blockers, in which nAChR internalization is sped up, direct electrical stimulation is sufficient to re-stabilize them (Fumagalli et al., 1990; Caroni et al., 1993; Akaaboune et al., 1999). The stabilizing effect of electrical stimulation on nAChRs is fast, dependent on L-type Ca^{2+} influx (Rotzler et al., 1991) and cAMP increases, and occurs without further nAChR synthesis (Caroni et al., 1993), suggesting that synaptic activity controls post-translational modifications of nAChRs. This is supported by studies in cultured myotubes, in which increased phosphorylation of nAChRβ was found to be associated with stabilization of nAChRs (Sava et al., 2001). Interestingly, nAChRs are mostly not phosphorylated in denervated and cultured myotubes, where nAChR stability is reduced. However, when cAMP concentration increases, more nAChRs are phosphorylated *in vitro* (Miles et al., 1987). Also *in vivo*, in mature NMJs of diaphragm muscles, synaptic nAChRs are heavily phosphorylated and, upon denervation, nAChR phosphorylation is reduced (Qu et al., 1990). Together, these data suggest that neuronal activity regulates Ca^{2+} influx and cAMP production, which modulate protein kinases responsible for nAChR phosphorylation, a signal for receptor stabilization.

Despite evidence for regulation of endocytosis as a key component for maintaining synaptic nAChR density, the endocytosis machinery for nAChRs remains unclear. In CHO-

K1/A5 cells heterologously expressing nAChRs, it appears to occur in a dynamin-, clathrin-, and caveolin-independent manner (Kumari et al., 2008). nAChR endocytosis is induced by the auto-phosphorylation of the c-Src kinase and subsequent activation of Rac1, which may modulate actin dynamics to form the endosomal compartment (Kumari et al., 2008). However, in contrast to the heterologous expression system, recent work *in vivo* has shown that treatment with the dynamin inhibitor dynasore leads to a significant decrease in receptor internalization from postsynaptic sites, highlighting the additional contribution of clathrin-mediated processes (Schmidt et al., 2011).

Upon internalization, most nAChRs are presumably targeted to degradation via the late endosome/lysosomal pathway. The progression of internalized receptors appears to be temporally graded, moving from the early endosome (co-localized with EEA1) to the late endosome (co-localized with LAMP1) with relatively stable kinetics (Kumari et al., 2008). Treatment of cultured muscle cells with leupeptin, a lysosomal proteinase inhibitor, increases the amount of labeled receptors in the late endosome, suggesting that most, if not all, late endosomal receptors are targeted for degradation by lysosomes (Hyman and Froehner, 1983; Kumari et al., 2008). Therefore, the regulation of nAChR likely occurs at the trafficking of the early endosomal compartment, by modulation of the nAChR pools targeted for degradation or recycling (see below).

The role of synaptic protein degradation via the ubiquitin-proteasome system (UPS) has been explored in detail at the CNS (Mabb and Ehlers, 2010). In the NMJ, ubiquitin is highly concentrated, but the role of ubiquitination and proteasome activity has only recently begun to be explored (Serdaroglu et al., 1992; Christianson and Green, 2004; Rezvani et al., 2010). Ubiquitin ligase activity as well as proteasome activity are highly regulated and have been shown to work in an activity-dependent manner in the CNS through CaMKII activity (Djakovic et al., 2009). In C2C12 myotubes, the UPS has also been shown to play an

important role during post-translational processing of receptor subunits in the ER (Christianson and Green, 2004). Inhibition of proteasome-mediated ER-associated degradation (ERAD) with lactacystin increased surface nAChR expression, without having a significant impact on fidelity of receptor assembly (Christianson and Green, 2004). This suggests that a significant amount of functional nAChR subunits are normally targeted to ERAD by the UPS as a regulatory mechanism of receptor density. More recently, it has been shown that the α-kinase-anchoring protein plays a crucial role to protect nAChRs in the synthetic pathway from proteosomal degradation, providing new insights into the possible role of the UPS on the regulation of nAChR density (Mouslim et al., 2012).

Recycling of nAChR into the postsynaptic membrane *in vivo*

For decades, it was widely believed that nAChRs were stable in the postsynaptic membrane until they were removed for degradation. Recent work from our lab has shown that, instead, many internalized nAChRs recycle back to the plasma membrane, and this 'recycled pool' contributes significantly to the steady-state of the postsynaptic receptor density (Bruneau et al., 2005; Bruneau and Akaaboune, 2006). This process has been shown to occur in an activity-dependent manner, as blocking synaptic activity depresses the recycling of receptors into synaptic sites. However, much of the molecular machinery governing the recycling and trafficking of receptor-containing vesicles remains unknown (Bruneau et al., 2005, 2008, 2009; Bruneau and Akaaboune, 2006; Wu et al., 2010). The discovery of recycled receptors at the NMJ has prompted us to re-evaluate the metabolic stability of receptors. Indeed, by monitoring the removal rate of receptor pools (recycled and pre-existing) from the same synapse, we found that the life-time of pre-existing nAChRs is much longer ($t_{1/2}$ ≈ 5-6 days) than that of recycled ones ($t_{1/2}$ ≈ 1 day) (Bruneau and Akaaboune, 2006). Recent studies have shown that the long-described stabilizing effect of

cAMP on synaptic nAChRs is at least partially mediated by the recruitment of myosin Va into the nAChR recycling pathway (Röder et al., 2008; Rudolf et al., 2011). Remarkably, the rate of recycling is tightly regulated by synaptic activity, via an intracellular Ca^{2+}/CaMKII pathway (Martinez-Pena y Valenzuela et al., 2010). Electrical stimulation increases intracellular Ca^{2+}, activates CaMKII and leads to increased delivery of recycled receptors to the synapse (Martinez-Pena y Valenzuela et al., 2010). Furthermore, upon inhibition of CaMKII, more receptors accumulated in the internal pool, suggesting that CaMKII activation is required in the translocation to the membrane (Martinez-Pena y Valenzuela et al., 2010). In the denervated muscle, where nAChR recycling is severely depressed, electrical stimulation and subsequent activation of CaMKII rescued internalized receptors from the degradation pathway and promoted their recycling back into the membrane (Martinez-Pena y Valenzuela et al., 2010). This significant shift in nAChR dynamics and accumulation of internalized receptors is due to a novel, specific modulation of the recycling pathway, as internalization of synaptic nAChRs is unaffected by CaMKII inhibition. It is tempting to say that the role of nAChR recycling in NMJ plasticity and its regulation by synaptic activity (denervation/stimulation) quite closely parallels the regulation of AMPA receptor recycling during long-term potentiation at central synapses (Park et al., 2004; Wang et al., 2008b).

The dystrophin glycoprotein complex and regulation of synaptic receptor dynamics

The dystrophin glycoprotein complex (DGC), which connects the extracellular basal lamina to the intracellular cytoskeleton, is critical for preserving the integrity of the skeletal muscle fiber. Its molecular composition consists of syntrophins and α-dystrobrevin (α-dbn) sub-complexes; dystrophin/utrophin, transmembrane dystroglycans and the sarcoglycan-sarcospan complex (Figure 1.2) (Pilgram et al., 2010). Mutations in genes encoding several DGC components cause muscular dystrophy in both human and animal models. In humans,

complete or partial loss of dystrophin results in Duchenne muscular dystrophy (DMD) or Becker muscular dystrophy, respectively. Deficiencies in sarcoglycans cause limb-girdle muscular dystrophies and deficiencies in α-dystroglycan glycosylation cause glycanopathies (Durbeej and Campbell, 2002). In mouse models, loss of DGC components also results in muscular dystrophy, as in the dystrophin-lacking *mdx* mouse or the α-dbn knockout (Durbeej and Campbell, 2002) (see below). In addition to maintaining the structural stability of myofibers, several DGC components play key roles in the maintenance of the postsynaptic receptor density.

Dystrophin and utrophin

Dystrophin is a large protein (427 kDa) of the DGC that associates with the sarcolemma throughout the entire muscle fiber and is highly concentrated at synaptic sites (Bonilla et al., 1988; Watkins et al., 1988; Zubrzycka-Gaarn et al., 1988; Arahata et al., 1989). In mice deficient in dystrophin (*mdx* model), postsynaptic nAChR clusters are fragmented and NMJ exhibit fewer postsynaptic folds. This synaptic remodeling seems to be secondary to muscle fiber regeneration, as changes in the distribution of synaptic proteins are only seen in regenerating myofibers (i.e., fibers with centrally located nuclei) (Torres and Duchen, 1987). The postsynaptic density of nAChRs appears normal and loss of dystrophin seems to have little effect on the electrophysiological properties (i.e., frequency and amplitude of mini-endplate potentials and quantal content) of the NMJ (Lyons and Slater, 1991).

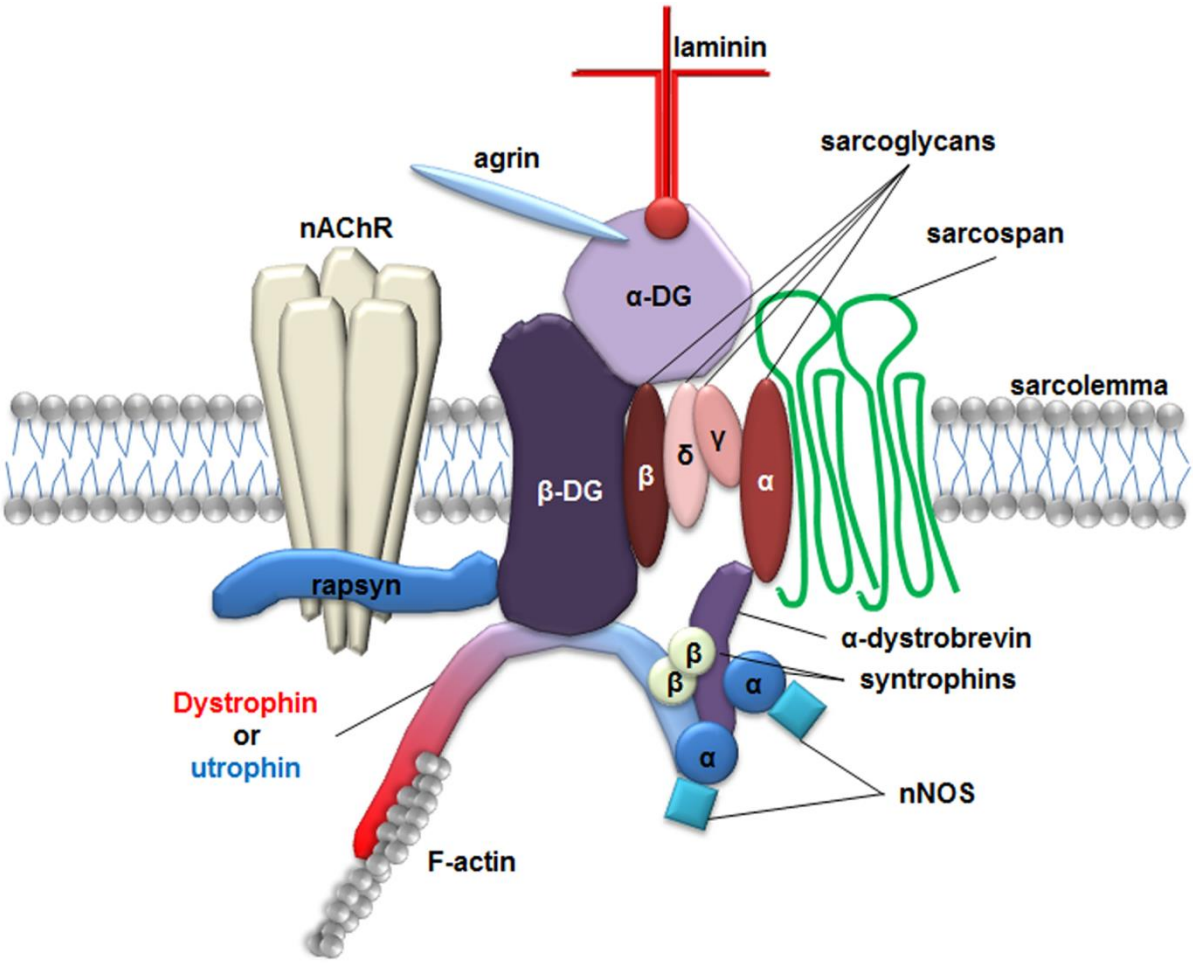

Figure 1.2. The dystrophin glycoprotein complex in the skeletal muscle. The dystrophin glycoprotein complex (DGC) anchors the sarcolemma to the intracellular cytoskeleton (actin) and extracellular matrix components (laminin). Its main cytosolic components are two large proteins, dystrophin and utrophin. While utrophin is exclusively found in the neuromuscular junction (NMJ), dystrophin is expressed throughout the sarcolemma, but is concentrated at the NMJ. Dystrophin/utrophin associate to the transmembrane β-dystroglycan (β-DG), which in turn recruits α-dystroglycan (α-DG). α-DG anchors extracellular matrix proteins such as laminin and agrin, both of which are involved in nicotinic acetylcholine receptor (nAChR) clustering in the developing fiber. α-DG also stabilizes the interaction of β-DG with the sarcospan-sarcoglycan sub-complex. In the NMJ, mainly α-, β-, γ- and δ-sarcoglycan are found in the sarcolemma, which in turn are required for stable association of oligomers of the four-transmembrane-loop protein, sarcospan. Rapsyn associates in a 1:1 ratio with nAChRs and binds them to the DGC through interactions with β-DG. In the cytoplasmic face of the sarcolemma, there are several dystrophin-associated proteins that are not crucial for DGC assembly, but that have key signaling role in the muscle fiber. Mainly, lack of α-dystrobrevin and α-syntrophins lead to heavily decreased nAChR density in the NMJ. α- and β-syntrophins are recruited to the DGC through interactions with dystrophin and α-dystrobrevin and are themselves crucial for neuronal nitric oxide synthase (nNOS) tethering to the sarcolemma and NMJ. α-Dystrobrevin is recruited to the DGC through interactions with dystrophin, α-syntrophin and the sarcoglycan complex. Deficiencies in DGC components shown in red lead to sarcolemma destabilization and muscle dystrophy; knockouts for components shown in blue have reduced nAChR density in the postsynaptic membrane. Therefore, the dystroglycans and α-dystrobrevin are shown in purple to represent both roles.

Earlier reports proposed that absence of dystrophin could lead to an increase in the rate of nAChR degradation (Xu and Salpeter, 1997). However, these studies were based on degradation measurements of radioactively-labeled nAChRs in whole-muscle homogenates, containing both dystrophic and intact muscle cells. In fact, in 2002, by monitoring single NMJ over time, Akaaboune et al. were able to show that the degradation rate of nAChRs is not affected in *mdx* mice and nAChR density is maintained at normal levels. Interestingly, dystrophin has been implicated in α3β4/β2 nAChR stability in sympathetic neurons (Di Angelantonio et al., 2011), suggesting that dystrophin may have distinct roles in stability of different nAChR subtypes, or that the loss of surface nAChRs in *mdx* sympathetic ganglion neurons is an indirect effect of the absence of dystrophin. Indeed, dystroglycans are crucial for nAChR stability in the NMJ (see below) and their expression was previously found to be reduced in the same *mdx* ganglia (Zaccaria et al., 2000).

Utrophin was initially identified as a transcript with 80% amino acid identity to dystrophin (Love et al., 1989), and has since been shown to be a close homolog of dystrophin that is highly clustered at the NMJ (Khurana et al., 1991; Ohlendieck et al., 1991). Interestingly, utrophin is upregulated in *mdx* muscle fibers (Matsumura et al., 1992), though loss of utrophin from the postsynaptic DGC leads to a very slight reduction (≈ 30%) in the density of postsynaptic nAChRs, with no detectable muscle dystrophy (Deconinck et al., 1997). Even when DGC assembly is severely impaired in a dystrophin and utrophin double knockout mouse, the effects on nAChR synaptic density and miniature endplate potential amplitude are very mild (Grady et al., 1997). The maintenance of a mostly unaltered synaptic nAChR density in *mdx* and/or utrophin$^{-/-}$ mice can be explained by the presence of an intact dystrobrevin-syntrophin sub-complex (Peters et al., 1998; Yoshida et al., 2000; Daval et al., 2010), because mice deficient in components of this sub-complex show marked alterations in nAChR distribution and dynamics.

The dystrobrevin-syntrophin sub-complex and nAChR dynamics

α-dbn is a cytosolic component of the DGC that is expressed in at least three alternatively-spliced isoforms in adult skeletal muscle: α-dbn1, α-dbn2 and α-dbn3 (Rees et al., 2007). α-dbn1 and α-dbn2 share a common NH_2-terminus, with two syntrophin-binding sites, but have distinct COOH-terminal domains (Blake et al., 1996; Peters et al., 1997). α-dbn1, the longest isoform, has an additional 188 amino acids which serve as a substrate for protein tyrosine kinases (Balasubramanian et al., 1998); it associates with utrophin and syntrophins and is highly concentrated at nAChR clusters in cultured muscle cells and the NMJ *in vivo* (Balasubramanian et al., 1998; Nawrotzki et al., 1998; Peters et al., 1998; Pawlikowski and Maimone, 2008) (Figure 1.2). α-dbn2 is predominantly present at extrasynaptic sites, where it associated mainly with dystrophin (Peters et al., 1998). α-dbn3, the shortest isoform, does not co-localize with nAChR clusters and lacks syntrophin-binding sites, and its function, if any, remains unclear (Pawlikowski and Maimone, 2008).

The importance of α-dbn for muscle integrity and synaptic nAChR stability is evidenced in mice deficient in α-dbn. These animals are mildly dystrophic (50% fibers), with a muscle phenotype similar to *mdx* mice, albeit with slower cycles of fiber degeneration and regeneration (Grady et al., 1999). The density of nAChRs is dramatically reduced (≈ 30% of wild-type mice) and synapses have a distinctly aberrant speckled appearance (Grady et al., 1999, 2000, 2003; Akaaboune et al., 2002). These alterations in nAChR distribution appear at least one week after birth, implicating α-dbn in maturation, but not formation, of the NMJ (Grady et al., 1999). Interestingly, these morphological alterations are accompanied by an increase in the rate of nAChR degradation (both in α-dbn$^{-/-}$ cultured myotubes and living mice), when compared to wild-type mice or mice deficient in dystrophin and/or utrophin (Grady et al., 2000; Akaaboune et al., 2002). In conclusion, α-dbn plays a key role in nAChR stability, despite the fact that α-dbn does not interact directly with nAChRs.

Interestingly, it appears the ability of α-dbn isoforms to stabilize nAChR clusters involves tyrosine phosphorylation. Only α-dbn1, which has tyrosine phosphorylation sites, is able to rescue fully the synaptic phenotype of α-dbn$^{-/-}$ NMJ, while a mutated form of α-dbn1 with no tyrosine phosphorylation sites is not (Grady et al., 2003). However, the signaling pathways regulating α-dbn phosphorylation, as well as its relevance for nAChR stabilization remain unknown, but their elucidation is likely to clarify the role of the DGC in stabilizing nAChRs. Of note is the fact that α-dbn is also widely present in the CNS (Rees et al., 2007), though α-dbn knockout mice exhibit no remarkable neurological phenotype (Grady et al., 1999, 2006; Rees et al., 2007). This is probably because neurons, unlike skeletal muscle, express the α-dbn homolog, β-dystrobrevin (Peters et al., 1997; Grady et al., 2006; Rees et al., 2007). Indeed, when both α-dbn and β-dystrobrevin are absent, $GABA_A$ receptor clustering is impaired in cerebellar synapses, leading to severe motor defects (Grady et al., 2006).

α-dbn also interacts with α- and β-syntrophins (Figure 1.2) (Butler et al., 1992), and in the absence of α1-syntrophin (α-syn), α-dbn is reduced in the NMJ (Adams et al., 2000). Syntrophins are a family of five dystrophin-binding adapter proteins (α1, β1, β2, γ1 and γ2) with a similar domain structure, containing a pleckstrin homology (PH), a PDZ protein interaction and a C-terminal domain unique to syntrophin (Adams et al., 1995b). In the mouse skeletal muscle, α1- and *β*1-syntrophins are found throughout the sarcolemma and are highly concentrated at the NMJ (Peters et al., 1997; Kramarcy and Sealock, 2000); β2-syntrophin is found almost exclusively at the NMJ (Peters et al., 1994, 1997; Kramarcy and Sealock, 2000) and γ2-syntrophin is present at the subsynaptic sarcoplasmic reticulum (Alessi et al., 2006). Of these, α-syn is the only isoform closely associated with nAChRs at the crests of the NMJ (Kramarcy and Sealock, 2000). Mice deficient in α-syn (α-syn$^{-/-}$) display synaptic aberrations, with markedly reduced nAChR density (≈ 30% of wild type synapses) and a

distinct speckled phenotype (Adams et al., 2000) that is similar to α-dbn$^{-/-}$ synapses. Despite these synaptic defects, α-syn$^{-/-}$ mice exercise voluntarily to the same extent as wild type mice (Adams et al., 2000) and show no muscle dystrophy or changes in contractile properties (Kameya et al., 1999).

Like α-dbn, α-syn does not seem to be involved in NMJ formation, as developing synapses are formed properly, but mature abnormally (Martinez-Pena y Valenzuela et al., 2011). Interestingly, recently published work from our lab shows the rate of nAChR degradation is also increased, similar to α-dbn$^{-/-}$ synapses (Martinez-Pena y Valenzuela et al., 2011). In contrast to α-syn$^{-/-}$, absence of β2-syntrophin does not cause any synaptic phenotype (Adams et al., 2004), though there is partial functional compensation between α-syn and β2-syntrophin, as evidenced by the severe synaptic defects of the α1/β2-syntrophin double knockout mouse, in which nAChR density is only 23% of wild type synapses (Adams et al., 2004).

Previous studies have shown that the synaptic defects of α-syn$^{-/-}$ mice include loss of several other components recruited by syntrophin protein-interaction domains. Consistent with the hypothesis of α-syn as a recruiter of key factors in maintaining synaptic receptor density, expression of syntrophin with intact PDZ and PH domains is required to rescue the synaptic α-syn$^{-/-}$ phenotype (Adams et al., 2010). Among these proteins, utrophin and neuronal nitric oxide synthase (nNOS) are completely absent and α-dbn is dramatically reduced in α-syn$^{-/-}$ NMJ (Kameya et al., 1999; Adams et al., 2000; Thomas et al., 2003). It is possible that loss of these proteins could contribute to the abnormal α-syn$^{-/-}$ synaptic phenotype. Indeed, mice deficient in nNOS display NMJ aberrations and possibly alterations in nAChR stability (Shiao et al., 2004). Similarly, loss of utrophin, could also contribute to the α-syn$^{-/-}$ synaptic phenotype, as utrophin-deficient NMJ also have reduced nAChR density, albeit much less pronounced (Deconinck et al., 1997; Grady et al., 1997). The reduced levels

of utrophin in α-syn$^{-/-}$ synapses are particularly puzzling, as utrophin is thought to associate to the DGC mainly through interactions with β-dystroglycan (Tommasi di Vignano et al., 2000; Pilgram et al., 2010). It is conceivable that syntrophin could play a role in targeting DGC molecules for assembly in the postsynaptic membrane. In support of this idea, in the *Torpedo* electrical organ, syntrophin first associates with nAChRs in post-Golgi vesicles throughout the exocytic pathway and is inserted into the postsynaptic membrane, where in turn it may recruit dystrophin/utrophin and dystrobrevin from the cytosol (Marchand et al., 2001).

More recently, we have found that rapsyn and α-dbn are also reduced in α-syn$^{-/-}$ muscles (Martinez-Pena y Valenzuela et al., 2011). The presence of fewer rapsyn molecules at the α-syn$^{-/-}$ NMJ could be a consequence of the loss of utrophin, as rapsyn is known to associate the DGC and nAChRs through utrophin (Apel et al., 1995; Cartaud et al., 1998). However, it is unlikely that loss of rapsyn could account for the reduced nAChR density, since rapsyn-GFP overexpression is unable to rescue the α-syn$^{-/-}$ phenotype, suggesting that rapsyn loss is a secondary event to the loss of synaptic nAChRs. On the other hand, α-dbn1 overexpression in α-syn$^{-/-}$ deficient muscle is able to partially rescue the aberrant nAChR distribution and slow the rate of receptor degradation, indicating that loss of dystrobrevin could contribute to synaptic deficiencies of α-syn$^{-/-}$ NMJ (Martinez-Pena y Valenzuela et al., 2011).

Dystroglycans and NMJ stability

Dystroglycans (DG) are encoded by a single gene that produces a precursor protein, which is then cleaved into α- and β-DG (Ibraghimov-Beskrovnaya et al., 1992; Deyst et al., 1995). β-DG is a transmembrane glycoprotein that links α-DG in the extracellular surface to dystrophin, and α-DG is a highly glycosylated protein that constitutes the core of the DGC

(Smalheiser and Schwartz, 1987). Through its glycosylated sites, it interacts with several proteins of the basal lamina, such as laminin and agrin (Figure 1.2) (Smalheiser and Schwartz, 1987). Abnormal function of α-DG has been shown to lead to dystrophic phenotypes (Grewal et al., 2001; Côté et al., 2002; Michele et al., 2002), but DG-null mice die at early embryonic stages, before muscle differentiation (Williamson et al., 1997), hindering the investigation of the role of DG on nAChR clustering and stability. Therefore, in 1999, Côté et al. generated chimeric mice with severe muscle DG deficiency to investigate the effect of DG on synaptic phenotype. These mice show severe synaptic disruption, even in non-dystrophic fibers (with fragmented NMJ and markedly reduced density of synaptic nAChRs) (Côté et al., 1999; Jacobson et al., 2001). However, it remains unknown whether these defects are related to abnormalities in nAChR molecular dynamics and whether they are caused by deficiencies in the dystrobrevin/syntrophin sub-complex.

Sarcoglycans and sarcospan

Sarcoglycans are transmembrane proteins encoded by separate, homologous genes. In the skeletal muscle, most sarcoglycan complexes are composed of α-, β-, γ-, and δ-sarcoglycans. The sarcoglycan complex appears to assemble sequentially: β- and δ-sarcoglycan are assembled first, followed by γ-, and α-sarcoglycan (Shi et al., 2004). Mice and hamsters deficient in sarcoglycans exhibit severe myopathy, without obvious synaptic aberrations (Yamanouchi et al., 1994; Duclos et al., 1998; Hack et al., 1998, 2000b; Araishi et al., 1999). Density of nAChRs appears not to be affected, indicating that sarcoglycans are not involved in the maintenance of receptor stability.

Sarcospan was identified as a four transmembrane spanning DGC component and part of the tetraspanin superfamily of proteins (Crosbie et al., 1997). Sarcospan is targeted to the

DGC through interaction with the sarcoglycan complex (Crosbie et al., 1999). The function of sarcospan has remained elusive for several years, since sarcospan null mice show no distinguishable phenotype and the DGC are assembled normally (Lebakken et al., 2000). Strikingly, transgenic mice overexpressing sarcospan have severe muscle degeneration (Peter et al., 2007). The mechanism seems to involve aberrant DGC assembly, with overexpression of most components and aggregation into insoluble complexes (Peter et al., 2007). Further insight into sarcospan function was provided by Peter et al. (Peter et al., 2008), who showed sarcospan directly interacts and stabilizes the utrophin-associated glycoprotein complex. These findings, together with the observation that sarcospan is enriched at the NMJ (Crosbie et al., 1999), indicate that sarcospan might have a role in the maintenance of the postsynaptic density. In fact, sarcospan is able to post-translationally stabilize the utrophin glycoprotein complex (Peter et al., 2008). Since utrophin is usually restricted to the NMJ, this might imply a physiological role of sarcospan in synaptic maintenance, but it is unclear whether the degenerative phenotype of sarcospan transgenic mice is accompanied by NMJ disassembly and/or nAChR loss.

Scaffolding protein rapsyn and nAChR dynamics

Rapsyn is a 43-kDa protein that is crucial for nAChR clustering, as NMJ fail to form in rapsyn$^{-/-}$ mice and nAChRs fail to cluster in rapsyn$^{-/-}$ myotubes (Gautam et al., 1995). Rapsyn associates to the postsynaptic plasma membrane through myristoylation (Musil et al., 1988) and binds to nAChRs in a 1:1 ratio (LaRochelle and Froehner, 1987). Despite the constant steady-state rapsyn:AChR ratio, there is significant divergence in their turnover at synaptic sites. Rapsyn is remarkably dynamic when compared to the nAChR, turning over 3-6 times more rapidly in receptor clusters in cultured myotubes (Bruneau and Akaaboune, 2007) and at the adult NMJ (Bruneau and Akaaboune, 2010). Also, while blockade of

synaptic activity is known to increase nAChR turnover (Akaaboune et al., 1999), it has no effect on the rates of rapsyn removal from and association to synaptic sites (Bruneau and Akaaboune, 2010).

These results show that the marked dynamism seen in the trafficking of synaptic receptors might be a hallmark of most or all synaptic components. In fact, receptor-associated proteins might play an even greater role on synaptic plasticity, as their turnover rate might be faster than the receptors' themselves. Therefore, a better understanding about the characteristics and mechanisms of receptor-associated protein turnover is warranted, in particular for those known to maintain synaptic receptor density, such as rapsyn and DGC components α-dystrobrevin and syntrophins.

Conclusion

Despite decades of work on the molecular regulation of nAChR clustering and trafficking at the postsynaptic density, the molecular mechanisms involved in maintaining the synaptic density of nAChRs are not yet fully elucidated. Also, despite our knowledge of several receptor-associated proteins of the DGC, it remains puzzling how those molecules, particularly the dystrobrevin-syntrophin sub-complex, are assembled and how they contribute to the stability of nAChRs. Presumably, a more complete understanding of the role of the postsynaptic DGC on nAChR stability will increase our understanding of neuromuscular diseases, which may help to define new therapeutic interventions.

Chapter II

Nicotinic acetylcholine receptor stability at the NMJ deficient in α-syntrophin *in vivo*

Previously published in the Journal of Neuroscience (J Neurosci. 2011 Oct;31(43):15586-96)

Isabel Martinez-Pena y Valenzuela*, Chakib Mouslim*, Marcelo Pires-Oliveira*, Marvin E. Adams, Stanley C. Froehner and Mohammed Akaaboune

* contributed equally to this work (I performed the qPCR and immunofluorescence experiments, assisted I. M-P. V. in the analysis of imaging data and helped draft the manuscript)

Abstract

α-syntrophin (α-syn), a scaffold protein, links signaling molecules to the dystrophin glycoprotein complex (DGC). Absence of α-syn from the DGC is known to lead to structurally aberrant neuromuscular junctions (NMJs) with few acetylcholine receptors (AChRs) clustered at synaptic sites. Using α-syn knockout mice, we show that during the first postnatal week, α -syn is not required for synapse formation. However, at postnatal day 7, the structural integrity of the postsynaptic apparatus is altered, the turnover rate of AChRs increases significantly, and the number/density of AChRs is impaired. At adult α-syn$^{-/-}$ NMJ, the turnover rate of AChRs is about 4 times faster than wild type synapses, and most removed receptors are targeted to degradation as few AChRs recycled to synaptic sites. Biochemical

analyses show that in muscle cells of adult knockout α-syn mice, total AChRs and scaffold protein rapsyn are significantly reduced, the 89 kDa and 75 kDa isoforms of tyrosine phosphorylated α-dystrobrevin (α-dbn) 1 (which are required for the maintenance and stability of AChR in α-dbn$^{-/-}$ synapses) are barely detectable. Electroporation of GFP- α-dbn1 in α-syn$^{-/-}$ muscle cells partially restored receptor density, turnover rate, and the structural integrity of the postsynaptic apparatus, whereas expression of rapsyn-GFP failed to rescue the α-syn$^{-/-}$ synaptic phenotype. These results demonstrate that α-syn is required for the maturation and stability of the postsynaptic apparatus and suggest that α-syn may act via α-dbn1.

Introduction

α-syntrophin (α-syn) is a component of the dystrophin glycoprotein complex (DGC), which also includes dystrophin/utrophin, dystroglycan, sarcoglycan, sarcospan, and α-dystrobrevin (α-dbn) (Straub and Campbell, 1997; Hack et al., 2000a; Dalkilic and Kunkel, 2003). It is thought to function as an adaptor molecule that recruits signaling and structural proteins to the transmembrane DGC. α-syn directly interacts with dystrophin/utrophin, dystrobrevins, neuronal nitric oxide synthase (nNOS), voltage-gated sodium channels, several kinases, aquaporin-4 and other channels and signaling proteins (Kramarcy et al., 1994; Ahn and Kunkel, 1995; Dwyer and Froehner, 1995; Brenman et al., 1996; Froehner et al., 1997; Gee et al., 1998; Adams et al., 2000; Neely et al., 2001).

At mature neuromuscular junctions (NMJs), α-syn is highly concentrated at both the troughs and the crests of the junctional folds and was found to accumulate with acetylcholine receptors (AChRs) at synaptic sites as early as postnatal day 1 (Kramarcy and Sealock, 2000). Adult animals deficient in α-syn show dramatic changes in the structural organization of the

synapses (Adams et al., 2000). AChRs are fewer in number and density, and the pattern in which they are clustered differs dramatically from wild type mice, with speckles of receptors extending from edges of mutant synapses. Several other proteins of the DGC are either decreased or completely absent from the postsynaptic apparatus (nNOS and utrophin, respectively) (Adams et al., 2000; Kramarcy and Sealock, 2000). However, it remains unknown how the absence of α-syn from synapses reduces receptor density and number in the postsynaptic membrane and at which stage of synaptic development the absence of α-syn begins to impair structural organization of the postsynaptic membrane.

The phenotype of the α-syn$^{-/-}$ NMJ appears very similar to the α-dbn null mice in many ways. α-dbn$^{-/-}$ NMJs have dramatically reduced levels of AChR, with an abnormal pattern of AChR distribution that resembles the α-syn mutant. In contrast to mice deficient in α-dbn, in which ≈50% of muscle fibers are dystrophic, α-syn null mice have no sign of muscular dystrophy (Adams et al., 2000; Grady et al., 2000). Previous studies have shown that α-dbn is necessary for tight tethering of AChRs in the postsynaptic membrane, and is required for the maturation of the synapse (Grady et al., 2000, 2003; Akaaboune et al., 2002). However, it is not known whether α-syn is involved in controlling the metabolic stability of AChRs and whether removed or decreased proteins of the DGC from α-syn$^{-/-}$ NMJ mediate the AChR postsynaptic phenotype of α-syn mutants.

In this work, we investigate the effect of the absence of α-syn from the postsynaptic membrane on synapse formation and maturation *in vivo*. Using a multidisciplinary approach, we show that α-syn is required for synaptic maturation and postsynaptic receptor stability and that α-syn acts in part through α-dbn1, as overexpression of α-dbn1 partially rescues the postsynaptic phenotype of α-syn deficient mice.

Materials and Methods

Animals and confocal microscopy

In this study, we used non-Swiss albino adult female mice (6–10 weeks old, 25–30 g) that were purchased from Harlan, mice deficient in α-syn that were bred in our animal facility from a pair provided by Dr. Froehner's laboratory, and mice deficient in α-dbn bred from a pair from Dr. Joshua Sanes's laboratory. All animal usage followed methods approved by the University of Michigan Committee on the Use and Care of Animals.

To determine whether α-syn is essential for synapse maturation, wild type and α-syn mutant mice from P0 to P60 were anesthetized by i.p. injection of 72 mg/kg ketamine and 12 mg/kg xylazine and their sternomastoid muscles were bathed with Alexa Fluor 488-conjugated α-bungarotoxin (BTX-Alexa488) (Invitrogen) to label AChRs (30 min, 5 μg/mL). Pups and adult mice were then fixed and NMJs were scanned with a confocal microscope (Leica SP5) using a 100× 1.46 NA oil immersion objective (Leica). The z-stacks were then collapsed and the contrast adjusted with Adobe Photoshop CS2.

Quantitative fluorescence assay

To determine whether absence of α-syn affects postsynaptic receptor density as synapses develop, the sternomastoid muscle of wild type and mutant mice from P0 to P60 were exposed and bathed with a saturating dose of BTX-Alexa488 to label all AChRs at superficial synapses (5 μg/mL, 1 h). The non-bound fluorescence was washed out with lactated Ringer's superfusion continuously for 10-15 min and synapses were imaged. The fluorescence intensity of labeled receptors at NMJ was assayed using a quantitative fluorescence imaging technique, as described by Turney and colleagues (Turney et al., 1996), with minor modifications.

In situ imaging of developing and mature synapses

The techniques of animal preparation, sternomastoid exposure, and neuromuscular imaging have been previously described in detail (Lichtman et al., 1987; van Mier and Lichtman, 1994; Akaaboune et al., 1999). The anesthetized mouse was placed on its back on the stage of a customized epifluorescence microscope, and superficial NMJs were viewed under a coverslip with a water-immersion objective (Olympus UAPO 20×W3/340 0.7 NA) and a digital CCD camera (Retiga EXi; Qimaging) and imaged (IPLap software; BioVision Technologies). At the end of an imaging session, the incision was closed and the mouse was allowed to recover until re-anesthetized and prepared for a second imaging session.

Several different experimental protocols were carried out. In each case, multiple animals were used (typically 5-8). In the first series of experiments, neonatal pups (3 days after birth) of control and mutant mice were injected in the tail with a low dose of BTX-Alexa488 (20 μL, 1 μg/mL). This concentration labels few receptors at the NMJ (less than 20%). At postnatal day 4 (P4), pups were anaesthetized and the sternomastoid muscle was exposed and superficial synapses were imaged immediately (time 0). Twenty-four hours later (P5), the same synapses were re-imaged and their fluorescence intensity was measured. When synapses were imaged multiple times, the wound was sutured (7-0 Ethilon monofilament Nylon), a local antiseptic was applied to prevent local infection of the neck after each session and the animal allowed to fully recover before the next imaging session.

In the second series of experiments, pups at P4 and P7 were injected with a low dose of BTX-Alexa488 and at P5 and P8, animals were anaesthetized, the sternomastoid muscle was exposed and superficial synapses were imaged immediately and re-imaged 24 hours later (P6 and P9).

In the last series of experiments, the sternomastoid muscle of adult wild type and mutant mice were bathed with a low dose of BTX-Alexa488 (0.1 μg/mL for 2 min) to label few receptors or injected with a low dose of BTX-Alexa488. The sternomastoid was then washed continuously for 10 min with lactated Ringer's solution. Under this condition of labeling, less than 30% of receptors were labeled with fluorescent α-bungarotoxin (BTX), leaving synapses functional (Akaaboune et al., 1999).

To investigate whether the absence of α-syn affects the insertion of newly synthesized receptors at adult synapses, the sternomastoid muscle was bathed with a single saturating dose of BTX-Alexa488 (5 μg/mL, 1 h). The superficial synapses were imaged and their fluorescence intensities were measured. Three days later, mice were anaesthetized, sternomastoid muscles exposed, and the same synapses were imaged and then re-saturated with the same fluorescently tagged BTX.

To investigate whether absence of α-syn has any effect on the recycling of AChRs, sternomastoid muscles of adult wild type and α-syn null mice were labeled with biotinylated α-bungarotoxin (BTX-biotin) (5 μg/mL, 1 h; Invitrogen) followed by a saturating dose of Alexa Fluor 488-tagged streptavidin (strept-Alexa488) (10 μg/mL, 3 h; Invitrogen), as described previously in details by Bruneau et al., 2005. Briefly, after three days of initial labeling (to allow more internalization of AChRs), the mouse was anaesthetized and the sternomastoid muscle was imaged, then incubated with strept-Alexa488 (10 μg/mL, 3 h) to label the recycled receptors; later, superficial synapses were re-imaged and their fluorescence intensities were measured to determine the contribution of recycled AChRs to total receptors at wild type and mutant synaptic sites. Control experiments for ruling out dissociation of streptavidin from biotin on the surface of the muscle cells were described in our previous work (Bruneau et al., 2005; Bruneau and Akaaboune, 2006; Martinez-Pena y Valenzuela et al., 2010). Based on the fact that after internalization of AChR-BTX-biotin/streptavidin

complexes inside the muscle, Alexa-labeled streptavidin dissociates rapidly from AChR-BTX-biotin within internal vesicles (likely endosomes), and on the extracellular surface the rate of dissociation of Alexa-labeled streptavidin from biotin was too slow to be detected even after several days, we can assess recycling by adding fresh Alexa-streptavidin hours or days after an initial saturating dose.

To determine the effects of the absence of α-syn on half-life of pre-existing and recycled pools, the sternomastoid muscle was exposed and bathed with BTX-biotin (5 μg/mL, 30 min) to label AChR following by a saturating dose of strept-Alexa488 (10 μg/mL, 3 h) (Bruneau et al., 2005; Bruneau and Akaaboune, 2006). Three days later, the animal was anaesthetized and the sternomastoid was exposed and bathed with Alexa Fluor 594-tagged streptavidin (10 μg/mL, 3 h; Invitrogen) to specifically label the recycled AChRs, as has been previously described in detail (Bruneau et al., 2005). Superficial doubly labeled synapses (red, recycled; and green, "pre-existing") were imaged and re-imaged several days later and their fluorescence intensities were assayed.

Western blot

Sternomastoid muscles were removed from wild type and α-syn null mice, minced, and homogenized on ice in a buffer containing 50 mM HEPES, pH 7.4, 2 mM EDTA, 250 mM sucrose, 150 mM NaCl, 1% NP-40, 0.25% sodium deoxycholate. Homogenates were shaken for 30 min and centrifuged at 10,000 × g for 10 min, giving a supernatant (S) and a pellet (P). The supernatant was collected and proteins were quantified using Pierce BCA protein assay. Identical amount of proteins were separated by 12% SDS-PAGE and transferred onto a polyvinylidene fluoride membrane. The membranes were bathed in PBS pH 7.4, 2% skimmed milk, 0.05% Tween 20, blocking solution for 1 h, incubated in either

monoclonal anti-rapsyn (R2029, clone 1234; Sigma) diluted at 0.5 μg/mL, anti-dystrobrevin (610766 Clone 23; BD biosciences) diluted at 1:4,000, or anti-α1-AChR subunit (MAB210; MMS-609R; Covance) diluted at 1:5,000 in PBS plus 0.05% Tween 20 at 4 °C overnight. The membranes were then incubated for 1 h in HRP-conjugated goat anti-rat or donkey anti-mouse secondary antibody at 1:20,000 (Jackson ImmunoResearch). After extensive washing, the membranes were incubated with SuperSignal West Femto Maximum Sensitivity Substrate (Pierce).

To determine the amount of receptors on the surface of muscle cells of mutant and wild type mice, sternomastoid muscles were exposed and bathed with 5 μg/mL of BTX-biotin for 1 h and receptors bound to BTX-biotin were pulled down using NeutrAvidin-coated agarose beads.

To determine the amount of intracellular AChR, sternomastoid muscles were bathed in 5 μg/mL of unlabelled BTX for 1 h to saturate all surface AChRs and non-bound unlabeled BTX was extensively washed out. Muscles were then removed, homogenized and muscle lysates were incubated with 300 nM BTX-biotin for 1 h at 4 °C. Receptors were then isolated using NeutrAvidin-coated agarose beads from 300 μg of total proteins.

In both intracellular and surface isolated receptors, the NeutrAvidin beads were collected by brief centrifugation and washed three times with homogenization buffer without detergents. The beads were resuspended in 75 μL of 2 × LDS buffer (Invitrogen) and boiled for 5 min to release proteins, which were separated on 12% SDS-PAGE and transferred onto a polyvinylidene fluoride membrane. After blocking in 2% non-fat milk, the membranes were incubated in rat anti-α1-AChR subunit at 4°C overnight. The membranes were then incubated for 1 h in HRP-conjugated goat anti-rat secondary antibody at 1:10,000 (Jackson ImmunoResearch). After extensive washing, the membranes were incubated with

SuperSignal West Pico Substrate (Pierce). Immunoblot quantitation was performed by scanning films and using the NIH ImageJ software.

Quantitative RT-PCR analysis of mRNA expression

RNA was isolated using TRIzol® (Invitrogen) from pairs of mouse sternomastoid muscles. Reverse transcription into cDNA was performed using 1 μg of total cellular RNA, 50 pmol oligo(dT)20 primer (Invitrogen) and SuperScript® III Reverse Transcriptase (Invitrogen). Quantitative real-time PCR was carried with 1 μL of cDNA product and the Power SYBR© Green PCR Master Mix (Applied Biosystems), using a 7500 Fast Real Time PCR System (Applied Biosystems). We used the following primers, designed to pair with different exons of mouse α1-AChR subunit (*Chrna1*; NM_007389.4): forward 5'-gaggaccaccgtgagattgt-3' and reverse 5'- aatcgacccattgctgtttc-3' (product size, 121 bp); rapsyn (*Rapsn*; NM_009023.3): forward 5'- ctcagatgcctgcaaaacaa-3' and reverse 5'-aggttgtgtggaaacccaag-3' (product size, 111 bp); α-dbn1 (*Dtna1*; NM_207650.3): forward 5'-ctccggctcctcagacag-3' and reverse 5'- ggcagatgctgaacggatg-3' (product size, 195 bp). Expression was normalized to WT using the $2^{-\Delta\Delta Ct}$ method (Livak and Schmittgen, 2001) and glyceraldehyde-3-phosphate dehydrogenase (*Gapdh*; NM_008084.2) as an internal reference, with primers 5'-aactttggcattgtggaagg-3' and 5'- ggatgcagggatgatgttct-3' (product size, 132 bp).

Immunofluorescence

To determine if absence of α-syn affects chromatin modification and transcriptional activation of postsynaptic nuclei, the sternomastoid muscle of wild-type and mutant adult mice were exposed and bathed with a saturating dose of BTX-Alexa488 (Invitrogen) to label

all superficial synapses (5 μg/mL, 30 min). The non-bound fluorescence was washed out with lactated Ringer's superfusion and the animals were perfused with 4% formaldehyde. After extraction and dissociation into thin fiber bundles, the sternomastoid muscle was permeabilized with 1% Triton X-100 Tris-buffered saline (TBS) for 30 min and then washed twice with TBS. Fiber bundles were immersed and incubated overnight in rabbit anti-phospho (Ser10)-acetyl (Lys14)-histone H3 (Millipore), diluted 1:500 in 1% bovine serum albumin (BSA) TBS. After washing with TBS, fiber bundles were incubated with DyLight 594-conjugated goat anti-rabbit IgG (Jackson Immunoresearch), diluted 1:1000 in 1% BSA TBS for 1 h. After washing with TBS, fibers were further dissociated, mounted in ProLong with DAPI (Invitrogen) and imaged with a confocal microscope (Leica SP5). The z-stacks were then collapsed and the contrast adjusted with Photoshop.

Electroporation of GFP-α-dbn1, rapsyn-GFP, and α-syn-GFP into the sternomastoid muscle and confocal microscopy

Adult mice deficient in α-syn (20–28 g) were anaesthetized, the sternomastoid muscle was surgically exposed and 10 μg of plasmid driving exogenous expression of GFP-α-dbn1, GFP-α-dbn1-P3$^-$ (three tyrosine phosphorylation sites at Y685, Y693 and Y710 mutated to phenylalanine), rapsyn-GFP, or α-syn-GFP was added (all constructs were driven by a CMV promoter). The plasmid solution was layered over the muscle surface as described by (Bruneau and Akaaboune, 2010). Gold electrodes were placed parallel to the muscle fibers on either side of the muscle, and eight monopolar square-wave pulses were applied perpendicularly to the long axis of the muscle. Following electroporation, the mouse was sutured and allowed to recover in a heated recovery chamber. One to two weeks later, the animal was re-anaesthetized and Alexa Fluor 594-labeled α-bungarotoxin (BTX-Alexa594) was added to the sternomastoid muscle to label AChRs (1 h). The animal was then perfused

transcardially with 2% formaldehyde and the sternomastoid muscle was removed, mounted and scanned with a confocal microscope (Leica SP5) and imaged. The z-stacks were then collapsed and the contrast adjusted with Photoshop.

Results

Effect of α-syntrophin deficiency on the maturation of developing synapses

To examine at which stage of synaptic development the absence of α-syn begins to alter normal postsynaptic apparatus development, sternomastoid muscles of α-syn null and wild type mice at different stages of development (P0, P5, P7, P15, and P60) were bathed with BTX-Alexa488 to label AChRs, then fixed, and imaged. High resolution confocal images of synapses show no significant differences in AChR distribution in mutant NMJs at P0 or P5, but abnormal patterning of AChRs was evident at P7 and became more pronounced at P15 where obvious patchy aggregates and extension of receptors from edges were observed. This abnormal patterning of AChR distribution persists and even worsens at mature synapses (P60) (Figure 2.1 A). Careful analyses of mutant and wild type synapses revealed that in mutants, the transition of synapses from plaque-like to perforated and to branched receptor distribution was delayed and the size of synapses remains relatively small compared to wild type (Figures 2.1 B, C). These observations suggest that α-syn is required for the maturation of the postsynaptic apparatus.

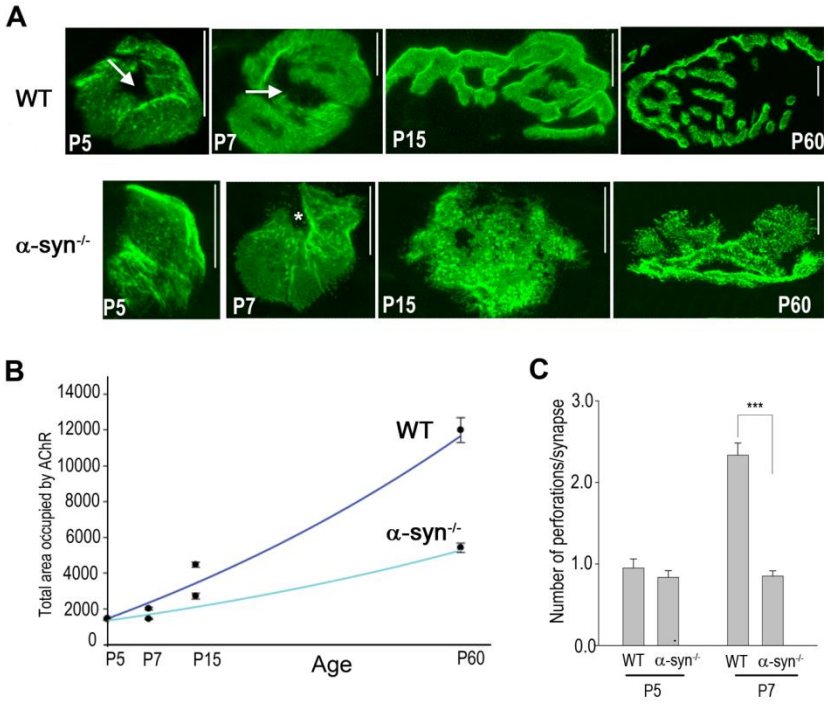

Figure 2.1. Absence of α-syn delays the maturation of the synapse. **A**) Sternomastoid muscles of mutant and wild type mice at different stages of development were bathed with BTX-Alexa488 to label AChRs and synapses were imaged with confocal microscope. Note that synapses at P5 of wild type and mutant look similar (there is no obvious abnormality in the pattern of receptor distribution). However, at P7, AChRs appear to have a patchy distribution in mutant synapses compared to wild-type synapses. At P15 and P60, the structural organization (many small, high-density aggregates of AChRs distributed both at the crests and troughs of junction folds, with frequent speckled extensions of AChRs from the edges) of mutant synapses is different from wild type at the same age. Arrows indicate synaptic perforations and asterisks, synaptic invaginations, as quantified in Figure 2.1 C. Scale bars are 10 μm. **B**) Graph shows the area occupied by AChRs as labeled with fluorescent BTX-Alexa488. Note that the overall synaptic area of mutant synapses is smaller than wild type as synapses mature. Each data point represents the mean and SEM of the area of several junctions. **C**) Graph shows fewer perforations/invaginations in developing mutant synapses than wild type, indicating that the maturation process is somewhat delayed in mutant synapses. Each bar represents the mean and SD of several junctions. *** $p < 0.0001$.

Next, we examined whether the abnormal patterning of receptor distribution in α-syn$^{-/-}$ NMJ is accompanied by alterations in the density and number of AChRs at synaptic sites. To do this, sternomastoid muscles from different developmental stages (P0 to P60) were labeled with BTX-Alexa488 to saturate all receptors. Superficial synapses were then imaged and their fluorescence intensity was assayed. The density of AChRs at different stages of development was expressed as a percentage of the fluorescence present at mature wild type

NMJs. As shown in Figure 2.2, no significant difference in receptor density between wild type and α-syn$^{-/-}$ NMJs was seen at P0 (WT: 13 ± 3% SD, n = 23; α-syn$^{-/-}$: 12.5 ± 2% SD, n = 16) and P5 (WT: 24.6 ± 5% SD, n = 21; α-syn$^{-/-}$: 24.2, ± 6% SD, n = 37). At P7, however, the density of AChR at α-syn$^{-/-}$ NMJs is (25 ± 6% SD, n = 20), 33% lower than the density of AChRs at wild type synapses (37 ± 9% SD, n = 20) of the same age (Figure 2.2). In contrast to wild type synapses, in which the density of AChRs continues to increase as synapses mature, the density of AChRs at α-syn$^{-/-}$ NMJs reaches a low maximum at P15 and remains unchanged thereafter (Figure 2.2). We also quantified the number of AChRs by calculating the product of average density and synaptic area, since during normal development of the synapse, both the size and average density within synaptic area increase. After postnatal day 7 and as synapses mature, the total number of receptors at synaptic sites begins to diverge from wild type synapses and remains low in α-syn mice compared to wild type (data not shown). Together these results indicate that α-syn is required for the increase of postsynaptic receptor density as synapses mature.

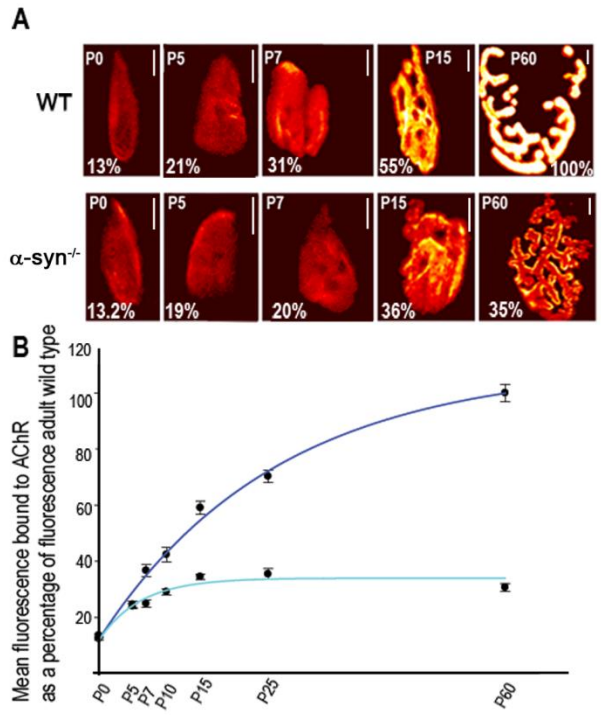

Figure 2.2. The density of postsynaptic receptors at the neuromuscular junction of α-syn null mice is dramatically affected as synapses mature. AChRs in sternomastoid muscles of control and mutant mice were labeled with BTX-Alexa488 until their saturation. Superficial synapses were imaged and their fluorescence intensity was measured and normalized to fluorescence intensity of adult wild type synapses. **A**) Examples of neuromuscular junctions imaged at different stages of development using a quantitative fluorescence assay. These pseudo-color images provide a linear representation of the density of AChR (white-yellow, high density; red-black, low density). **B**) Quantification of the density of AChRs using the same approach shown in A. Each data point represents the mean and SEM of several NMJs. Note that at P0 and P5, the density of postsynaptic receptors is the same between wild type and mutant synapses. At wild type synapses, the density of postsynaptic receptors increases steadily as synapses mature, but the density of postsynaptic receptors at mutant synapses rises slowly and remains low as synapses mature. Scale bars are 10 μm.

AChR dynamics in developing synapses of mice lacking α-syntrophin

Having found that absence of α-syn from NMJs impairs postsynaptic receptor density and distribution as early as P7, we asked whether failure to increase the density and number of postsynaptic receptors is accompanied by an accelerated rate of receptor loss from the postsynaptic membrane. To test this, labeled AChRs on the sternomastoid of α-syn$^{-/-}$ and wild type pups at postnatal day (P4) were imaged and then re-imaged 24 hours later. Twenty-four hours after initial imaging, fluorescence intensity of the labeled receptors had decreased 39 ± 8% SD (n = 26) in mutant synapses [$t_{1/2} \approx 34$ hours] and 35 ± 8% SD (n = 20) in wild type synapses [$t_{1/2} \approx 38$ hours], ($p > 0.05$) (Figure 2.3 A). This result indicates that absence of α-syn has no significant effect on receptor turnover rate during the first five days after birth. However, at 6 days after birth, fluorescence intensity of the labeled receptors had decreased 54 ± 6% SD (n = 18) over 24 hours in mutant synapses [$t_{1/2} \approx 21$ hours] and only 36 ± 6% SD (n = 25) in wild type synapses [$t_{1/2} \approx 37$ hours] over the same period ($p < 0.0001$) (Figure 2.3 B). At P9, fluorescence intensity of the labeled AChR decreased 48 ± 6% SD (n = 24) [$t_{1/2} \approx 26$ hours] in the α-syn$^{-/-}$ synapses, but only 26 ± 6% SD (n = 20) [$t_{1/2} \approx 55$ hours] in wild type synapses over 24 hours ($p < 0.0001$) (Figure 2.3 C). This indicates that α-syn is involved in receptor removal from postsynaptic sites as synapses mature.

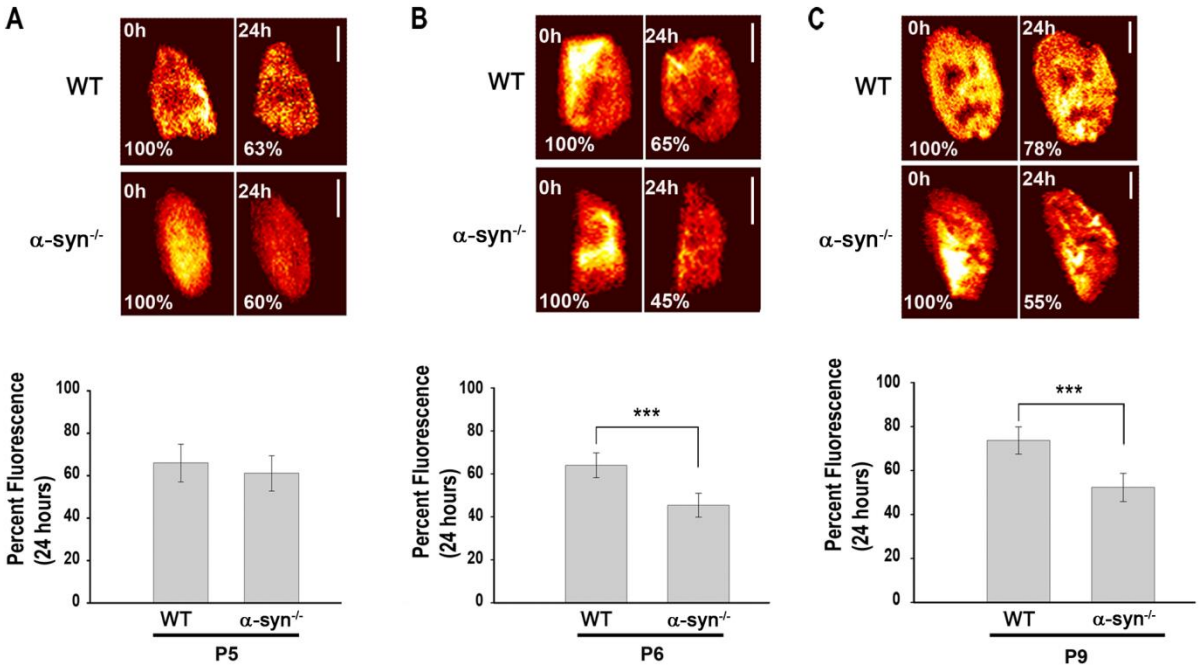

Figure 2.3. Absence of α-syn accelerates the loss rate of AChRs at developing synapses. **A**) Neonatal pups of wild type and mutant mice aged 3 days after birth were injected with a low dose of BTX-Alexa488 in their tails (less than 20% of AChR were labeled), and 24 hours later they were anesthetized and synapses on the sternomastoid muscle were imaged immediately (time 0) and re-imaged 24 hours later. Example of two views of the same neuromuscular synapses of mutant and wild type imaged and re-imaged at 0 and 24 hours later. The total fluorescence intensity (a measure of the total number of AChRs) was expressed as 100% at the initial labeling (time 0) and normalized to this on the successive view (24 hours). Graph summarizes the data from many synapses using the approach in A. Note that the remaining fluorescently labeled AChR in mutant synapses was not significantly different from wild type synapses. **B**) Example of two images of wild type and mutant NMJ of pups 6 days old at time 0 and 24 hours later. Graph shows data from many synapses. Note that the loss of fluorescence from labeled AChR is increased in mutant synapses compared to wild type. **C**) At P9, the loss of fluorescence of labeled AChR from wild type synapses averaged at 26% after 24 h, whereas the loss of fluorescence from α-syn$^{-/-}$ synapses was 48%. Note that α-syn deficiency dramatically decreases the half-life of AChRs. Each data point represents the mean percentage of fluorescence intensity (± SD) at each view. Scale bars are 10 μm. *** $p < 0.0001$.

AChR dynamics at mature synapses of mice lacking α-syntrophin

The observation that α-syn$^{-/-}$ synapses bear fewer AChRs than controls prompted us to examine the possible mechanisms that lead to decreased AChR density at postsynaptic sites. We investigated this issue in adult mutant mice. First, we examined whether absence of α-syn from adult synapses decreases the half-life of AChRs. To examine this, sternomastoid muscles were labeled with a non-saturating dose of fluorescent BTX (less than 30% of

receptors were labeled, leaving synapses functional) and the loss of fluorescently tagged AChRs was monitored over the next 24 hours. We found that the fluorescence intensity of the labeled receptors had decreased 8 ± 3% SD (n = 31) of original fluorescence in wild type synapses [$t_{1/2} \approx 9$ days] and 30 ± 7% SD (n = 25) of original fluorescence in mutant synapses [$t_{1/2} \approx 2$ days] (Figure 2.4 A). Therefore, the half-life of AChRs at α-syn$^{-/-}$ synapses is about four times faster than AChR at wild type synapses.

Next, we used the loss rate to calculate the insertion rate of new AChRs into the postsynaptic membrane. Knowing that the size of mature synapses remains relatively constant for at least several weeks, the sternomastoid muscle was bathed with a single saturating dose of BTX-Alexa488 to label all AChRs on the surface of the muscle cell, and superficial synapses were imaged immediately (time 0). Three days later, the same synapses were located, re-imaged and the loss of their fluorescence intensity was measured. A second saturating dose of BTX-Alexa488 was added to label new AChRs and synapses were imaged again. We found that most lost receptors were replaced with new AChRs, indicating that the rate of insertion of new receptors into the postsynaptic membrane was not impaired by the absence of α-syn (Figure 2.4 B).

Then, we explored whether a defect in the number of recycled receptors could account for the low number and density of receptors at α-syn$^{-/-}$ NMJs, since this pool of receptors contributes to the density and number of AChRs in the postsynaptic membrane(Bruneau et al., 2005; Bruneau and Akaaboune, 2006). The sternomastoid muscle of mutant and wild type animals was labeled with BTX-biotin, followed by a saturating dose of strept-Alexa488, as described previously (Bruneau et al., 2005) and superficial synapses were imaged immediately (time 0). Three days after the initial labeling (to allow for a sizable amount of receptor internalization), the same synapses were imaged to measure the loss of fluorescence and then the sternomastoid muscle was bathed with strept-Alexa488 to label recycled AChRs

(receptors that had lost their initial strept-Alexa488 tag while retaining BTX-biotin during the process of internalization and reinsertion in the postsynaptic membrane). The same synapses were re-imaged and the percentage of recycled AChRs at mutant synapses was measured and compared to wild type synapses. We found that only 9 ± 4% SD (n = 21) of the original fluorescence had recovered at mutant synapses, while the recovery was 22 ± 3% SD (n = 23) in wild type synapses (Figure 2.4 C). This result indicates that in the absence of α-syn, fewer recycled receptors are clustered in synaptic sites.

Having shown that AChRs are removed faster from mutant than wild type synapses, next we asked which of the receptor pools [recycled receptors and/or not yet internalized AChRs (pre-existing)] is affected by the absence of α-syn. To address this, AChRs in the sternomastoid muscle of wild type and mutant mice were sequentially labeled with BTX-biotin followed by a single saturating dose of (green) strept-Alexa488 as described by Bruneau et al. (2005). Three days after the initial labeling, the sternomastoid muscle was bathed with Alexa Fluor 594-tagged streptavidin (red) to specifically label recycled AChRs and doubly labeled synapses were immediately imaged (time 0) and re-imaged three days later. The fluorescence intensity of labeled recycled AChRs at wild type and α-syn$^{-/-}$ synapses decreased to 22 ± 6% SD (n = 16) and 15 ± 3% SD (n = 22) of the original fluorescence, respectively ($p < 0.0001$), while the fluorescence intensity of labeled pre-existing AChRs decreased to 59 ± 6% SD (n = 21) in wild type synapses and to 42 ± 8% SD (n = 18) in mutant synapses ($p < 0.0001$) (Figures 2.4 D, E). This result indicates that the stability of both recycled and pre-existing AChRs is affected by the absence of α-syn from synapses.

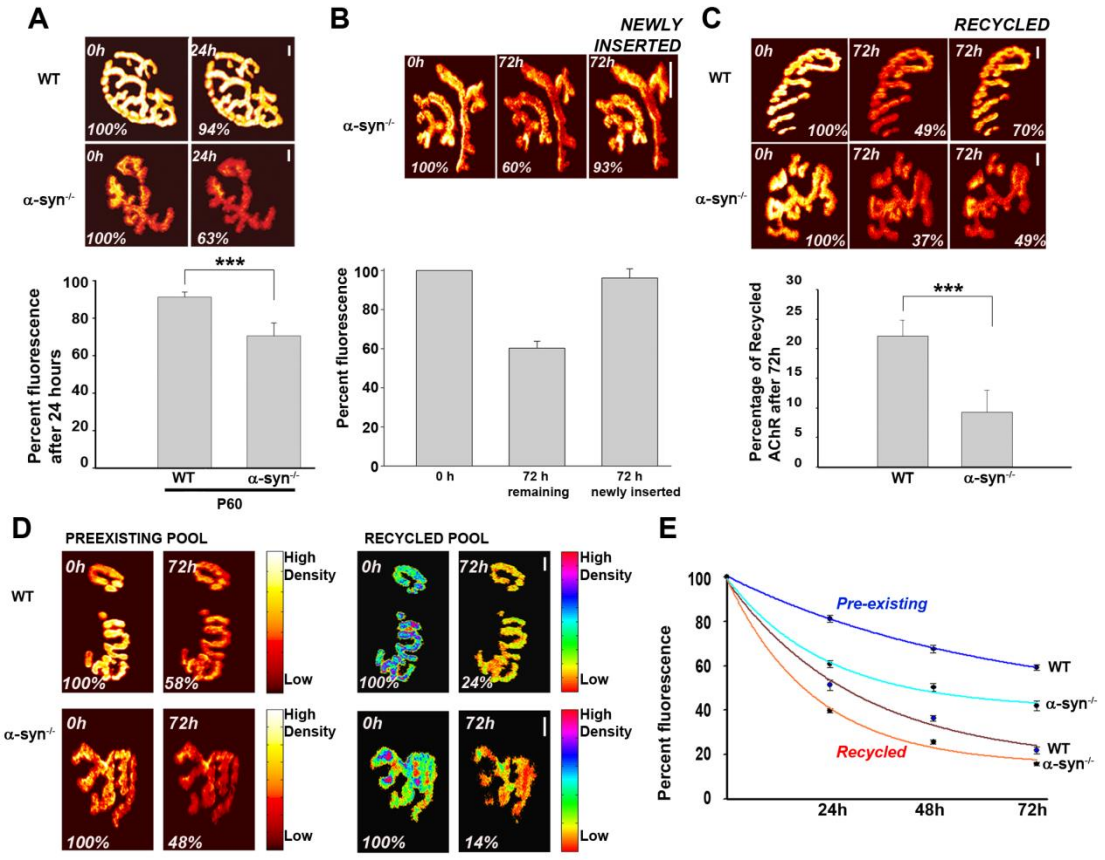

Figure 2.4. Dynamics of AChRs at mature neuromuscular junctions deficient in α-syn. **A)** Adult wild type and mutant mice were injected with a low dose of BTX-Alexa488 in their tails (less than 30% of AChR were labeled, so synapses are still functional), and 24 hours later they were anesthetized and synapses on the sternomastoid muscle were imaged immediately and re-imaged 24 hours later. Example of two views of the same neuromuscular synapses of mutant and wild-type imaged and re-imaged at 0 and 24 hours later. Graph summarizes the data from many synapses using the approach in A. Note that the loss rate of labeled AChRs from mutant synapses was significantly higher than that of wild type synapses. **B**) The sternomastoid muscles of mice deficient in α-syn were labeled with a saturating dose of BTX-Alexa488 and superficial synapses were immediately imaged. Three days later, the same synapses were located, re-imaged and the loss of their fluorescence intensity was measured (72 h remaining). A second saturating dose of BTX-Alexa488 was added to label new AChRs that had been inserted during the 72 h and synapses were imaged again (72 h newly inserted). The total fluorescence intensity was expressed as 100% at the initial labeling and normalized to this on each successive view. Graph summarizes the data from many NMJs. **C)** The sternomastoid muscles of mice deficient in α-syn and wild type mice were labeled with a saturating dose of BTX-biotin followed by a saturating dose of strept-488 and superficial synapses were imaged. The total fluorescence intensity was expressed as 100% at the initial labeling and normalized to this on each successive view. To assess the amount of recycled receptors that had been re-inserted between time 0 and 3 days, strept-488 was then added to the muscle and the same synapses were re-imaged. Graph summarizes the amount of recycled receptors present at synaptic sites, obtained from many junctions. Each bar represents the mean percentage of original fluorescence intensity ± SD. **D**) Absence of α-syn increases the removal rates of pre-existing and recycled AChRs from the same synapse as assayed by loss of fluorescence intensities compared to wild type synapses. The total fluorescence intensity of each AChR pool was normalized to 100% at initial imaging. Pseudo-color images provide a linear representation of the density of AChRs. Scale bars are 10 μm. *** $p < 0.0001$. **E**) Graph shows loss of fluorescently labeled pre-existing and recycled AChRs from several synapses. Note that removal of AChRs from both pools is faster in the absence of α-syn. Each data point represents the mean percentage of original fluorescence intensity ± SD.

We also asked whether a mistargeting of the insertion of receptors into non-synaptic zones could also account for the low number/density of receptors at synaptic sites of mice deficient in α-syn. To test this, the sternomastoid muscles of mutant and wild type mice were labeled with BTX-biotin. Receptors on the muscle surface were isolated with NeutrAvidin-coated beads, and analyzed by western blot using anti-α1-AChR subunit antibody (MAB210). If absence of α-syn specifically impairs the insertion of AChRs into the postsynaptic membrane, the amount of receptors on the surface should be smaller in mutant than wild type and greater in the internal pool of mutant than that of wild type. Conversely, if loss of α-syn mistargets receptors into non-synaptic zones, the amount of receptors on the surface of muscle cells should be comparable to wild type. Western blot analysis of receptors reveals the presence of few receptors in both surface and internal compartments of mutant muscle cells compared to wild type (Figures 2.5 A, B). This result was further confirmed by western blot analysis of total homogenates (membrane and internal fractions) from mutant and wild type muscle cells using rat anti-α1-AChR subunit, showing that the amount of total AChRs is significantly reduced in mutant mice compared to wild-type (Figures 2,5 A, B).

This finding prompted us to test whether the low number of receptor is a consequence of a low level of AChR transcripts. To test this, the mRNA levels of α1-AChR subunit from mutant and wild type were measured by real-time RT-PCR using glyceraldehyde 3-phosphate dehydrogenase as an internal control. We found that AChR mRNA (α1 subunit) expression level was similar between mutants and controls, indicating that loss of α-syn has no effect on receptor gene expression (Figures 2.5 C). These results were further confirmed by immune-fluorescence with antibodies against phospho (Ser10)-acetyl (Lys14)-histone H3 (Figure 2.5 D), which indicated normal activity of subsynaptic nuclei gene expression. Together, these results strongly imply that α-syn is involved in controlling the stability and trafficking of AChRs at multiple points during the secretory process.

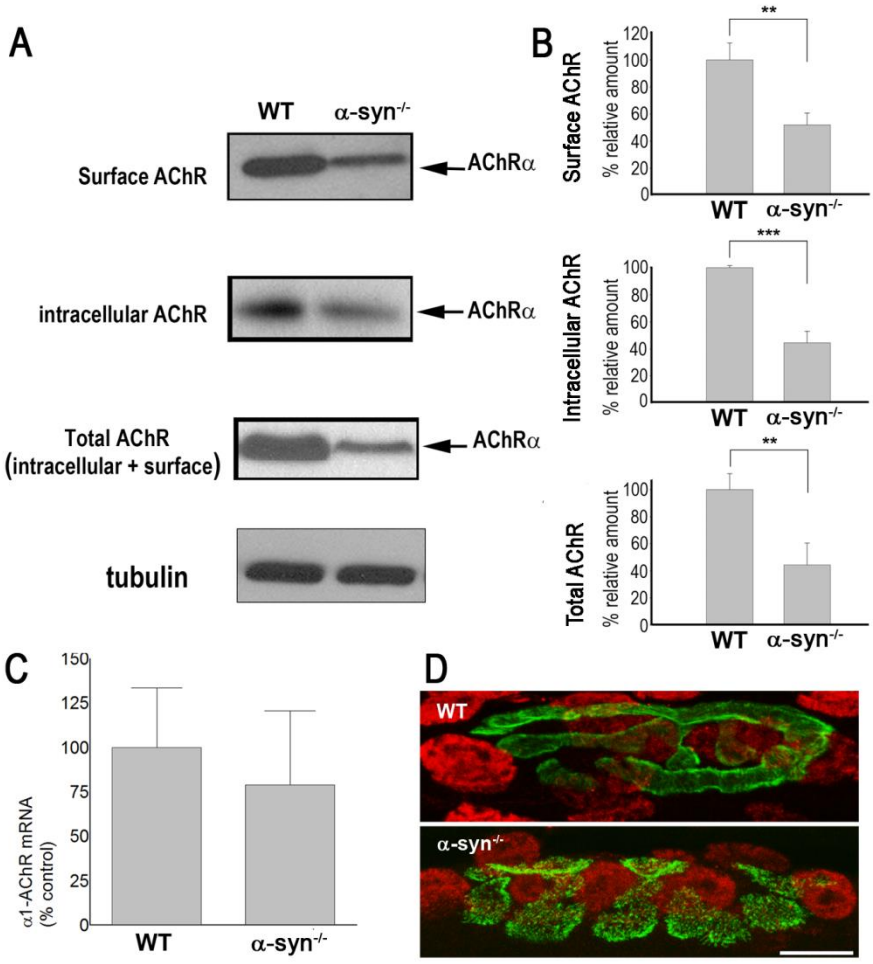

Figure 2.5. Absence of α-syn reduces both surface and internal receptors. **A**) Receptors on the surface of sternomastoid muscles of mutant and wild type mice were saturated with BTX-biotin, pulled down with NeutrAvidin-agarose beads and immunoblotted with anti-α1-AChR subunit. To assess the amount of AChRs in the internal compartment, sternomastoid muscles of mutant and wild type mice were incubated with unlabelled BTX to saturate all surface receptors; then muscle homogenates were incubated with BTX-biotin to bind AChRs in the internal pool, pulled down with NeutrAvidin-agarose beads and probed for α1-AChR subunit. Total amount of AChRs (on the surface and in the internal compartment) was probed by western blotting of homogenates from sternomastoid muscles of mutant and wild type mice. Tubulin was used as a loading control. **B**) Quantitative analysis of the amounts of AChRs on the surface, in the internal pool, and the total of mutant and wild type muscle cells. At least three independent repetitions were performed in each experiment. Data are shown as mean ± SD; n = 5. **C**) Real-time PCR of α1-AChR subunit mRNA expression levels are similar in sternomastoid muscles of wild type (WT) and α-syn$^{-/-}$; error bars are SD with n = 3 mice. **D**) Transcriptional activation is similar in subsynaptic nuclei of wild-type (WT) and α-syntrophin knock-out (α-syn$^{-/-}$) mice. Muscle fibers were stained with Alexa Fluor 488-BTX (green) for the neuromuscular junction and anti-phospho (Ser10)-acetyl (Lys14)-histone H3 (red). Representative images are shown. Scale bar is 10 μm. ** $p < 0.01$; *** $p < 0.001$.

Absence of α-syntrophin sharply reduced AChR-associated scaffold protein levels in muscle cells

Next, we investigated whether loss of α-syn also affects the expression levels of other postsynaptic scaffolding proteins, such as α-dbn and rapsyn. Previous studies have shown that the concentration of α-dbn was reduced at synaptic sites of muscle fibers deficient in α-syn (Adams et al., 2000), but it was not clear whether absence of α-syn leads to a reduction in total amount of α-dbn in the muscle cells and/or a decrease in recruitment of α-dbn to synapses. To examine this, the sternomastoid muscle was removed and muscle homogenates were examined by western blot analysis using antibodies against α-dbn. We found that isoforms of α-dbn1 and 2 expressed by the muscle were reduced. As shown in Figure 2.6, the 89 kDa isoform of α-dbn1 was reduced more than 85% of the control, and the 75 kDa isoform was undetectable. It is worth mentioning that both α-dbn1 isoforms have been shown to be phosphorylated, but the 75 kDa isoform is more heavily phosphorylated, and contains more phosphotyrosine than the 89 kDa isoform in the presence of the tyrosine phosphatase inhibitor, pervanadate (Nawrotzki et al., 1998). This severe reduction is not due to low levels of α-dbn transcript, as qRT-PCR shows that mRNA levels were not affected (Figure 2.6 C). The concentration of α-dbn 2 (non-phosphorylated isoform) was reduced by half (Figures 2.6 A, B). Rapsyn, a scaffolding protein required for AChR aggregation, is also reduced in mutant syntrophin mice. As displayed in Figure 2.6, both western blot and qRT-PCR show that rapsyn was reduced by half compared to wild type (Figure 2.6), indicating that α-syn is involved in controlling rapsyn gene expression (see discussion).

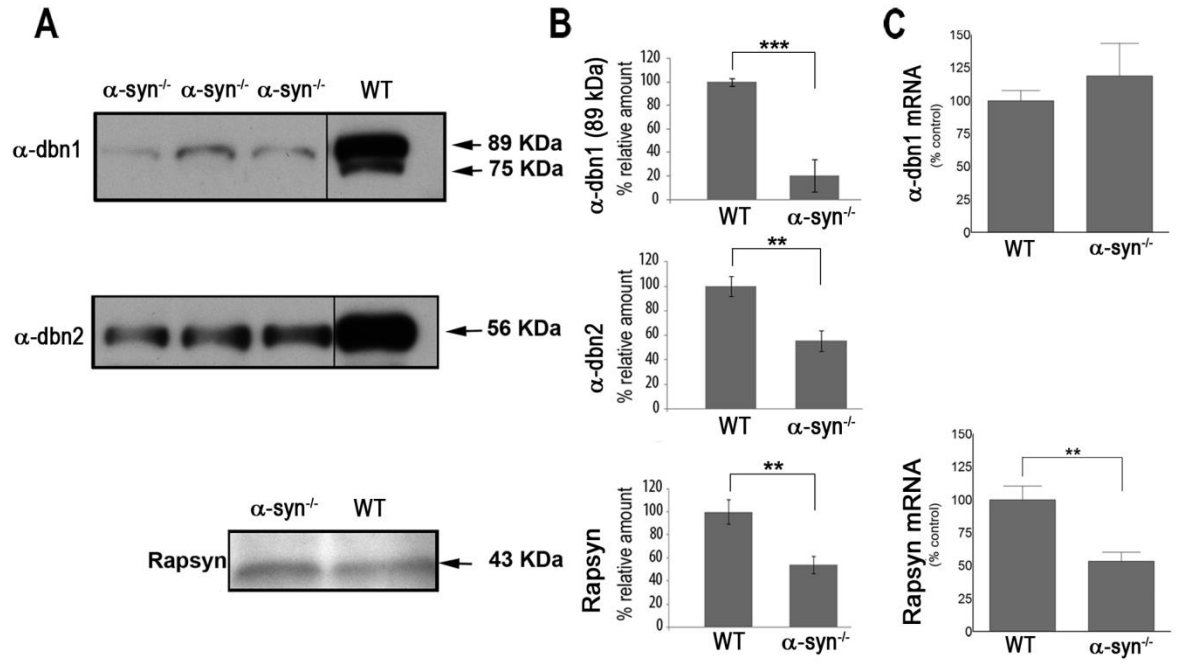

Figure 2.6. Absence of α-syn induces a severe reduction of α-dbn isoforms. Equal amounts (50 µg) of protein form total sternomastoid muscle extracts of α-syn mutant and wild type mice were separated on SDS-polyacrylamide gels, and subjected to immunoblotting with a pan-α-dbn antibody. **A**) Blots show a severe reduction of 89 kDa α-dbn and undetectable 75 kDa α-dbn isoforms in α-syn mutant compared to wild type, whereas 59 kDa α-dbn2 isoform is reduced to about 50% of wild type levels. Rapsyn was reduced to ~50% of wild-type. **B**) Graphs show quantification of western blots. **C**) Graph shows that real-time PCR of α-dbn1 mRNA expression levels are similar in sternomastoid muscles of wild type (WT) and α-syntrophin knockout (α-syn$^{-/-}$), whereas rapsyn mRNA expression level was reduced by half in α-syn knockout compared to wild type. Error bars are SD with n = 3 mice. ** $p < 0.01$; *** $p < 0.001$.

To investigate whether the phenotype of α-syn$^{-/-}$ NMJ might be caused by loss of recruited scaffold proteins, we electroporated GFP-α-dbn1 into the sternomastoid muscle of mice deficient in α-syn. One to two weeks later, mice were perfused, muscles were removed, and AChRs were labeled with fluorescent BTX-Alexa594. As shown in Figure 2.7 A, GFP-α-dbn1 was concentrated at synaptic sites of electroporated deficient muscle cells. High resolution images show that GFP-α-dbn1 constructs partially restored the AChR distribution shape (categories 2 and 3; Figure 2.7 B). The restoration was more pronounced in some synapses than other, most likely depending on the expression level of constructs (Figure 2.7 B). However, we found no significant difference in AChR pattern at synapses expressing

GFP-α-dbn1 or GFP-tyrosine-mutated dystrobrevin isoform (Figure 2.7 A). Conversely, overexpression of rapsyn-GFP alone in α-syn$^{-/-}$ muscle fibers does not restore the normal synaptic phenotype (Figures 2.7 A, B), nor does it change the distribution of AChR in WT synapses (data not shown) (Bruneau and Akaaboune, 2010).

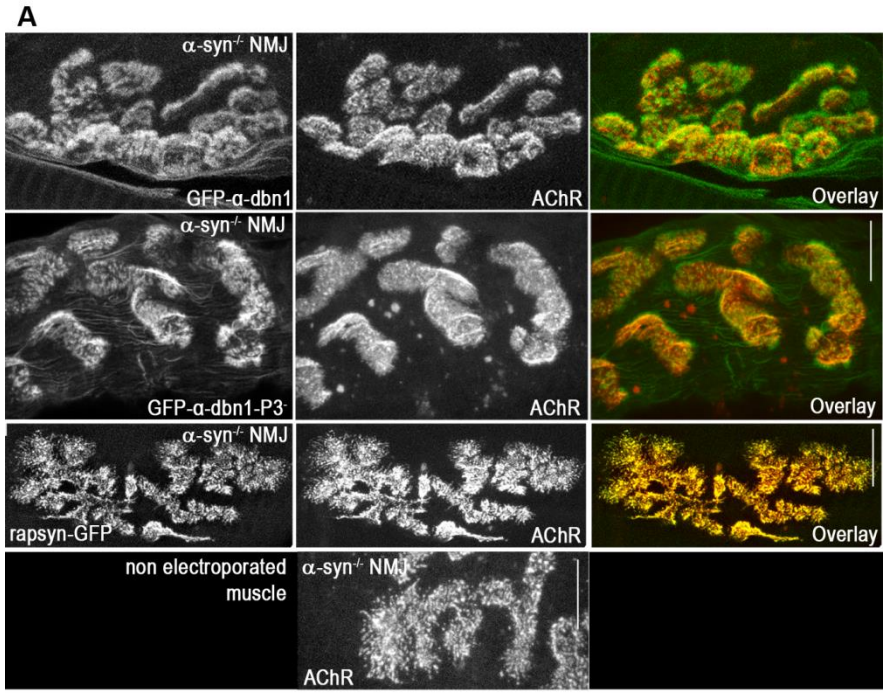

	category (%)				
	1	2	3	4	N
WT	95	5	0	0	19
α-syn$^{-/-}$	0	0	7	93	27
α-syn$^{-/-}$ + GFP-α-dbn1	0	15	33	51	39
α-syn$^{-/-}$ + GFP-α-dbn1-P3^{-}	0	14	32	54	28
α-syn$^{-/-}$ + rapsyn-GFP	0	0	10	90	20

Figure 2.7. Electroporation of α-dbn1 partially rescues the pattern of AChR distribution at α-syn$^{-/-}$ NMJ. **A**) The sternomastoid muscle of adult α-syn null mice was electroporated with GFP-α-dbn1 or GFP-α-dbn1 with three tyrosine phosphorylation sites mutated to phenylalanine (GFP-α-dbn1-P3^{-}). One to two weeks later, the mouse was perfused with 2% formaldehyde, and receptors were labeled with BTX-Alexa594. Neuromuscular synapses on electroporated and non-electroporated muscles were imaged with the confocal microscope. Representative high resolution images show that GFP-constructs are expressed and localized at postsynaptic sites. Expression of either α-dbn1 and α-dbn1-P3^{-} in α-syn$^{-/-}$ muscle partially restored the AChR pattern of distribution. Note that synapses in muscle cells deficient in α-syn electroporated with GFP-α-dbn1 appear to have relatively smooth borders with few patchy clusters of AChR and less extensions of receptor beyond the edge. However, non-electroporated α-syn$^{-/-}$ muscle synapses exhibit hot spots of receptors and fragmented branch borders with many speckles. Rapsyn-GFP was similarly electroporated into adult α-syn knock-out muscles. While rapsyn-GFP is found at postsynaptic sites, rapsyn-GFP does not rescue the synaptic phenotype

in muscle cells deficient in α-syn. **B**) Synapses were categorized according to their AChR distribution, ranging from category 1, showing well defined troughs and synaptic borders, where most WT synapses are found, to 4, with markedly disorganized and patchy AChR distribution and fuzzy synaptic borders, typical of α-syn$^{-/-}$ synapses. Categories 2 and 3 show intermediate phenotypes, as exemplified by the synapses shown. The table shows the frequency distribution (in percentages) for each category per group, as well as the number of synapses analyzed (N). Scale bars are 10 μm.

To analyze in more detail the rescue of α-syn$^{-/-}$ synaptic phenotype by GFP-α-dbn1, we examined first whether expression of GFP-α-dbn1 rescues the density of postsynaptic receptors of α-syn$^{-/-}$ NMJs. To do this, the sternomastoid muscle of mice deficient in α-syn was electroporated with GFP-α-dbn1 and 7 days later, the sternomastoid was bathed with a saturating dose of BTX-Alexa594 to label all receptors. Superficial synapses of electroporated with GFP-α-dbn1 and non-electroporated muscle fibers from the same sternomastoid were imaged and the fluorescence intensity of labeled AChRs was measured. The density of AChRs (expressed as a percentage of the fluorescence present at mature wild type NMJ) at α-syn$^{-/-}$ NMJ over-expressing GFP-α-dbn1 (66 ± 4% of WT synapses, n = 26 NMJs) is 78% higher than the density of AChRs at non electroporated synapses (31 ± 6% SD, n = 20 NMJs), but lower than wild type (Figure 2.8 A). Next, we examined whether over-expression of GFP-α-dbn1 increases the half-life of AChRs at α-syn$^{-/-}$ NMJ. Twenty-four hours after initial imaging, fluorescence intensity of the labeled receptors had decreased 16 ± 3% SD (n = 16 NMJs) in mutant synapses expressing GFP-α-dbn1 [$t_{1/2} \approx 4$ days], compared to 31 ± 5% SD (n = 7 NMJs) in non-electroporated synapses [$t_{1/2} \approx 2$ days] ($p < 0.0001$) and 8 ± 3% SD [$t_{1/2} \approx 9$ days] (n = 9 NMJs) in wild type synapses ($p < 0.0001$) (Figure 2.8 B). Finally, we tested whether the number of recycled receptor has increased in α-syn$^{-/-}$ NMJs expressing GFP-α-dbn1. We found that, three days after initial labeling, 74% more AChRs recycled back into mutant synapses expressing GFP-α-dbn1 (n = 10 NMJs), when compared to non-electroporated fibers (n = 12 NMJs) (Figure 2.8 C). These results indicate that α-dbn1 partially rescued synaptic phenotype including AChR half-life, recycling

and postsynaptic density. Conversely, overexpression of α-syn-GFP into the sternomastoid muscle of mice deficient in α-dbn, which have a similar NMJ phenotype to α-syn$^{-/-}$ NMJ, does not restore the normal synaptic phenotype (Figure 2.8 D), suggesting that the synaptic effects of α-dbn and α-syn are not merely additive. Also, overexpression of α-dbn in wild type synapses does not increase receptor density (data not shown). Not all proteins lost from α-syn null synapses are involved in the increase of the turnover rate of receptor. In mice lacking utrophin, which is highly concentrated at wild type synaptic sites, but lost in the absence of α-syn, the AChR turnover rate is unaffected (data not shown) (Akaaboune et al., 2002).

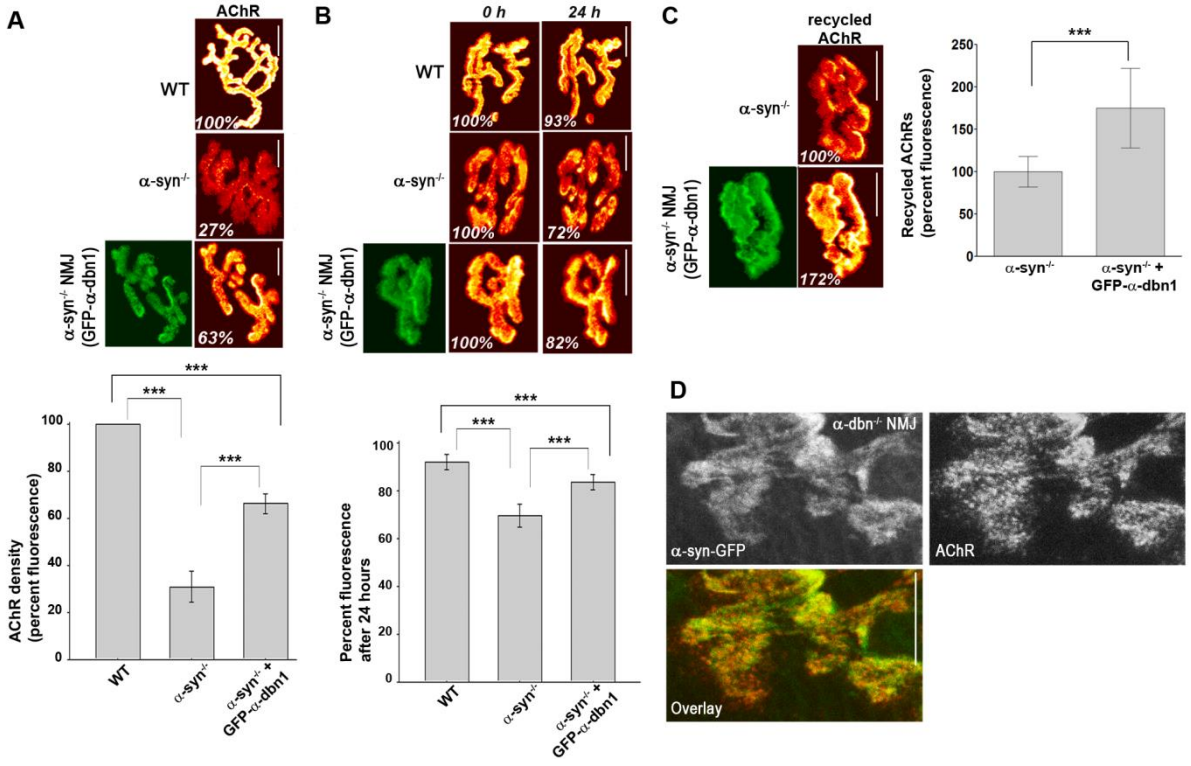

Figure 2.8. Electroporation of α-dbn1 partially rescues the density, stability and recycling of AChRs at expressing α-syn$^{-/-}$ NMJs. **A**) The sternomastoid muscle of adult α-syn null mice was electroporated with GFP-α-dbn1. One week later, AChRs were labeled with a saturating dose of BTX-Alexa594 and superficial synapses, with or without GFP-α-dbn1, from the same sternomastoid muscle were imaged. Fluorescence intensity was measured and normalized to wild type (WT) synapses. Total fluorescence was normalized to WT synapses. Graph summarizes the data from many synapses. **B**) One week after electroporation of GFP-α-dbn1, AChRs were labeled with BTX-Alexa594, and superficial synapses, with or without GFP-α-dbn1, from the same sternomastoid muscle were imaged immediately (time 0) and re-imaged 24 h later. Note that there are more remaining fluorescently tagged AChRs in synapses electroporated with GFP-α-dbn than in non electroporated synapses, though comparably less than WT

NMJs. Graph summarizes the data from many synapses. **C)** Sternomastoid muscles from α-syn$^{-/-}$ mice were electroporated with GFP-α-dbn1. One week later, surface AChRs were labeled with BTX-biotin, followed by a saturating dose of unlabeled streptavidin, then bathed with strept-Alexa594 to label the AChRs recycled for 3 days. Graph summarizes the data from many synapses. Each bar represents the mean percentage of fluorescence intensity ± SD. *** $p < 0.0001$. **D**) The sternomastoid muscle of adult α-dbn null mice was electroporated with α-syn-GFP, AChRs were labeled with BTX-Alexa594, and imaged with a confocal microscope. Note that α-syn-GFP does not rescue the α-dbn$^{-/-}$ synaptic phenotype. Scale bars are 10 μm.

Discussion

The importance of the DGC in muscle integrity is well established. However, little is known about the role of this complex in the molecular dynamics of receptors at postsynaptic sites *in vivo*. In this study, we examined the mechanisms by which absence of α-syn leads to fewer receptors at mature synaptic sites and whether α-syn is required for synaptic development. The main results are as follows: (1) absence of α-syn dramatically destabilizes AChRs at mature synapses; (2) the AChR recycling pathway is impaired in the absence of α-syn; (3) postsynaptic defects coincide with an abnormal shift in turnover rate of AChR in developing synapses; (4) in the absence of α-syn, there is a dramatic reduction in the total amount of AChRs, rapsyn, and α-dbn in muscle cells; (5) AChR transcript levels are not affected by lack of α-syn; and (6) electroporation of fused GFP-α-adn1 into muscle fibers deficient in α-syn restores to some extent the phenotype of the NMJ. Taken together, these results establish a role for α-syn in the maintenance and stability of AChRs *in vivo*.

Previous studies have shown that NMJs of α-syn$^{-/-}$ muscle contain few receptors, raising the possibility that α-syn may be critical for the maintenance of receptor density and stability. The present work provides direct evidence for this idea by showing that synapses lacking α-syn have a significantly increased turnover rate of AChRs and drastically reduced density of AChRs both in developing and mature synapses. This high turnover is not a consequence of muscular dystrophy, since no sign of muscular dystrophy is seen in muscle fibers (Adams et al., 2000).

α-syntrophin is a component of the DGC which is present in both the troughs and the crests of the junctional folds (Kramarcy and Sealock, 2000), and links signaling proteins to the DGC (Brenman et al., 1996; Gee et al., 1998). However, no direct link between α-syn and AChR has been reported so far, raising the question of how α-syn might control the density/number and stability of receptors at the crest of the postjunctional folds. It is possible that absence of α-syn from the complex may change the conformation of the DGC and its association with other postsynaptic components, leading to instability of the complex as a whole, which in turn may affect the stability and/or tethering of AChRs into the postsynaptic membrane. At NMJs deficient in α-syn, several components of the DGC are either reduced or completely lost (Adams et al., 2000). For example, the total amount of α-dbn in muscle (Figure 2.6) is reduced, and utrophin and nNOS are completely lost from synaptic sites (Adams et al., 2000). From our studies, it appears that absence of α-syn has no effect on the gene expression of α-dbn, since we see no difference in α-dbn transcript levels between α-syn null and wild type animals. This raises the question of how loss of α-syn might control the stability and trafficking of α-dbn from the ER into the cell surface. This issue warrants further investigation, particularly with regard to signaling processes associated with the DGC, such as those involving nNOS.

The absence of utrophin from α-syn$^{-/-}$ NMJ is likely not responsible for the rapid turnover rates of AChR at α-syn$^{-/-}$ NMJ. The turnover rate of AChR was no faster in utrophin null than in control mice (Akaaboune et al., 2002). Interestingly, however, in α-adbn$^{-/-}$ synapses, which bear few receptors and have a higher turnover rate of AChRs (Grady et al., 2000; Akaaboune et al., 2002), α-syn appears to be unaltered and remains highly concentrated at the NMJ (Grady et al., 1999). Thus, it is conceivable that accelerated turnover rate of receptors in the α-syn mutant may be secondary to the dramatic reduction of α-dbn at the NMJ and muscle cells. Due to the fact that full length phosphorylated α-dbn isoforms are

severely reduced in α-syn mutants, that α-syn$^{-/-}$ and α-dbn$^{-/-}$ NMJ have similar phenotypes, and that α-dbn isoforms are able to rescue α-dbn mutant synapses (Grady et al., 2003), it is plausible that the NMJ phenotype and receptor stability in α-syn$^{-/-}$ are controlled by α-dbn alone or synergistically with other factors. If the α-syn$^{-/-}$ NMJ phenotype is caused by α-dbn reduction, then we expect at least some sign of muscular dystrophy. However, α-syn$^{-/-}$ mice do not exhibit any sign of muscular dystrophy. Perhaps the presence of α-dbn2, which is less reduced (Figure 2.5), may be sufficient to prevent muscular dystrophy in these mutant mice. Consistent with this, previous results have shown that transgenic expression of either α-dbn2 or 1 isoforms in α-dbn$^{-/-}$ mice, in which muscular dystrophy was observed (Grady et al., 1999), is sufficient to rescue the dystrophic phenotype (Grady et al., 2003).

Our present data argue that the α-syn$^{-/-}$ NMJ phenotype results, at least in part, from α-dbn reduction, since electroporation of exogenous of α-dbn restores synaptic distribution of AChR to some extent. In contrast to α-dbn$^{-/-}$ NMJs, in which overexpression of phosphorylatable α-dbn1 is able to fully rescue the synaptic phenotype, phosphorylated and non-tyrosine-phosphorylated α-dbn1 isoforms partially rescue the syn$^{-/-}$ NMJ phenotype in the same way, possibly because α-syn is required for the tethering and/or the signaling pathway of α-dbn phosphorylation.

Deficiencies in certain DGC components do not cause defects in NMJ (Duclos et al., 1998; Hack et al., 1998). Interestingly, only components that control localization of nNOS at NMJ are involved in the maintenance of the NMJ structure and mice deficient in components that induce removal of nNOS from synapses exhibit structural defects of NMJ similar to those observed in nNOS null mice (Shiao et al., 2004). This suggests that nNOS may be the common factor that contributes to defects in NMJ of missing DGC molecules. nNOS is lost from synapses deficient in α-syn and α-dbn, which raises the possibility that nNOS along with α-dbn may be involved in the stability of receptors at the postsynaptic sites. Indeed,

expression of a nNOS transgene can partially rescue NMJ phenotype in α-syn$^{-/-}$ extensor digitorum longus and quadriceps muscles (Shiao et al., 2004).

Results presented here show that loss of α-syn induces abnormal AChR distribution and a decrease in AChR density and stability as early as postnatal day 7. α-syntrophin is expressed at the postsynaptic membrane at birth (Kramarcy and Sealock, 2000), but its absence from synapses has no effect on receptor distribution or stability before P6, suggesting that α-syn is not required for the early steps of synapse maturation. While the mechanism by which α-syn may induce abnormal patterning of AChRs after P7 is not known, it is possible that such events might be triggered by loss of α-dbn, nNOS and/or other proteins. In support of this, α-dbn$^{-/-}$ mice show a decrease in AChR density and abnormal patterning of AChR distribution as early as 7 days postnatal (Grady et al., 2000). Thus, it is conceivable that a partial loss of α-dbn in the α-syn mutant may initiate AChR instability during synaptic development, leading to a decline in the density of AChRs as development proceeds.

One interesting finding of the current study is that the contribution of receptor recycling to total receptors present at α-syn$^{-/-}$ NMJs was very low compared to mature wild type NMJs, where a significant number of recycled AChRs contribute to the steady-state of the postsynaptic receptor density (Bruneau et al., 2005). This raises the question of how α-syn may regulate the trafficking and degradation of internalized AChR. Previous studies have shown that α-dbn interacts with several cytoskeletal proteins, including the cargo-binding domain of the kinesin heavy chain (Ceccarini et al., 2005) and intermediate filaments (Mizuno et al., 2001; Newey et al., 2001). Kinesin motor proteins and other cytoskeleton elements have been found to be involved in the trafficking and delivery of receptors to synaptic sites (Setou et al., 2002). Thus, alteration in AChR recycling may involve α-dbn, since this later is dramatically reduced in α-syn mice.

Here we show that loss of α-syn is also associated with a reduction in rapsyn concentration, a 43-kDa protein that is critical for receptor clustering (Gautam et al., 1995). Conversely, AChR are necessary for the clustering of rapsyn in both mammals and fish (Ono et al., 2001, 2004; Bruneau et al., 2008). A threshold density of AChR likely provides a critical signal that enables proteins of the DGC and intracellular scaffold to remain aggregated. However, it is possible that α-syn reduces the levels of rapsyn, which then controls receptor number and density. Consistent with this, previous reports showed that rapsyn and receptors are trafficked in the same intracellular vesicle from the ER to cell surface (Marchand et al., 2002). However, in our experiments, overexpression of rapsyn-GFP was unable to restore the α-syn$^{-/-}$ synaptic phenotype. While the mechanism by which absence of α-syn leads to instability of AChRs remains largely unknown, the present study implies that the effect of α-syn on AChR is in part mediated by α-dbn1. Understanding how DGC components are involved in regulating the postsynaptic receptor number/density at the NMJ will be the focus of future study.

Chapter III

PKC and PKA regulate AChR dynamics at the neuromuscular junction of living mice

Previously published in Plos ONE (Plos ONE. 2013 Nov;8(11):e81311)

Isabel Martinez-Pena y Valenzuela, Marcelo Pires-Oliveira and Mohammed Akaaboune (I assisted I. M-P. V. in the analysis of imaging data and helped draft the manuscript)

Abstract

The steady state of the acetylcholine receptor (AChR) density at the neuromuscular junction (NMJ) is critical for efficient and reliable synaptic transmission. However, little is known about signaling molecules involved in regulating the equilibrium between the removal and insertion of AChRs that establishes a stable postsynaptic receptor density over time. In this work, we tested the effect of activities of two serine/threonine kinases, PKC and PKA, on the removal rate of AChRs from and the re-insertion rate of internalized recycled AChRs into synaptic sites of innervated and denervated NMJs of living mice. Using an in vivo time-lapse imaging approach and various pharmacological agents, we showed that PKC and PKA activities have antagonistic effects on the removal and recycling of AChRs. Inhibition of PKC activity or activation of PKA largely prevents the removal of pre-existing AChRs and promotes the recycling of internalized AChRs into the postsynaptic membrane. In contrast, stimulation of PKC or inactivation of PKA significantly accelerates the removal of postsynaptic AChRs and depresses AChR recycling. These results indicate that a balance

between PKA and PKC activities may be critical for the maintenance of the postsynaptic receptor density.

Introduction

The maintenance of a high density of nicotinic acetylcholine receptors (AChRs) at the postsynaptic membrane of a neuromuscular junction (NMJ) is essential for the effectiveness of synaptic impulse transmission. This high concentration of AChRs is established by rates of removal, re-insertion of recycled, insertion of newly synthesized and lateral diffusion of AChRs (Bruneau and Akaaboune, 2006; Bruneau et al., 2009; Pires-Oliveira et al., 2013). Several mechanisms have been implicated in the regulation of these rates, including synaptic activity, neural factors and receptor-associated scaffold proteins (Akaaboune et al., 1999, 2002; Grady et al., 2003; Bruneau et al., 2009; Bruneau and Akaaboune, 2010; Martinez-Pena y Valenzuela et al., 2010, 2011; Pires-Oliveira et al., 2013). Several studies have also reported that serine/threonine kinases PKC and PKA activities are implicated in the clustering and stability of AChRs in cultured muscle (Miles and Huganir, 1988; Nimnual et al., 1998; Lanuza et al., 2000, 2002, 2006; Nelson et al., 2003). However, it remains unknown at which steps of AChR trafficking PKC and PKA are involved.

PKA and PKC have been extensively studied in many cell types, including muscle cells. Predominantly, two isoforms of PKC are found to be expressed in skeletal muscle cells: conventional (c)PKCα (Nakano et al., 1992), mainly localized in the cytosol and sarcolemma, and novel (n)PKCθ, mostly localized postsynaptically at the NMJ (Ohno et al., 1991; Nishizuka, 1992; Johannes et al., 1994; Newton, 2001). The skeletal muscle also abundantly expresses cAMP-dependent PKA, whose Rα-isoform is enriched in the NMJ region (Perkins et al., 2001).

In the present work, we explored the role of the serine/threonine kinases PKC and PKA on AChR dynamics in living mice, particularly on the removal of AChRs from and the re-insertion of recycled AChRs into the postsynaptic membrane. We found that PKC and PKA have antagonistic effects on the removal of pre-existing receptors and the recycling of AChRs into the postsynaptic membrane. These results suggest that a tight balance between PKC and PKA activities is crucial for the stability of the postsynaptic receptor density.

Materials and Methods

Receptor pools labeling and neuromuscular junction imaging in living mice

This study was carried out according to the recommendations in the NIH Guide for the Care and Use of Laboratory Animals. The protocol was approved by the University Committee on the Use and Care of Animals of the University of Michigan (protocol number 3939). Non-Swiss Albino adult female mice (6–10 weeks old, 25–30 g) were anesthetized with an intraperitoneal injection of a mixture of 80 mg/kg ketamine and 20 mg/kg xylazine and the sternomastoid muscle was exposed, labeled, and the whole animal was placed on its back on the stage of a customized epifluorescence microscope as described previously (Lichtman et al., 1987; Balice-Gordon and Lichtman, 1993; Turney et al., 1996; Bruneau and Akaaboune, 2006). Superficial neuromuscular junctions were imaged with a water-immersion objective (x20 UApo 0.8 NA Olympus BW51; Optical Analysis Corp.)

The recycled receptor pool was identified using a method of labeling that allows one to selectively label recycled receptors, as described in our previous work in detail (Bruneau et al., 2005; Bruneau and Akaaboune, 2006). Briefly, receptors on the sternomastoid muscle were labeled with biotinylated bungarotoxin (BTX-biotin) (5 μg/ml, 30 min; Invitrogen) followed by a single saturating dose of streptavidin-Alexa Fluor 488 (strept-Alexa488; green; 10 μg/ml, 3 h; Invitrogen). A second color of (red) streptavidin Alexa-594 (10 μg/ml, 10–

30 min) was then added to the sternomastoid muscle to be sure that all biotin sites are saturated. Four days later (after initial labeling, to allow more internalization of AChRs and formation of a sizeable pool), the mouse was anaesthetized and the recycled AChR pool on the sternomastoid muscle was specifically labeled with strept-Alexa 594 (10 µg/ml, 1 h) (receptors that had lost their streptavidin tag and were re-inserted in the synapses with their BTX-biotin tag). Superficial synapses were then imaged and re-imaged at the end of the experiment and their fluorescence intensities were measured. Experiments showing that the dissociation of streptavidin from biotin does not occur on the surface of the muscle cells but instead inside the muscle fiber were worked out in our previously published work (Bruneau et al., 2005; Bruneau and Akaaboune, 2006; Martinez-Pena y Valenzuela et al., 2010).

Pharmacological treatment

To test the effect of PKC on the removal of pre-existing AChRs form the postsynaptic membrane and the insertion of internalized recycled AChRs into synaptic sites, several experiments were performed. In the first series of experiments, the sternomastoid muscle was bathed with calphostin C (5 µM; Sigma), a potent, selective light-activated inhibitor for PKC isolated from the fungus *Cladosporium cladosporioides* (Iida et al., 1989; Kobayashi et al., 1989; Bruns et al., 1991). Staurosporine (100 nM; Sigma), an agent that blocks a broad spectrum of kinases depending on the concentration was also used to block PKC. In a second series of experiments, we used phorbol-12-myristate-13-acetate (PMA), (200 nM; Sigma) (Bursztajn et al., 1988), a pharmacological agent that stimulates PKC.

Stimulation of PKA was performed by using the membrane-permeant and metabolically resistant agonist 8-bromoadenosine-3’-5’-cyclic monophosphorothioate, Sp-8-

Br-cAMP, (1 mM; BIOLOG) (Pacheco et al., 2003). Inhibition of PKA activity was performed by using H89 (5 μM; Sigma) (Blazev et al., 2001).

Muscle denervation

Adult mice were anaesthetized, the sternomastoid was exposed and the nerve was excised by removing a 5 mm piece to prevent a possible re-innervation. Four days after denervation, the sternomastoid muscled was bathed with BTX-biotin followed by a saturating dose of streptavidin (strept-Alexa488). Three days after the initial labeling, the mouse was reanesthetized and the sternomastoid muscle was bathed with strept-Alexa594 (to label recycled nAChRs), and superficial synapses were imaged. PKC and PKA activators and inhibitors were used and the pre-existing receptor removal rate and recycled pool number were measured after 7 hours of drug treatments.

Quantitative fluorescence imaging

Quantitative fluorescence imaging was used to measure the fluorescence intensity of labeled receptor pools (Turney et al., 1996; Akaaboune et al., 1999; Martinez-Pena y Valenzuela et al., 2010). Briefly, images were calibrated to a non-fading reference standard to compensate for spatial and temporal changes in the light source and camera between imaging sessions at different time points. The same fluorescent ligands were repetitively imaged and as long as we verified that the image pixel intensity was not saturated, it was possible to get an accurate quantitative measurement of the relative number of nAChRs. Images were analyzed with algorithms for IPLAB (Scanalytics) and Matlab (The Mathworks). Background fluorescence was determined by manual selection of a boundary region around the each NMJ

and subtracting it from the original image, and the mean of the total fluorescence intensity (which corresponds to receptor density) was measured (Turney et al., 1996).

Results

Effect of PKC on stability of AChR pools at the NMJ *in vivo*

Previous studies have reported that PKC is involved in the stability of AChRs (Wallace, 1988; Lanuza et al., 2000, 2006, 2010; Nelson et al., 2003). In this work, we wanted to know which steps of AChR trafficking are regulated by PKC activity at the mature NMJs of living mice. To address this, we first tested whether activation or inhibition of PKC has any effect on the removal of AChRs from postsynaptic sites. To examine this, AChRs on the sternomastoid muscle were labeled with a non-saturating dose of biotinylated α-bungarotoxin (BTX-biotin) followed by (green) streptavidin-Alexa Fluor488 (strept-Alexa488) to saturate all biotin sites (see Methods). Four days later, the sternomastoid muscle was exposed and superficial synapses were imaged (time 0) (Figure 3.1 A). The sternomastoid was bathed with PKC inhibitor, calphostin C, continuously for 7 hours and the same synapses were then re-imaged. The loss of fluorescence intensity from NMJs was assayed and compared with untreated synapses. In muscles treated with calphostin C, fluorescence intensity of pre-existing AChRs (not yet internalized) decreased by only 4% (96 ± 6% of original fluorescence; n = 33 NMJs, 3 mice), compared to untreated muscles ($p < 0.001$), where the fluorescence intensity decreased by 12% (88 ± 5% of original fluorescence; n = 19 NMJs, 3 mice) (Figure 3.1 B, C). In contrast, in muscles treated with PKC activator, phorbol-12-myristate-13-acetate (PMA), a widely used PKC activator (Wallace, 1988; Nishizuka, 1992), pre-existing AChRs fluorescence decreased significantly to 82 ± 9% (n = 39 NMJs, 5 mice), compared to untreated muscles ($p < 0.05$). (Figure 3.1 B, C).

Next, we asked whether PKC also affects the normal rate of recycling of previously internalized AChRs into the postsynaptic membrane. To this end, AChRs on the sternomastoid muscle were sequentially labeled with BTX-biotin, followed by a saturating dose of strept-Alexa488, as described in our previous work (Bruneau et al., 2005; Bruneau and Akaaboune, 2006). Four days later, recycled receptors were specifically labeled by adding (red) streptavidin-Alexa594 (strept-Alexa594) to the sternomastoid muscle (strept-Alexa594 binds to receptors that have lost their initial strept-Alexa488 tag while retaining BTX-biotin) (Bruneau et al., 2005). Superficial synapses were imaged immediately (time 0), and the sternomastoid muscle was then bathed with calphostin C, a highly specific PKC blocker, to inhibit PKC (Kobayashi et al., 1989; Bruns et al., 1991) for the duration of the experiment (7 hours). At the end of the experiment, a second dose of strept-Alexa594 was added to label recycled receptors that had been inserted during the treatment of muscles and the same synapses were imaged for a second time (Figure 3.1 D). The fluorescence intensity of labeled recycled AChRs was measured before and after treatment. Quantification of recycled AChRs shows that after 7 hours of calphostin C treatment, the fluorescence intensity increased to 114 ± 8% (n = 57 NMJs, 7 mice) of their original fluorescence at time 0 (normalized at 100%) compared to untreated synapses where fluorescence remains unchanged, as previously described by Bruneau et al. (Bruneau et al., 2005) (102 ± 3%, n = 15 NMJs, $p < 0.001$, 3 mice) (Figure 3.1 E, F). As a second test of PKC inhibition, we used staurosporine (100 nM), a moderately potent PKC blocker, and found that the re-insertion of recycled AChRs at synaptic sites after 7 hours of treatment was also increased, albeit slightly less than with calphostin C (fluorescence intensity of recycled receptors was 106 ± 5% (n = 17 NMJs, 4 mice) versus untreated synapses, 99 ± 3% (n = 21 NMJs, 4 mice, $p < 0.001$).

The observation that PKC inhibition promotes the recycling of AChRs into synaptic sites prompted us to examine whether activation of PKC would depress the recycling of

AChR. AChRs were labeled as described above, and four days later, the sternomastoid muscle was treated with PMA, and 7 hours after treatment, recycled receptors that had been inserted during the treatment of muscles were assessed. Quantification of fluorescently labeled recycled AChRs shows that the density of recycled receptors in muscles treated with PKC activator was significantly decreased (91 ± 7% of original fluorescence; n = 31 NMJs, 5 mice) when compared to untreated synapses (102 ± 3% of original fluorescence; n = 15 NMJs, 3 mice) (Figure 3.1 E, F).

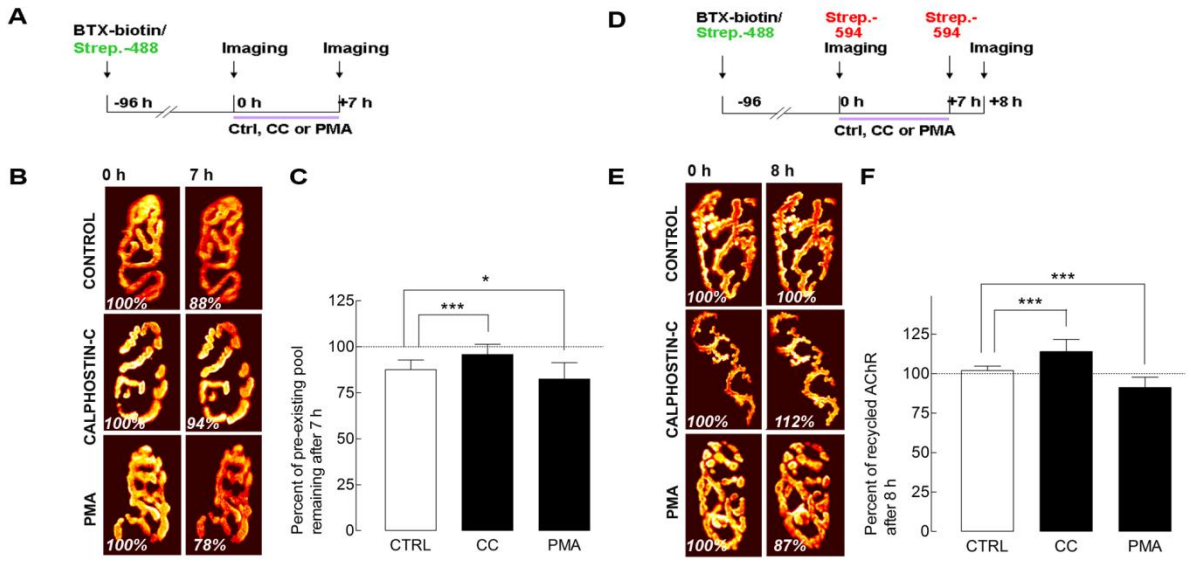

Figure 3.1. PKC activation accelerates the removal of receptors from synaptic sites *in vivo.* **A**) Labeling protocol for assessing the removal of preexisting AChRs from the postsynaptic membrane. Sternomastoid muscles were labeled with biotinylated α-bungarotoxin (BTX-biotin)/Alexa Fluor 488-streptavidin (strept-Alexa488; green). Four days later, superficial synapses were then imaged (time 0) and the sternomastoid muscles were bathed with or without PKC pharmacological agents for 7 h. At the end of the experiment, the same synapses were then imaged. **B**) Examples of control, and neuromuscular junctions treated with PKC inhibitor calphostin C (CC) and PKC activator phorbol-12-myristate-13-acetate (PMA), that were imaged at time 0 and 7 h later. The total fluorescence intensity of labeled preexisting AChRs was expressed as 100% at the time 0 and 7 hours later. Pseudo-color images provide a linear representation of the density of AChRs. Note that PKC inhibition with CC largely prevents the removal of preexisting AChRs while PKC activation accelerates their loss from postsynaptic membrane. **C**) Histogram summarizes the amount of preexisting receptors present at synaptic sites, obtained from many junctions by the approach shown in B. Each bar represents the mean percentage of original fluorescence intensity ± SD. **D**) Labeling method to analyze the insertion of recycled AChRs into the postsynaptic membrane. Sternomastoid muscles were labeled with BTX-biotin/strept-Alexa488; green. Four days later, muscles were bathed again with a saturating dose of strept-Alexa594, red, to selectively label the recycled receptors that had lost their initial strept-Alexa488 tag, while retaining BTX-biotin during the process of internalization and reinsertion.

Superficial synapses were then imaged (time 0) and the sternomastoid muscles were bathed with PKC activators and inhibitors. At the end of the experiment, a second saturating dose of strept-Alexa594 was added to label receptors that have been recycled during the treatment. **E**) Example of control, and neuromuscular junctions treated with PKC inhibitor calphostin C (CC) and PKC activator PMA, that were imaged at time 0 and 8 h later. The total fluorescence intensity of labeled recycled AChRs was expressed as 100% at the time 0 and the fluorescence intensity 8 h later was compared with the fluorescence intensity of the synapse at the previous view. Note that PKC inhibition with CC increases the fluorescence intensity of recycled AChRs while PKC activation with PMA decreases their recycling. **F**) Histogram summarizes the amount of recycled receptors present at synaptic sites, obtained from many junctions by the approach shown in D. Each bar represents the mean percentage of original fluorescence intensity ± SD. *, $p < 0.05$; ***, $p < 0.001$.

Given the involvement of PKC activity on AChR recycling, we asked whether the increase of the recycled pool is due to an enhanced stability of recycled receptors in the membrane and/or to the promotion of the insertion of new recycled receptors. To distinguish between these two possibilities, AChRs on the sternomastoid muscles were labeled with BTX-biotin/strept-Alexa488 and four days later, the sternomastoid muscle was exposed and bathed with strept-Alexa594 to specifically label AChRs that had recycled after the initial labeling, and then the superficial synapses were imaged. The muscles were then treated with either PKC inhibitor calphostin C or PKC activator PMA for 7 hours; the same synapses were re-imaged, and their fluorescence intensity was measured. The muscles were bathed again with a second dose of strept-Alexa594, and the same synapses were imaged for a third time (Figure 3.2 A). Quantification of recycled AChR loss treated with calphostin C showed that the loss of fluorescence was largely prevented, as only 8% of labeled AChR was lost (92 ± 5% of original fluorescence; n = 9 NMJs, 3 mice) (Figure 3.2 D, E), compared to 19% in non-treated muscles ($p < 0.05$; 81 ± 3% of original fluorescence; n = 11 NMJs, 3 mice) (Figure 3.2 B, C). At the same synapses, the number of recycled receptors that had been inserted during the treatment was about 19% (111% – 92%) of the original fluorescence (up to 111 ± 7%; n = 9 NMJs, 3 mice) (Figure 3.2 D, E), similar ($p > 0.05$) to the 17% (98% – 81%) increase in control NMJs (up to 98 ± 2%; 11 NMJs, 3 mice) (Figure 3.2 B, C). In

contrast, when muscles were treated with PKC activator PMA, the loss of recycled AChR was significantly increased ($p < 0.001$) to 34% of the original fluorescence ($66 \pm 6\%$; $n = 8$ NMJs, 3 mice) (Figure 3.2 F, G), compared to 19% in non-treated muscles. When the number of receptors recycled during the treatment was assessed, it was 17% (83% – 66%) of the original fluorescent pool (up to $83 \pm 11\%$; $n = 8$ NMJs, 3 mice), not significantly different ($p > 0.05$) from the 17% (98% – 81%) in non-treated muscles. These results suggest that PKC regulates the AChR recycled pool by reducing the half-life of recycled receptors in the postsynaptic membrane.

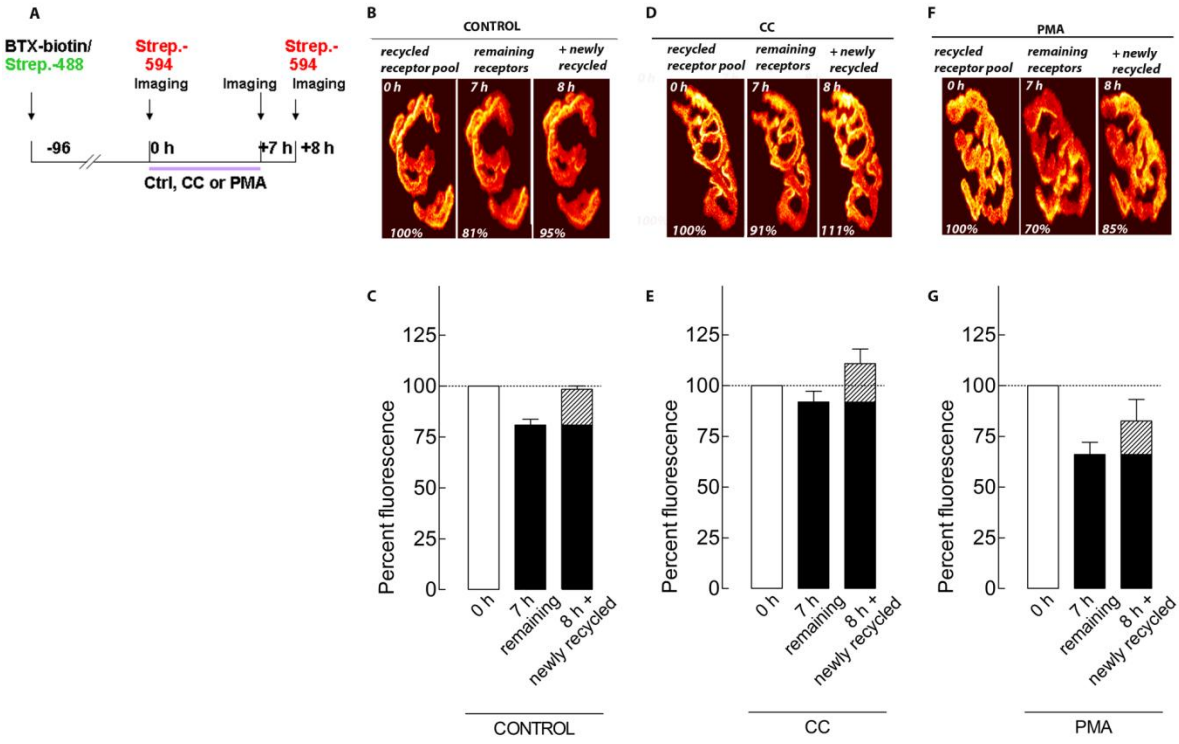

Figure 3.2. Activation of PKC accelerates the removal of recycled AChRs from the postsynaptic membrane *in vivo.* **A**) Labeling protocol of receptors as described above. Superficial synapses were imaged (time 0) and the sternomastoid muscles were treated with PKC inhibitors or activators for 7 h. At the end of the treatments, the same superficial synapses were imaged again to assess the loss of fluorescence from the first view (7 h). To test whether the loss of recycled matches the re-insertion of newly recycled receptors, the sternomastoid muscles were incubated with the same new fresh strept-Alexa594; (red) to selectively label the receptors that recycled during those 7 h. **B**, **D**, **F**) Examples of NMJs that were imaged immediately (time 0; recycled receptor pool), after 7 h of incubation with vehicle (**B**; control), calphostin C (**D**; CC), or phorbol-12-myristate-13-acetate (**F**; PMA), and then re-imaged after labeling of recycled receptors that were inserted during 7 h of treatment (newly

recycled). **C**, **E**, **G**) Graphs summarizing data obtained from many synapses treated with vehicle (**C**; control), calphostin C (**E**; CC), phorbol ester (**G**; PMA) with the approach shown in B, D and F. Each bar represents the mean percentage of original fluorescence intensity ± SD.

PKA activity antagonizes the effect of PKC on stability of AChR pools

PKA activity has been previously shown to enhance the stability of AChRs (Shyng et al., 1991; Nelson et al., 2003); here, we sought to examine whether PKA activity has a similar effect on AChR dynamics at the NMJ of adult living mice. In particular, we investigated the effect of PKA on AChR removal and recycling. First, we examined the effect of PKA activity on the removal of pre-existing AChRs. AChRs on the sternomastoid muscle were labeled as described above and PKA activity was inhibited with the highly specific blocker H89 (Lee and Linstedt, 2000; Dong et al., 2013). Quantification of the fluorescence intensity of pre-existing AChRs showed significant loss after 7 h (to 77 ± 9% of original fluorescence; n = 21 NMJs, 3 mice), compared to 88 ± 5% in non-treated muscles (n = 21 NMJs, 3 mice, $p < 0.001$). However, when PKA was stimulated with the metabolically stable activator of cAMP-dependent protein kinases, Sp-8-Br-cAMPS, receptor loss was minor (to 97 ± 7% of fluorescence remained; n = 23 NMJs, 3 mice, $p < 0.001$) (Figure 3.3 A, B).

Next, we evaluated whether PKA also affects AChR recycling. Quantification of recycled AChRs that had been inserted during treatment for 7 h with H89 showed that fluorescence decreased to 82 ± 11% (n = 59 NMJs, 6 mice) of the original value, compared to untreated synapses (98 ± 3%, n = 27 NMJs 4 mice, $p < 0.001$) (Figure 3.3 C, D). In contrast, when sternomastoid muscles were treated with Sp-8-Br-cAMPS, the fluorescence intensity of recycled receptors increased to 114 ± 12% (n = 55 NMJs, 6 mice) of their original fluorescence ($p < 0.001$ versus untreated synapses) (Figure 3.3 C, D).

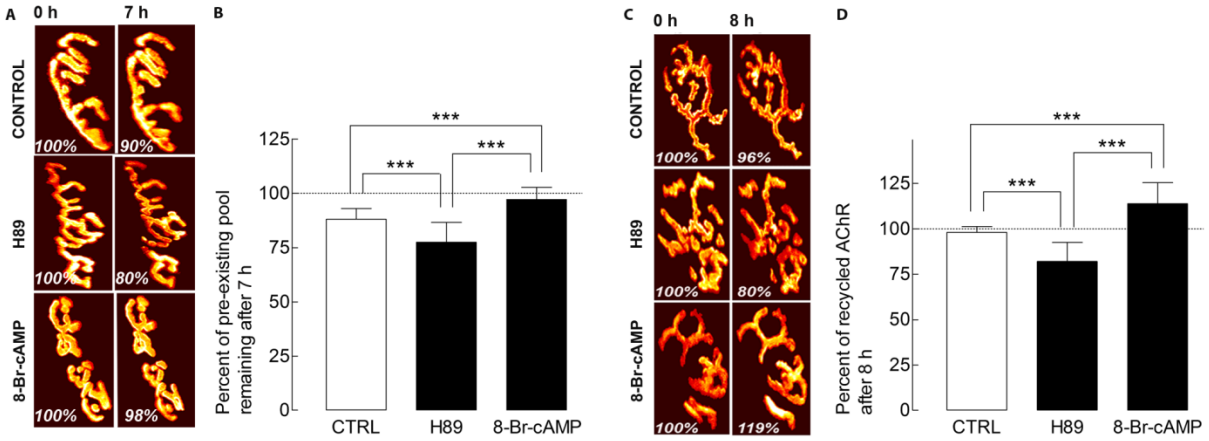

Figure 3.3. Stimulation of PKA increases the stability of AChRs at NMJ *in vivo.* Sternomastoid muscles were labeled as described above (Figure 3.1). **A**) Examples of two views of the same NMJ before and after treatment with PKA inhibitor and activator. Note that the loss of labeled preexisting receptors was largely prevented in muscles treated with PKA activator 8-Br-cAMP and was significantly accelerated in synapses treated with PKA inhibitor H89 compared to control synapses. **B**) Graph showing pre-existing receptors (retaining their strept-Alexa488 after initial labeling) from the same synapses as assessed in A. Each bar represents the mean percentage of original fluorescence intensity ± SD. ***, $p < 0.001$. **C**) Examples of recycled AChRs from control and NMJs incubated with PKA inhibitor H89 and PKA activator 8-Br-cAMP that were imaged at time 0 and 8 h later. **D**) Histogram summarizes the amount of recycled receptors present at synaptic sites, obtained from many junctions by the approach shown in A. Each bar represents the mean percentage of original fluorescence intensity ± SD. ***, $p < 0.001$.

To investigate whether PKA regulates the insertion of newly recycled receptors or their stability in synaptic sites, we measured the loss and insertion of recycled receptors during treatments with PKA inhibitors and activators. Inhibition of PKA with H89 accelerated the loss of recycled AChR, as 33% of the original fluorescence was lost (67 ± 9%; 10 NMJs, 3 mice), when compared ($p < 0.01$) to 19% in control synapses. The insertion of recycled receptors was 16% (84% – 67%) of the original labeled pool (up to 84 ± 8%; 10 NMJs, 3 mice) (Figure 3.4 C, D), which was not significantly lower than 17% (98% – 81%) in control muscles ($p > 0.05$) (Figure 3.4 A, B). When PKA was activated with Sp-8-Br-cAMPs, loss of recycled AChR was only 9% of the original fluorescence (91 ± 9%; 17 NMJs, 4 mice) (Figure 3.4 E, F), reduced from 19% in control NMJs ($p < 0.001$). Insertion of

newly recycled receptors was 22% (113% – 91%) of the original labeled pool (up to 113 ± 6%; 17 NMJs, 4 mice), but not significantly higher than the 17% in control NMJs.

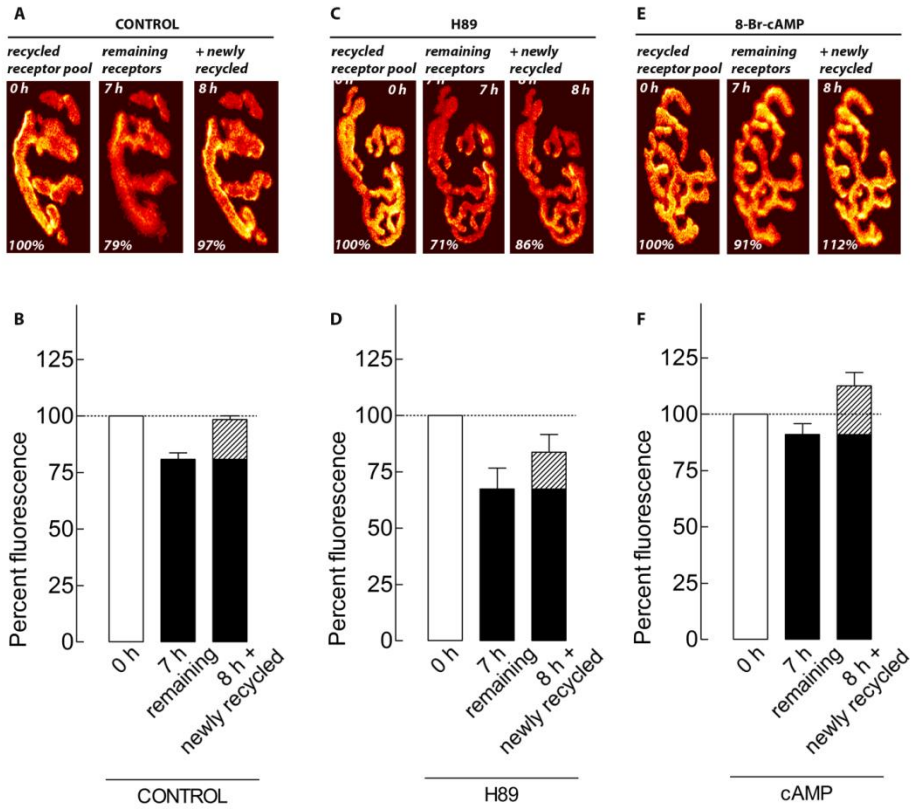

Figure 3.4. Activation of PKA prevents largely the removal of recycled AChRs at NMJ from postsynaptic membrane *in vivo.* Sternomastoid muscles were labeled with BTX-biotin/strept-Alexa488; green and 4 days later were bathed again with a saturating dose of strept-Alexa594; red as described above (Figure 3.2). The muscles were then treated with vehicle, PKA inhibitor (H89), PKA activator cAMP, for 7 h. the loss and insertion of recycled AChRs during treatment was assessed. **A**, **C**, **E**) Examples of NMJs that were imaged immediately (time 0; recycled receptor pool), after 7 h of incubation with vehicle (**A**; control), inhibitor (**C**; H89) or 8-Br-cAMP (**E**; cAMP) and then re-imaged after labeling of recycled receptors that were inserted during 7 h of treatment (newly recycled). **B**, **D**, **F**) Graphs summarizing data obtained from many synapses treated with vehicle (**B**; control), PKA inhibitor (**D**; H89), 8-Br-cAMP (**F**; cAMP) with the approach shown in A, C and E. Each bar represents the mean percentage of original fluorescence intensity ± SD.

PKC and PKA regulate removal of AChRs from synaptic sites and AChR recycling through a similar pathway

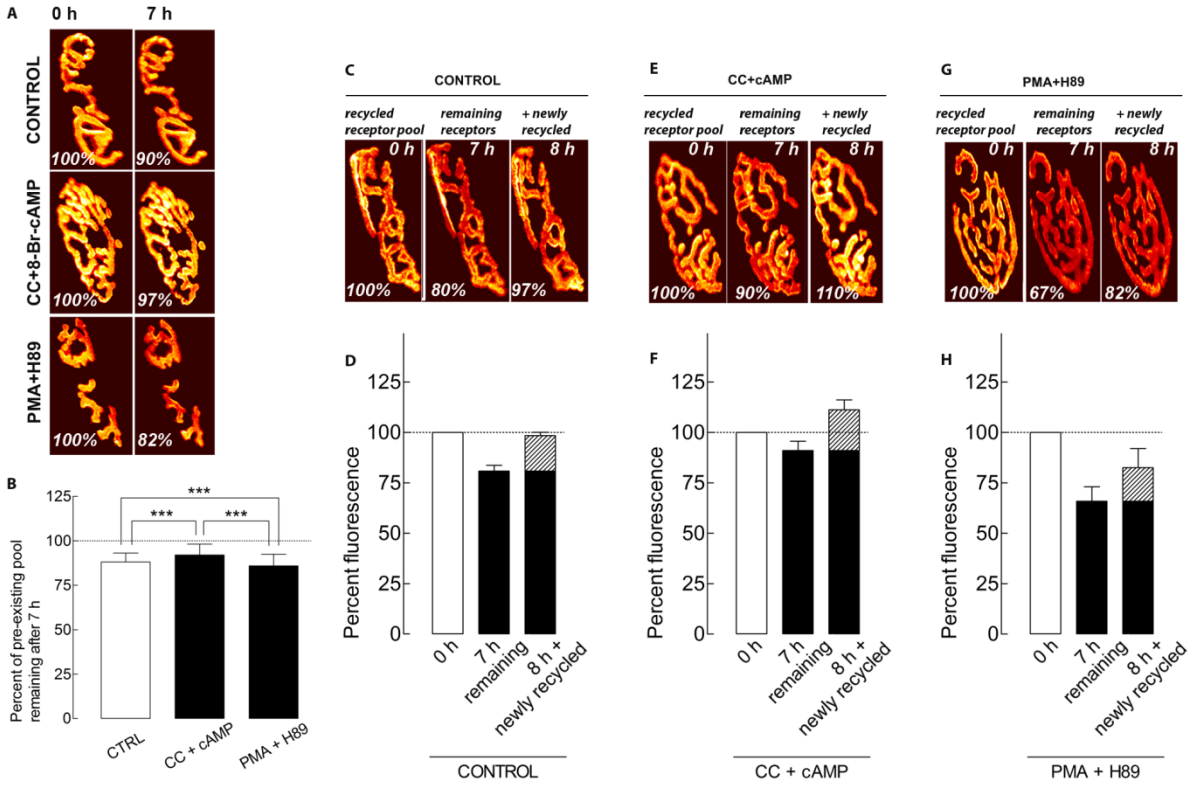

Figure 3.5. PKC inhibition and PKA activation do not act synergistically on the stability of receptors. **A**, Examples of two views of the same labeled pre-existing AChRs (AChRs that are not yet internalized) before (time 0) and after treatment (7 h later) with both PKC inhibitor CC and PKA activator 8-Br-cAMP, or PKC activator PMA and PKA inhibitor H89. Note that PKC inhibition in combination with PKA activation significantly decreased the removal of labeled preexisting AChRs compared to non-treated synapses but no more than one single treatment (Figures 3.1 and 3.3). Simultaneous PKC activation and PKA inhibition treatment accelerate the removal of preexisting AChRs, but comparable to one single treatment (Figures 3.1 and 3.3). **B**, Histogram summarizes the amount of preexisting receptors present at synaptic sites, obtained from many junctions by the approach shown in A. Each bar represents the mean percentage of original fluorescence intensity ± SD. ***, $p < 0.001$. **C**, **E**, **G**, Examples of NMJs (**C**; control, **E**; CC + cAMP, **G**; PMA+H89), showing that the loss of labeled recycled pool is also affected by PKC and PKA treatment. Note that the loss of recycled AChRs after 7 hours is prevented in the CC+cAMP treatment, but is increased in the PMA+H89 treatment, though the results are similar to each treatment alone (Figures 3.1 and 3.3). **D**, **F**, **H**, Graphs summarizing data obtained from many synapses with the approach shown in C, E and G.

Next, we asked whether PKC and PKA activities have a synergistic effect on AChR removal and recycling. We first examined the effect of a PKC inhibitor and a PKA stimulator on the removal of AChRs from the same synapses. In muscles treated concomitantly with

calphostin C and Sp-8-Br-cAMP, the fluorescently labeled pre-existing AChRs decreased by 8% (92 ± 6% of the original fluorescence; n = 15 NMJs, 4 mice) (Figures 3.5 A, B), similar ($p > 0.05$) to either treatment alone, suggesting no additive effects of the agents used on AChR removal. In the second set of experiments, muscles were treated with both the PKC activator PMA, and PKA inhibitor H89. When both were used in combination, the loss of AChRs was 14% (86 ± 7% of the original fluorescence; 8 NMJs, 3 mice) (Figures 3.5 A, B), which was not different ($p > 0.05$) from either treatment alone. We also investigated the combined effect of PKC and PKA on AChR recycling. Treatment with calphostin C and cAMP did not further reduce removal of recycled AChR (91 ± 5%, 13 NMJs, 3 mice) nor increase insertion (20%; 111% – 91%) (Figures 3.5 E, F) beyond any treatment alone (up to 111 ± 5%; 14 NMJs, 3 mice). Similarly, when both PMA and H89 were added together, removal of recycled AChR (68 ± 9%, 9 NMJs, 3 mice) or their insertion (16%, up to 84 ± 9%; 9 NMJs, 3 mice) (Figures 3.5 G, H) were affected similarly as when the treatments were isolated.

Effect of PKC and PKA activities on AChR dynamics in denervated synapses

Previous studies have shown that in denervated muscles the loss of receptors is accelerated and only few internalized AChRs were able to recycle back into the synaptic original sites (Bruneau and Akaaboune, 2006; Martinez-Pena y Valenzuela et al., 2010). Here we asked whether PKC or PKA activity could prolong the metabolic stability of receptors in the postsynaptic membrane and promote the recycling of internalized ones. Receptors on denervated sternomastoid muscles (four days after nerve section) were labeled with BTX-biotin followed by strept-Alexa488 and three days later (seven days after denervation), the sternomastoid muscle was exposed and superficial synapses were imaged, and muscles were

bathed with either PKC inhibitor calphostin C or PKA activator Sp-8-Br-cAMPS (both agents have been shown to largely prevent the removal of AChRs from innervated synapses, see Figures 3.1 and 3.3) for the duration of the experiment. Seven hours after treatment, the same synapses were re-imaged and changes in fluorescence intensities of labeled AChRs before and after treatment were assessed. In muscles treated with calphostin C, the loss of fluorescence intensity of pre-existing AChRs was only 8% of the original fluorescence (92 ± 7%, n = 18 NMJs, 3 mice, $p < 0.001$) compared to 29% of receptor loss in non-treated denervated synapses (71 ± 9%; n = 22 NMJs, 3 mice, $p < 0.001$). Similar results were obtained when denervated muscles were treated with PKA activator Sp-8-Br-cAMP, the loss was 14% of the original fluorescence; 86 ± 8%; n = 22 NMJs, 3 mice, $p < 0.001$ compared to non-treated denervated synapses) (Figures 3.6 A, B).

Given that PKC inhibition and PKA activation were able to promote AChR recycling, we asked whether these treatments could rescue AChRs from degradation and promote their recycling into denervated NMJs. To test this, denervated sternomastoid muscle (four days after nerve section) was labeled as described above and three days later, recycled AChRs that had been inserted after the initial labeling were imaged. In muscles treated with calphostin C, the fluorescence intensity of recycled receptors at the NMJs increased to 100 ± 7% (n = 30 NMJs, 3 mice) compared to untreated denervated synapses 86 ± 8% (n = 26 NMJs, 3 mice, $p < 0.001$) after 7 h. Similarly, treatment of muscles with PKA activator Sp-8-Br-cAMPS increased the number of recycled AChRs to 101 ± 17% of original fluorescence (n = 23 NMJs, 3 mice, $p < 0.001$ compared to non-treated denervated, 86 ± 8%) (Figures 3.6 C, D).

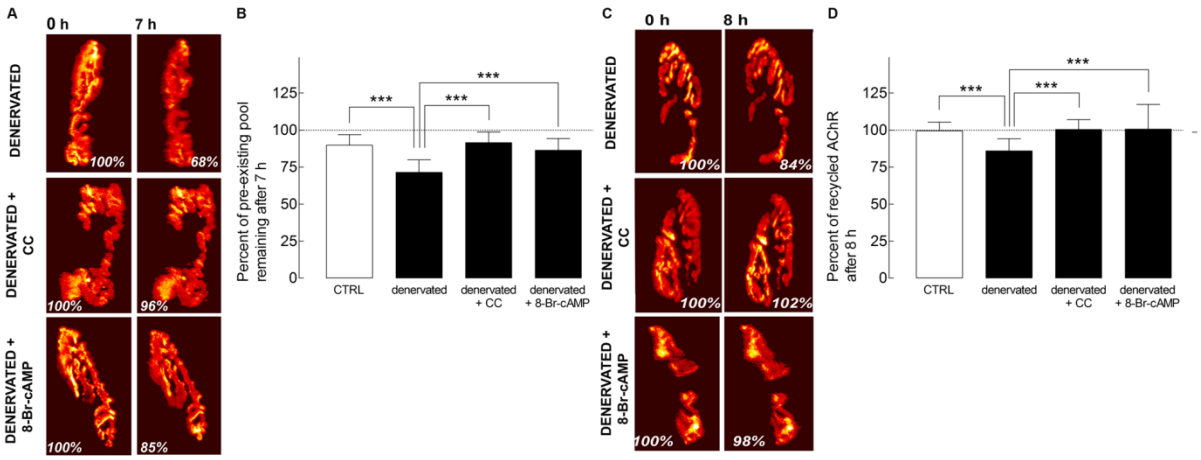

Figure 3.6. PKC inhibition and PKA activation restore recycled AChRs at denervated synapses. Denervated sternomastoid muscles (four days after denervation) were labeled with BTX-biotin/strept-Alexa488 and 3 days later, superficial synapses were then imaged (time 0) and the sternomastoid muscles were bathed with PKC inhibitor calphostin C or PKC activator phorbol-12-myristate-13-acetate (PMA) for 7 h. At the end of the experiment, the same synapses were then imaged. **A**, Example of denervated NMJs, non-treated or treated with CC and 8-Br-cAMP, imaged at time 0 and 7 h later. Fluorescence intensity of both treated denervated synapses increased compared to untreated denervated NMJs. **B**, Histogram summarizing the fluorescence measurements obtained from many NMJs by the approach shown in A. Each bar represents the mean percentage of original fluorescence intensity ± SD. ***, $p < 0.001$. **C**, Examples of recycled AChRs from the same denervated synapses as assessed by the change in fluorescence over the 7 h period of the experiments. Fluorescence intensity of labeled recycled receptors from denervated synapses was less than CC or 8-Br-cAMP treated denervated synapses. **D**, Graph showing the fluorescence measurements of recycled receptors obtained from many synapses by the approach shown in C. Each bar represents the mean percentage of original fluorescence intensity ± SD. ***, $p < 0.001$.

Discussion

In this work, we show that the serine/threonine kinases PKA and PKC have antagonistic effects on the removal of pre-existing AChRs and the size of the recycled pool of AChRs at mature innervated and denervated neuromuscular junctions. Particularly, we show that inhibition of PKC or stimulation of PKA promotes the recycling of internalized AChR into synaptic sites and the anchoring of receptors at the postsynaptic membrane, while stimulation of PKC or inhibition of PKA depresses the recycling of AChR and accelerates the removal rate of receptors from the postsynaptic membrane. Furthermore, we show that inhibition of PKC and stimulation of PKA have no synergistic effects on AChR dynamics.

The present experiments show that both PKA and PKC kinase activities are linked to the trafficking and stability of AChRs. However, it is difficult to determine whether this process is a direct consequence of receptor phosphorylation or an indirect effect induced by phosphorylation of other proteins by PKA and PKC (effector molecules involved in internalization or proper delivery, for example). Previous studies have shown that all AChR subunits are subject to phosphorylation by different kinases. For instance, α and δ subunits are phosphorylated by PKC, δ and γ/ε are phosphorylated by PKA (Changeux et al., 1984; Huganir et al., 1984). Thus, it is tempting to speculate that phosphorylation of AChR subunits can either promote or alter the trafficking and metabolic stability of AChR. For instance, when cultured myotubes were treated with PKC activators, receptor clusters failed to form in response to agrin, the insertion of new receptors in the membrane was impaired, and the disassembly of preexisting AChR clusters was enhanced (Ross et al., 1988; Wallace, 1988; Lanuza et al., 2000; Li et al., 2001). Similarly, when PKC was overexpressed in muscle cells, the stability of receptors was reduced (Miles and Wagner, 2003). Conversely, inhibition of PKC activity (either by pharmacological agents or by genetic manipulations) enhanced the stability of receptor clusters in cultured myotubes and in living mice. Notably, in mice deficient in PKCθ isoform, the disassembly of receptor clusters (redistribution and dispersion), which normally occurs during the early stage of postnatal development, was delayed (Lanuza et al., 2010). The phosphorylation of δ subunit in this mutant mouse is reduced (Lanuza et al., 2006), suggesting that the loss of PKC activity enhances the stability of receptors (at least through the phosphorylation state of δ subunit). It is possible that, in mature synapses, changes in the phosphorylation state of δ subunit by manipulations of PKC may have an effect on the fate of internalized AChRs (either degradation or recycling) and those anchored in the postsynaptic membrane (they remain stable or disassemble).

The current work shows that not only is PKC involved in receptor stability, but also PKA. Stimulation of PKA promotes both the recycling and stability of AChRs. Consistent with these observations, previous studies have reported that PKA stabilizes the receptors on the surface of cultured myotubes (Nelson et al., 2003) and in cultured explants denervated diaphragms from mouse (Shyng et al., 1991). It is conceivable that phosphorylation of ε (Miles and Huganir, 1988) or δ subunits (sites that are different from PKC phosphorylation sites) by PKA may stabilize the clustering of AChRs. It is also plausible that phosphorylation of scaffold proteins by PKA or other kinases may play a critical role in the stability of AChRs. Along these lines, it was reported that the loss of tyrosine phosphorylation of α-dystrobrevin reduces the stability of agrin-induced AChRs in cultured myotubes and in mice deficient in neuregulin receptors (*erb2/4*$^{-/-}$) (Schmidt et al., 2011). Recently, it was suggested that PKA is also involved in the recycling of AChRs through its interaction with myosin Va, and in the stability of AChRs in the postsynaptic membrane through its anchoring by rapsyn (Röder et al., 2010; Choi et al., 2012). It is also possible that phosphorylation of other effector molecules by PKA may play an important role in the sorting and proper delivery of AChRs to the plasma membrane. In the central nervous system, PKA activity has also been found to regulate AMPAR trafficking and insertion as its inhibition reduces AMPAR insertion and synaptic strength (Ehlers, 2000). While it appears that the phosphorylation of receptors, receptor associated-scaffold proteins, and/or effector molecules by PKC and PKA are instrumental for the stability of AChRs, further studies are warranted to investigate when and how antagonistic effects of PKA and PKC are linked to receptor stability and trafficking.

Finally, our findings suggest that PKA and PKC do not have synergistic effects on the removal of AChRs from or recycling into the postsynaptic membrane (Figure 3.5). This implies that these kinases might act to regulate receptor removal and recycling through a similar, overlapping pathway. In the present work, our quantitative fluorescence assay is not

sensitive enough to test the effect of PKC and/or PKA on the synthesis of new AChRs over the short time window of our experiments. Since the detection of the pool of newly synthesized receptors requires that all pre-existing AChRs be completely saturated with α-bungarotoxin (and these synapses are then non-functional), insertion of new AChRs is heavily depressed (Akaaboune et al., 1999).

Based on this and on previously published work, it appears that PKC and PKA act on a pathway distinct from CamKII, since when muscles were treated with KN93 (an inhibitor that blocks CamKII activity), PKC activator PMA and PKA inhibitor H89, the loss of AChRs from the synaptic membrane was increased significantly compared to PMA and H89 alone. While the mechanism by which these kinases activity control AChR removal and recycling is not known, it is possible that these kinases act on different receptor subunits and/or substrate proteins involved in anchoring and/or clustering receptors at synapses. Of note, all of these kinases are found to be concentrated at the postsynaptic membrane of the NMJ with different localizations; most notably, muscle specific CaMKII βm is precisely co-localized with receptors at the crests of the junctional folds (Martinez-Pena y Valenzuela et al., 2010). Thus, it is conceivable that a spatial cellular compartmentalization of kinases in the postsynaptic density may play an important role in the trafficking and stability of receptors. Overall, the current work and other studies suggest that a balance between kinases (phosphorylation by PKC, PKA or CamKII) is important in controlling the molecular dynamics of AChRs at mature neuromuscular synapses.

Chapter IV

Conclusion

In this work, we explored different aspects of the regulation of nAChR dynamics in the NMJ, focusing on the role of α-syn, a member of the nAChR-associated DGC, and serine-threonine kinases PKC and PKA. Interest in studying the function of the cytosolic dystrophin-associated protein α-syn began in the early 2000s, when it was shown that mice deficient in α-syn have severely reduced numbers of nAChRs. This was somewhat puzzling, as α-syn does not interact directly with nAChRs. This clearly pointed at an indirect, regulatory role for this protein on receptor clustering. Our data elucidate the crucial role of α-syn in controlling the rate of internalization and recycling of nAChRs in developing and mature synapses.

We showed that synapses form normally in the absence of α-syn, but mature aberrantly and lag behind in nAChR density even in adulthood. This is likely because nAChR are removed more promptly from the postsynaptic membrane, while recycling is heavily inhibited. Interestingly, our results also suggest that the role of α-syn is mediated by an associated protein, α-dbn1, since α-syn$^{-/-}$ muscle is severely depleted of α-dbn, and α-dbn overexpression attenuates the deficiencies of the mutant NMJ. Meanwhile, in α-dbn$^{-/-}$ muscle fibers, the expression of α-syn is unaffected, despite severe NMJ defects (Grady et al., 1999). This seems to point at α-dbn as the crucial component for the maintenance of postsynaptic nAChR density. α-dbn, much like α-syn, is a cytosolic dystrophin-associated protein whose loss leads to increased removal of nAChRs from synaptic sites.

Since proper function of α-dbn1 requires intact tyrosine phosphorylation sites (Grady et al., 2003), it is possible that α-dbn is a point of convergence for kinases and other signaling mechanisms that regulate nAChR dynamics. The mechanisms regulating α-dbn phosphorylation and the kinases involved are poorly understood, but PKA itself can also phosphorylate α-dbn (Ceccarini et al., 2007). Further experiments are required to investigate if the effects of the PKA/PKC modulation of nAChR dynamics (see Chapter III) depend on α-dbn phosphorylation, and what other kinases and signaling pathways converge directly ot indirectly on α-dbn regulation. Also, it remains unknown how α-dbn can modulate nAChR dynamics; further investigation of its interactions, especially with signaling molecules or cytoskeletal components, are therefore warranted.

Among these partners, dysbindin was initially identified as a dystrobrevin-binding protein in skeletal muscle and other tissues (Benson et al., 2001). Its encoding locus, DTNBP1, was later identified as a susceptibility locus for schizophrenia (Straub et al., 2002). Since dysbindin has been implicated in endosome-lysosome trafficking (Di Pietro et al., 2006; Gokhale et al., 2012), it is tempting to speculate that it is a possible candidate member of the elusive molecular machinery involved in sorting nAChRs to degradation or recycling in the skeletal muscle fiber. In fact, Orozco et al. (2014) showed recently that in mice deficient in dysbindin, LTP is enhanced, consistent with mis-trafficking of AMPA glutamate receptors for recycling. While no dramatic NMJ phenotypes are reported in dysbindin-deficient sandy mice (Li et al., 2003a), it is possible that this deficiency is either too small for a detectable effect in the NMJ or that there are altered nAChR density and recycling in these synapses, even while their overall anatomy is preserved. Therefore, the role of dysbindin on the regulation of nAChRs in the NMJ and the functional consequences of its association to α-dbn remain to be investigated.

In the second part of this work, we looked to other signaling pathways that regulate nAChR density. We showed that PKC and PKA activities balance each other, regulating removal and recycling of AChRs. While PKC inhibits recycling and increases removal, PKA has the opposite, nAChR stabilizing effect. Since PKA and PKC had long been known to regulate nAChR in vitro, it was presumed that they would have a role in the development and initial clustering of nAChRs at the NMJ. This assumption was confirmed by developmental in vivo studies. For the first time, however, we show a crucial role for PKA and PKC in the modulation of nAChR density at the adult NMJ. In fact, activation of PKA or inhibition of PKC were sufficient to counteract the loss of receptors induced by short-term denervation (Figure 3.6). This opens new avenues for therapeutic interventions to attenuate postsynaptic degeneration in myasthenic syndromes and traumatic transient denervations. Further work is required to clarify the targets of PKA and PKC phosphorylation that regulate nAChR dynamics. These kinases could regulate nAChR trafficking in three different ways: a) direct phosphorylation of nAChRs on different sites; b) phosphorylation of receptor-associated scaffold proteins and/or c) phosphorylation of cytosolic signaling proteins. At this point, mostly because the nAChR internalization and recycling machineries are still unknown (see Chapter I), the possible targets of PKA and PKC at the NMJ remain to be investigated.

A caveat that must be considered in the interpretation of all our results is the reliance on BTX as a marker for nAChRs. BTX has been used for several decades to study nAChR dynamics (Changeux et al., 1970; Axelrod et al., 1976; Akaaboune et al., 1999; Bruneau et al., 2005; Martinez-Pena y Valenzuela et al., 2011), but it also silences the receptors that are being monitored. At this point, we cannot discard the possibility that BTX-tagged receptors internalize and/or recycle at a different rate from the non-labeled pool, even when a small percentage of receptors is blocked and neuromuscular junction activity is intact (Akaaboune et al., 1999; Bruneau et al., 2005). To circumvent this issue, one should think about

developing new approaches to investigate nAChR dynamics without using antagonists that block receptor activity. Some promising future developments might include introduction of nAChR subunits with non-antagonistic exogenous binding sites for labels or receptor subunits tagged with photoactivatable fluorescent proteins, either expressed *in vitro* or in genetically modified animals.

In sum, we show that the density of nAChRs at the NMJ is tightly regulated by the receptor-associated proteins of the DGC, as well as serine-threonine kinases PKA and PKC. Therefore, receptor density can be finely tuned to several extracellular cues, such as nerve-released factors and electromechanical activity. Our work adds new insights into our understanding of the signaling network regulating synaptic receptor density, particularly in neuromuscular diseases where the density of receptor is highly compromised. For instance, in myasthenic syndromes where nAChR density is severely reduced (Drachman et al., 1980; Gilhus, 2012); the use of α-syn$^{-/-}$ and α-dbn$^{-/-}$ animal models may provide mechanism(s) for the loss of receptor from the synaptic folds in these devastating diseases. Additionally, while no primary mutations in α-syn or α-dbn have been associated with myasthenias in humans, several patients were identified with secondary loss of these proteins at the NMJ (Jones et al., 2003; Compton et al., 2008), so it is likely that loss of α-syn and/or α-dbn might also explain the loss of nAChRs and the myasthenia of these patients, similarly to mice models (Grady et al., 1999; Adams et al., 2000).

In the central nervous system, nAChR density is also severely affected in Alzheimer's disease (AD) (Picciotto and Zoli, 2002; Buckingham et al., 2009; Schliebs and Arendt, 2011), due to defects intracellular trafficking pathways and reduced receptor stability. Similar loss of nAChRs is also a hallmark of schizophrenia (Breese et al., 2000; Miwa et al., 2011) and bipolar disorder (Severance and Yolken, 2007). Synaptic plasticity involving modulation of postsynaptic receptor density is also seen in models of drug addiction, where AMPA

glutamate receptors are trafficked for insertion into the extrasynaptic membrane, then relocated into the synaptic compartment, in a PKA-dependent process (Quintero, 2013). Considering the crucial role for regulate synapses, the signaling pathways explored in this work might help elucidate the pathological mechanisms, as well as open new therapeutic avenues to be explored for the attenuation of morbidity of many peripheral and central neurological diseases.

Appendix

β-catenin interacts with receptor-associated proteins at the neuromuscular junction *in vivo*

Introduction

During the development of the NMJ, nAChRs shift from diffuse expression throughout the whole surface of the muscle fiber to a pre-pattern of small clusters around the center of the muscle fiber (Kim and Burden, 2008). Throughout the early postnatal weeks, in mice, the approaching nerve releases two main factors, agrin and acetylcholine that contribute to the maturation of the NMJ. Agrin induces the synthesis and clustering of nAChRs at the postsynaptic region, while acetylcholine-induced depolarizations are required for the dispersion of extrasynaptic receptor clusters. By P15, most muscle fibers are monoinnervated, with the only postsynaptic nAChR cluster with a more characteristic, branched, 'pretzel'-like shape (Balice-Gordon and Thompson, 1988; Sanes and Lichtman, 1999). In addition to agrin and acetylcholine, other signaling pathways are crucial for the regulation of NMJ development; particularly, the Wnt signaling pathway has been repeatedly implicated in the development of invertebrate and vertebrate synapses. These signaling pathways, including the role of Wnts, have been recently reviewed by Wu et al. (2010).

Briefly, Wnt proteins are a family of phylogenetically conserved, secreted glycoproteins with ubiquitous function in development. These proteins bind Frizzled (Fzd) receptors in target cells, activating Disheveled, which in turn inhibits glycogen synthase

kinase 3β (GSK3β), allowing accumulation of the cadherin-associated protein β, β-catenin (β-cat), and its translocation into the nucleus to activate gene transcription (Wu et al., 2010). β-cat plays key roles in cell adhesion, signaling and regulation of gene expression. The Wnt signaling pathway and β-cat have also been implicated in several steps of the development and maturation of the NMJ (Wu et al., 2010).

In vitro, β-cat mediates Wnt signaling and inhibits rapsyn expression through the canonical pathway (Wang et al., 2008a). Additionally, the non-transcriptional activity of β-cat is required for agrin-induced nAChR clustering, since it is thought to bridge rapsyn and cytoskeletal α-catenin (Zhang et al., 2007). Specific suppression of β-cat in the postsynaptic skeletal muscle disrupts differentiation of motor nerve presynaptic terminals, leading to ectopic nerve branches, defects in neurotransmitter release, and perinatal death, but with no defects in postsynaptic nAChR density (Li et al., 2008). Interestingly, overexpression of stable β-cat in the skeletal muscle produces a remarkably similar phenotype (Liu et al., 2012; Wu et al., 2012). Since these animals die shortly after birth, any possible role of β-cat in the adult NMJ remains to be investigated. Previously, electroporation of β-cat into adult muscles was described as leading to reduced NMJ area and branching after six weeks (Wang et al., 2008a). This raised the possibility that β-cat is involved in regulating nAChR density in adult NMJs. Here, we investigated the possible role of the Wnt signaling pathway in the stability of a mature NMJ. My results from preliminary work aimed at investigating the role of β-cat in mature synapses are presented here.

Materials and Methods

Generation of β-catenin BiFC constructs

β-cat was amplified from peGFP-β-cat (a gift from Dr. Lin Mei, Georgia Regents University) using Pfu polymerase (Agilent) and primers to introduce flanking restriction sites. Amplification products (≈ 2.4 kb) and BiFC vectors were digested and ligated; specifically, β-cat was cloned between EcoRI and XbaI sites into pBiFC-VN173 and EcoRI and KpnI sites into pBiFC-VC155. pBiFC-β-cat-VN173 contains β-cat with its C-terminus fused to the 173 N-terminal aminoacids of the Venus fuorescent protein through the linker RRSIAT (Shyu et al., 2008). pBiFC-β-cat-VC155 contains β-cat with its C-terminus fused to the 155 C-terminal aminoacids of Venus through the linker ACKIPNELKGKVMNH (Shyu et al., 2008). We used a stabilized form of β-cat, in which glycogen synthase kinase 3β phosphorylation sites S33, S37, T41 and S45 are mutated to alanine, blocking ubiquitination and β-cat degradation (Yu and Malenka, 2003). pBiFC- α-syn-VC155, pBiFC-α-dbn-VC155 and pBiFC-rapsyn-VN173 were previously generated in our lab by Dr. Mohamed Aittaleb.

Electroporation of BIFC constructs into the sternomastoid muscle and confocal microscopy

Adult mice (3-month-old), wild-type or deficient in α-syn, were anaesthetized, the sternomastoid muscle was surgically exposed and to a mix of 5 μg of each plasmid of the pair driving exogenous expression of half of the BiFC construct dissolved in water. The following pairs were used: pBiFC-β-cat-VN173 and pBiFC-β-cat-VC155 (positive control); pBiFC-β-cat-VN173 and pBiFC-α-syn-VC155; pBiFC-β-cat-VN173 and pBiFC-α-dbn-VC155; and pBiFC-rapsyn-VN173 and pBiFC-β-cat-VC155. The plasmid solution was layered over the muscle surface and the muscle electroporated as described above (Chapter II). Three days

later, the animal was re-anaesthetized and Alexa Fluor 594-labeled α-bungarotoxin (BTX-Alexa594; red) was added to the sternomastoid muscle to label nAChRs (30 min). The animal was then perfused transcardially with 2% formaldehyde PBS and the sternomastoid muscle was removed, dissected, mounted and imaged with a confocal microscope (Leica SP5). The z-stacks were then processed with Photoshop CS6 (Adobe). When there is interaction between the two proteins fused to the Venus halves, these are able to reform into the Venus full structure and emit green fluorescence (Figure A.1).

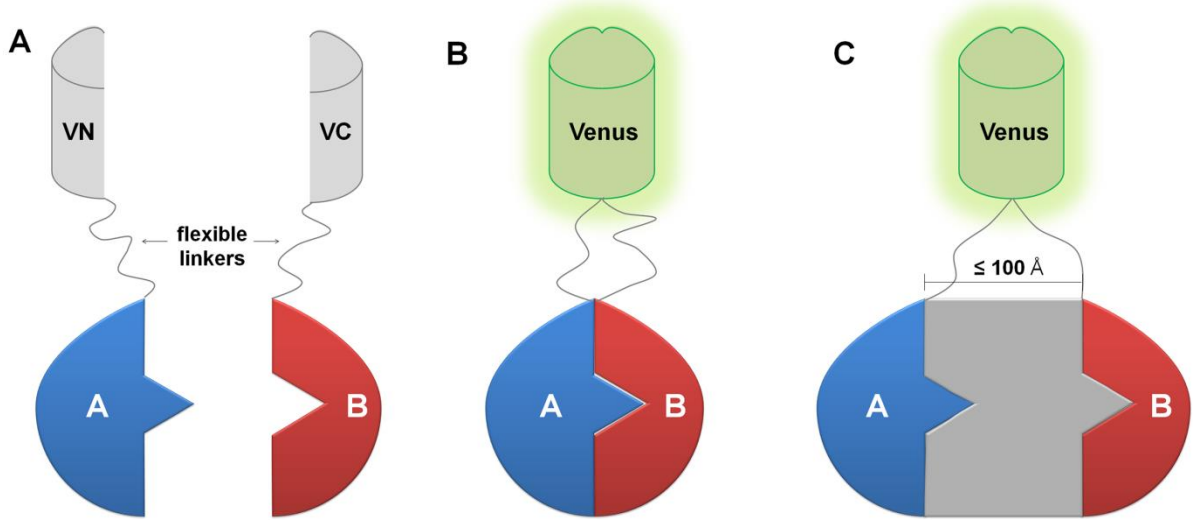

Figure A.1. The bimolecular fluorescence complementation (BiFC) assay allows detection of protein-protein interactions in the same macromolecular complex. **A)** A scheme of a pair of BiFC constructs; the C-terminus of protein A was fused to the 173 N-terminal aminoacids of the fluorescent Venus protein (VN) through the RRSIAT flexible linker. The C-terminus of protein B was fused to the 155 C-terminal aminoacids of Venus (VC) through the linker ACKIPNELKGKVMNH. Either construct when expressed by itself does not emit fluorescence; **B)** Direct interaction between proteins A and B leads to pairing of both Venus halves and emission of green fluorescence; **C)** Indirect interactions between proteins A and B in the same macromolecular complex can also lead to Venus complementation and positive BiFC signal. Since the linkers, as well as the C-termini of the proteins considered in this studied are flexible, we estimate BiFC signals will be detected if both halves of Venus are linked to points within about 100 Å of each other (Shyu et al., 2008).

Results and Discussion

Since biochemical evidence in vitro suggested β-cat interacted with rapsyn, we first investigated β-cat interaction with nAChR-associated proteins in vivo, taking advantage of the bimolecular fluorescence complementation (BiFC) assay. For this technique, we co-electroporated β-cat and scaffold proteins α-syn, α-dbn and rapsyn, with each of the pair fused to a half of the fluorescent protein Venus. When and wherever these exogenous proteins interact, both halves of Venus complement each other, leading to the emission of green fluorescence. BifC allows for the detection of direct or indirect protein interactions in the same macromolecular complex (Hu et al., 2002). In our system, considering the use of flexible linkers described above and the long, flexible sequences at both the N- and C-termini of β-cat (Gottardi and Peifer, 2008; Xing et al., 2008), we expect to detect interactions when both halves of Venus are fused to points within 100 Å of each other (Hu et al., 2002) (Figure A.1).

We started by testing our self-generated β-cat BiFC constructs by co-expressing β-cat fused to either half of Venus. We saw diffuse BiFC signal throughout the electroporated muscle fibers, consistent with the signal of GFP-β-cat (Figure A.2; β-cat-VN + β-cat-VC). Next, we looked at the interaction between β-cat and nAChR-associated proteins. When we co-electroporated β-cat with α-syn or α-dbn, we saw a clear, albeit low-intensity signal in the synaptic region. The BiFC fluorescence was seen mostly 'surrounding' the α-BTX-stained nAChRs (Figure A.2; β-cat-VN + α-syn-VC and β-cat-VN + α-dbn-VC), due to the localization of α-syn or α-dbn at the troughs of the NMJ (Pires-Oliveira et al., 2013). When β-cat was expressed with rapsyn, there was strong BiFC emission restricted to the NMJ, which co-localized perfectly with nAChRs (Figure A.2; rapsyn-VN + β-cat-VC), similar to GFP-rapsyn (Bruneau and Akaaboune, 2010). These results indicate that β-cat interacts with rapsyn at the NMJ in vivo; while a direct interaction of β-cat with α-syn or α-dbn cannot be

discarded, the difference in signal intensity is likely explained by recruitment of β-cat by rapsyn to close proximity of the DGC (Figure 1.2), allowing for BiFC. The signal between β-cat and α-syn or α-dbn is also consistent and similar to the BiFC signal seen between rapsyn and α-syn or α-dbn (M. Aittaleb, unpublished observations). We will further confirm these β-cat molecular interactions using biochemical methods. Also, mutation of the α-catenin interaction site on β-cat was shown to abrogate rapsyn binding in vitro (Zhang et al., 2007); we will develop a similarly mutated β-cat BiFC construct to further investigate the specificity of this in vivo interaction.

The presence of β-cat in the NMJ in association with rapsyn and, through it, the DGC, suggested the possibility that β-cat might be involved not only in the clustering of nAChRs during development, but also in the maintenance of receptor density at the adult NMJ. We therefore hypothesized whether β-cat expression or activation might be affected in α-syn$^{-/-}$ and NMJs, where drastic reduction of nAChRs is seen. However, when comparing muscle lysates from WT and α-syn$^{-/-}$ mice, we found no reduction of β-cat expression or in the ratio of active β-cat (data not shown). These results implied that the synaptic phenotype of α-syn$^{-/-}$ mice is not associated with loss or deficient activation of β-cat.

In our hands, we did not see any changes in NMJ morphology after electroporation with β-cat, though we did not investigate the NMJ after one week of electroporation. Additionally, β-cat expression and activity were not affected in α-syn$^{-/-}$ skeletal muscles. Therefore, the role of β-cat on regulating nAChRs at the mature NMJ, if any, remains unclear. The generation of conditional β-cat muscle knockouts inducible at adulthood could elucidate these post-developmental functions. Alternatively, we are working to optimize a GFP-tagged β-cat-shRNA construct viable for muscle electroporation. With these techniques, we hope to finally clarify the role of β-cat and the molecular interactions that localize it to the NMJ in the regulation of nAChR density.

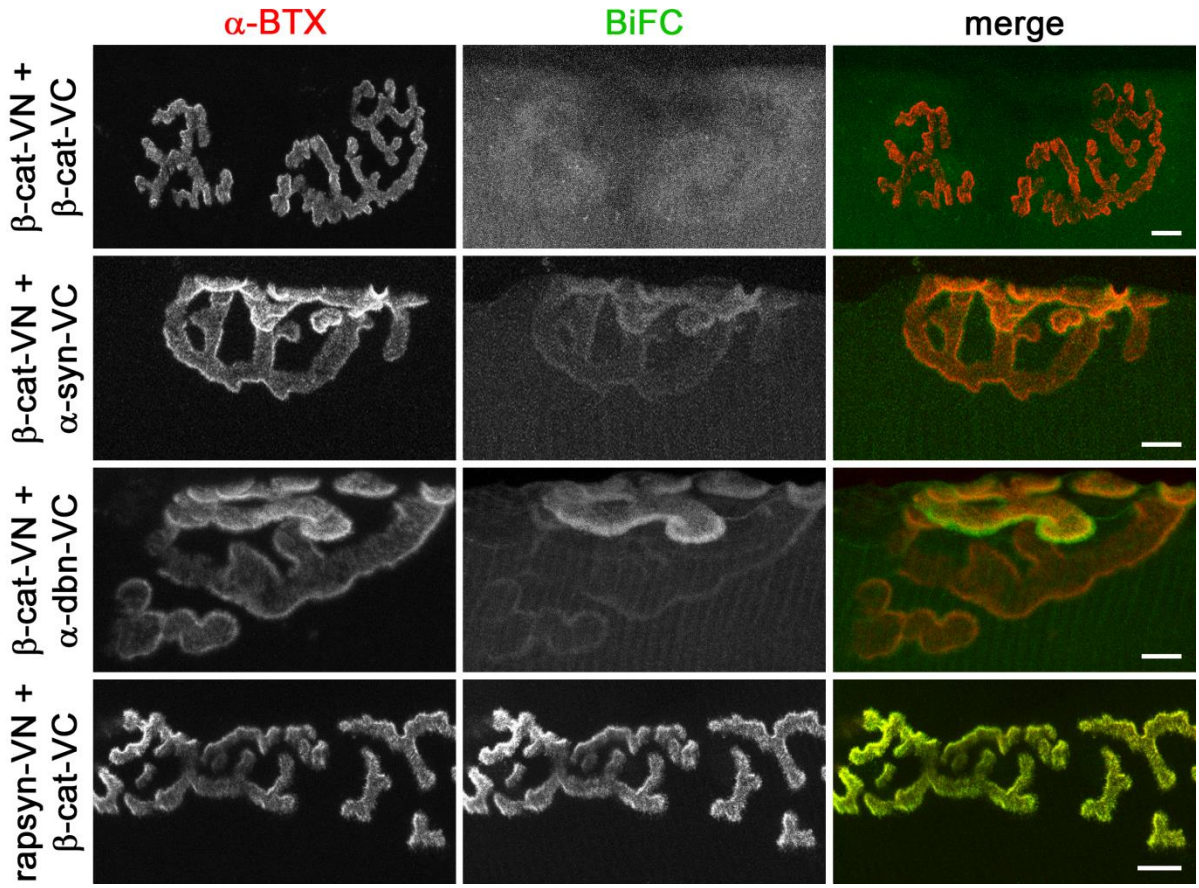

Figure A.2. β-catenin interacts with nAChR-associated proteins in mouse NMJs. When β-catenin (β-cat) is fused to both halves of Venus (β-cat-VN and β-cat-VC), BiFC signal is diffuse throughout the whole muscle fiber, as expected for the cytosolic and membrane-associated distribution of activated β-cat. β-cat-VN showed a weak interaction with α-syn-VC and α-dbn-VC, with signal clearly, albeit only slightly, above the background at the troughs of the NMJ, a localization consistent with α-syn and α-dbn. Interestingly, rapsyn-VN and β-cat-VC showed strong BiFC signal at the NMJ, which perfectly co-localized with α-BTX-labeled nAChRs, similar to rapsyn-GFP by itself. Scale bars are 20 μm.

References

Adams L, Carlson BM, Henderson L, Goldman D (1995a) Adaptation of nicotinic acetylcholine receptor, myogenin, and MRF4 gene expression to long-term muscle denervation. J Cell Biol 131:1341–1349.

Adams ME, Anderson KNE, Froehner SC (2010) The alpha-syntrophin PH and PDZ domains scaffold acetylcholine receptors, utrophin, and neuronal nitric oxide synthase at the neuromuscular junction. J Neurosci 30:11004–11010.

Adams ME, Dwyer TM, Dowler LL, White RA, Froehner SC (1995b) Mouse alpha 1- and beta 2-syntrophin gene structure, chromosome localization, and homology with a discs large domain. J Biol Chem 270:25859–25865.

Adams ME, Kramarcy N, Fukuda T, Engel AG, Sealock R, Froehner SC (2004) Structural abnormalities at neuromuscular synapses lacking multiple syntrophin isoforms. J Neurosci 24:10302–10309.

Adams ME, Kramarcy N, Krall SP, Rossi SG, Rotundo RL, Sealock R, Froehner SC (2000) Absence of alpha-syntrophin leads to structurally aberrant neuromuscular synapses deficient in utrophin. J Cell Biol 150:1385–1398.

Ahn AH, Kunkel LM (1995) Syntrophin binds to an alternatively spliced exon of dystrophin. J Cell Biol 128:363–371.

Akaaboune M, Culican SM, Turney SG, Lichtman JW (1999) Rapid and reversible effects of activity on acetylcholine receptor density at the neuromuscular junction in vivo. Science 286:503–507.

Akaaboune M, Grady RM, Turney S, Sanes JR, Lichtman JW (2002) Neurotransmitter Receptor Dynamics Studied In Vivo by Reversible Photo-Unbinding of Fluorescent Ligands. Neuron 34:865–876.

Alessi A, Bragg AD, Percival JM, Yoo J, Albrecht DE, Froehner SC, Adams ME (2006) gamma-Syntrophin scaffolding is spatially and functionally distinct from that of the alpha/beta syntrophins. Exp Cell Res 312:3084–3095.

Altiok N, Altiok S, Changeux JP (1997) Heregulin-stimulated acetylcholine receptor gene expression in muscle: requirement for MAP kinase and evidence for a parallel inhibitory pathway independent of electrical activity. EMBO J 16:717–725.

Apel ED, Roberds SL, Campbell KP, Merlie JP (1995) Rapsyn may function as a link between the acetylcholine receptor and the agrin-binding dystrophin-associated glycoprotein complex. Neuron 15:115–126.

Arahata K, Hoffman EP, Kunkel LM, Ishiura S, Tsukahara T, Ishihara T, Sunohara N, Nonaka I, Ozawa E, Sugita H (1989) Dystrophin diagnosis: comparison of dystrophin abnormalities by immunofluorescence and immunoblot analyses. Proc Natl Acad Sci U S A 86:7154–7158.

Araishi K, Sasaoka T, Imamura M, Noguchi S, Hama H, Wakabayashi E, Yoshida M, Hori T, Ozawa E (1999) Loss of the sarcoglycan complex and sarcospan leads to muscular dystrophy in beta-sarcoglycan-deficient mice. Hum Mol Genet 8:1589–1598.

Axelrod D, Ravdin P, Koppel DE, Schlessinger J, Webb WW, Elson EL, Podleski TR (1976) Lateral motion of fluorescently labeled acetylcholine receptors in membranes of developing muscle fibers. Proc Natl Acad Sci U S A 73:4594–4598.

Axelrod D, Ravdin PM, Podleski TR (1978) Control of acetylcholine receptor mobility and distribution in cultured muscle membranes. A fluorescence study. Biochim Biophys Acta 511:23–38.

Balasubramanian S, Fung ET, Huganir RL (1998) Characterization of the tyrosine phosphorylation and distribution of dystrobrevin isoforms. FEBS Lett 432:133–140.

Balice-Gordon RJ, Lichtman JW (1993) In vivo observations of pre- and postsynaptic changes during the transition from multiple to single innervation at developing neuromuscular junctions. J Neurosci 13:834–855.

Balice-Gordon RJ, Thompson WJ (1988) Synaptic rearrangements and alterations in motor unit properties in neonatal rat extensor digitorum longus muscle. J Physiol 398:191–210.

Benson M a, Newey SE, Martin-Rendon E, Hawkes R, Blake DJ (2001) Dysbindin, a novel coiled-coil-containing protein that interacts with the dystrobrevins in muscle and brain. J Biol Chem 276:24232–24241.

Berg DK, Hall ZW (1975) Loss of alpha-bungarotoxin from junctional and extrajunctional acetylcholine receptors in rat diaphragm muscle in vivo and in organ culture. J Physiol 252:771–789.

Bessereau JL, Stratford-Perricaudet LD, Piette J, Le Poupon C, Changeux JP (1994) In vivo and in vitro analysis of electrical activity-dependent expression of muscle acetylcholine receptor genes using adenovirus. Proc Natl Acad Sci U S A 91:1304–1308.

Blake DJ, Nawrotzki R, Peters MF, Froehner SC, Davies KE (1996) Isoform diversity of dystrobrevin, the murine 87-kDa postsynaptic protein. J Biol Chem 271:7802–7810.

Blazev R, Hussain M, Bakker AJ, Head SI, Lamb GD (2001) Effects of the PKA inhibitor H-89 on excitation-contraction coupling in skinned and intact skeletal muscle fibres. J Muscle Res Cell Motil 22:277–286.

Bonilla E, Samitt CE, Miranda a F, Hays a P, Salviati G, DiMauro S, Kunkel LM, Hoffman EP, Rowland LP (1988) Duchenne muscular dystrophy: deficiency of dystrophin at the muscle cell surface. Cell 54:447–452.

Breese CR, Lee MJ, Adams CE, Sullivan B, Logel J, Gillen KM, Marks MJ, Collins a C, Leonard S (2000) Abnormal regulation of high affinity nicotinic receptors in subjects with schizophrenia. Neuropsychopharmacology 23:351–364.

Brenman JE, Chao DS, Gee SH, McGee a W, Craven SE, Santillano DR, Wu Z, Huang F, Xia H, Peters MF, Froehner SC, Bredt DS (1996) Interaction of nitric oxide synthase with the postsynaptic density protein PSD-95 and alpha1-syntrophin mediated by PDZ domains. Cell 84:757–767.

Bruneau E, Akaaboune M (2007) The dynamics of the rapsyn scaffolding protein at individual acetylcholine receptor clusters. J Biol Chem 282:9932–9940.

Bruneau E, Sutter D, Hume RI, Akaaboune M (2005) Identification of nicotinic acetylcholine receptor recycling and its role in maintaining receptor density at the neuromuscular junction in vivo. J Neurosci 25:9949–9959.

Bruneau EG, Akaaboune M (2006) The dynamics of recycled acetylcholine receptors at the neuromuscular junction in vivo. Development 133:4485–4493.

Bruneau EG, Akaaboune M (2010) Dynamics of the rapsyn scaffolding protein at the neuromuscular junction of live mice. J Neurosci 30:614–619.

Bruneau EG, Brenner DS, Kuwada JY, Akaaboune M (2008) Acetylcholine receptor clustering is required for the accumulation and maintenance of scaffolding proteins. Curr Biol 18:109–115.

Bruneau EG, Esteban J a, Akaaboune M (2009) Receptor-associated proteins and synaptic plasticity. FASEB J 23:679–688.

Bruns RF, Miller FD, Merriman RL, Howbert JJ, Heath WF, Kobayashi E, Takahashi I, Tamaoki T, Nakano H (1991) Inhibition of protein kinase C by calphostin C is light-dependent. Biochem Biophys Res Commun 176:288–293.

Buckingham SD, Jones AK, Brown LA, Sattelle DB (2009) Nicotinic acetylcholine receptor signalling: roles in Alzheimer's disease and amyloid neuroprotection. Pharmacol Rev 61:39–61.

Bursztajn S, Schneider LW, Jong YJ, Berman SA (1988) Phorbol esters inhibit the synthesis of acetylcholine receptors in cultured muscle cells. Biol Cell 63:57–65.

Butler MH, Douville K, Murnane a a, Kramarcy NR, Cohen JB, Sealock R, Froehner SC (1992) Association of the Mr 58,000 postsynaptic protein of electric tissue with Torpedo dystrophin and the Mr 87,000 postsynaptic protein. J Biol Chem 267:6213–6218.

Caroni P, Rotzler S, Britt JC, Brenner HR (1993) Calcium influx and protein phosphorylation mediate the metabolic stabilization of synaptic acetylcholine receptors in muscle. J Neurosci 13:1315–1325.

Cartaud a., Coutant S, Petrucci TC, Cartaud J (1998) Evidence for in situ and in vitro association between beta-dystroglycan and the subsynaptic 43K rapsyn protein.

Consequence for acetylcholine receptor clustering at the synapse. J Biol Chem 273:11321–11326.

Ceccarini M, Grasso M, Veroni C, Gambara G, Artegiani B, Macchia G, Ramoni C, Torreri P, Mallozzi C, Petrucci TC, Macioce P (2007) Association of dystrobrevin and regulatory subunit of protein kinase A: a new role for dystrobrevin as a scaffold for signaling proteins. J Mol Biol 371:1174–1187.

Ceccarini M, Torreri P, Lombardi DG, Macchia G, Macioce P, Petrucci TC (2005) Molecular basis of dystrobrevin interaction with kinesin heavy chain: structural determinants of their binding. J Mol Biol 354:872–882.

Chang CC, Huang MC (1975) Turnover of junctional and extrajunctional acetylcholine receptors of the rat diaphragm. Nature 253:643–644.

Changeux JP, Devillers-Thiéry A, Chemouilli P (1984) Acetylcholine receptor: an allosteric protein. Science 225:1335–1345.

Changeux JP, Kasai M, Lee CY (1970) Use of a snake venom toxin to characterize the cholinergic receptor protein. Proc Natl Acad Sci U S A 67:1241–1247.

Choi K-R, Berrera M, Reischl M, Strack S, Albrizio M, Röder I V, Wagner A, Petersen Y, Hafner M, Zaccolo M, Rudolf R (2012) Rapsyn mediates subsynaptic anchoring of PKA type I and stabilisation of acetylcholine receptor in vivo. J Cell Sci 125:714–723.

Christianson JC, Green WN (2004) Regulation of nicotinic receptor expression by the ubiquitin-proteasome system. EMBO J 23:4156–4165.

Cohen TJ, Barrientos T, Hartman ZC, Garvey SM, Cox G a, Yao T-P (2009) The deacetylase HDAC4 controls myocyte enhancing factor-2-dependent structural gene expression in response to neural activity. FASEB J 23:99–106.

Cohen TJ, Waddell DS, Barrientos T, Lu Z, Feng G, Cox G a, Bodine SC, Yao T-P (2007) The histone deacetylase HDAC4 connects neural activity to muscle transcriptional reprogramming. J Biol Chem 282:33752–33759.

Collingridge GL, Isaac JTR, Wang YT (2004) Receptor trafficking and synaptic plasticity. Nat Rev Neurosci 5:952–962.

Compton AG, Albrecht DE, Seto JT, Cooper ST, Ilkovski B, Jones KJ, Challis D, Mowat D, Ranscht B, Bahlo M, Froehner SC, North KN (2008) Mutations in contactin-1, a neural adhesion and neuromuscular junction protein, cause a familial form of lethal congenital myopathy. Am J Hum Genet 83:714–724.

Côté PD, Moukhles H, Carbonetto S (2002) Dystroglycan is not required for localization of dystrophin, syntrophin, and neuronal nitric-oxide synthase at the sarcolemma but regulates integrin alpha 7B expression and caveolin-3 distribution. J Biol Chem 277:4672–4679.

Côté PD, Moukhles H, Lindenbaum M, Carbonetto S (1999) Chimaeric mice deficient in dystroglycans develop muscular dystrophy and have disrupted myoneural synapses. Nat Genet 23:338–342.

Crosbie RH, Heighway J, Venzke DP, Lee JC, Campbell KP (1997) Sarcospan, the 25-kDa transmembrane component of the dystrophin-glycoprotein complex. J Biol Chem 272:31221–31224.

Crosbie RH, Lebakken CS, Holt KH, Venzke DP, Straub V, Lee JC, Grady RM, Chamberlain JS, Sanes JR, Campbell KP (1999) Membrane targeting and stabilization of sarcospan is mediated by the sarcoglycan subcomplex. J Cell Biol 145:153–165.

Dalkilic I, Kunkel LM (2003) Muscular dystrophies: genes to pathogenesis. Curr Opin Genet Dev 13:231–238.

Daval S, Rocher C, Cherel Y, Le Rumeur E (2010) Several dystrophin-glycoprotein complex members are present in crude surface membranes but they are sodium dodecyl sulphate invisible in KCl-washed microsomes from mdx mouse muscle. Cell Mol Biol Lett 15:134–152.

Deconinck a E, Potter a C, Tinsley JM, Wood SJ, Vater R, Young C, Metzinger L, Vincent A, Slater CR, Davies KE (1997) Postsynaptic abnormalities at the neuromuscular junctions of utrophin-deficient mice. J Cell Biol 136:883–894.

Deyst KA, Bowe MA, Leszyk JD, Fallon JR (1995) The alpha-dystroglycan-beta-dystroglycan complex. Membrane organization and relationship to an agrin receptor. J Biol Chem 270:25956–25959.

Di Angelantonio S, De Stefano ME, Piccioni A, Lombardi L, Gotti C, Paggi P (2011) Lack of dystrophin functionally affects α3β2/β4-nicotinic acethylcholine receptors in sympathetic neurons of dystrophic mdx mice. Neurobiol Dis 41:528–537.

Di Pietro SM, Falcón-Pérez JM, Tenza D, Setty SRG, Marks MS, Raposo G, Dell'Angelica EC (2006) BLOC-1 interacts with BLOC-2 and the AP-3 complex to facilitate protein trafficking on endosomes. Mol Biol Cell 17:4027–4038.

Djakovic SN, Schwarz L a, Barylko B, DeMartino GN, Patrick GN (2009) Regulation of the proteasome by neuronal activity and calcium/calmodulin-dependent protein kinase II. J Biol Chem 284:26655–26665.

Dong Z, Chai W, Wang W, Zhao L, Fu Z, Cao W, Liu Z (2013) Protein kinase A mediates glucagon-like peptide 1-induced nitric oxide production and muscle microvascular recruitment. Am J Physiol Endocrinol Metab 304:E222–8.

Drachman DB, Adams RN, Stanley EF, Pestronk a (1980) Mechanisms of acetylcholine receptor loss in myasthenia gravis. J Neurol Neurosurg Psychiatry 43:601–610.

Duclos F, Straub V, Moore S a, Venzke DP, Hrstka RF, Crosbie RH, Durbeej M, Lebakken CS, Ettinger a J, van der Meulen J, Holt KH, Lim LE, Sanes JR, Davidson BL, Faulkner

J a, Williamson R, Campbell KP (1998) Progressive muscular dystrophy in alpha-sarcoglycan-deficient mice. J Cell Biol 142:1461–1471.

Dupuis L, Loeffler J-P (2009) Neuromuscular junction destruction during amyotrophic lateral sclerosis: insights from transgenic models. Curr Opin Pharmacol 9:341–346.

Durbeej M, Campbell KP (2002) Muscular dystrophies involving the dystrophin-glycoprotein complex: an overview of current mouse models. Curr Opin Genet Dev 12:349–361.

Dwyer TM, Froehner SC (1995) Direct binding of Torpedo syntrophin to dystrophin and the 87 kDa dystrophin homologue. FEBS Lett 375:91–94.

Ehlers MD (2000) Reinsertion or degradation of AMPA receptors determined by activity-dependent endocytic sorting. Neuron 28:511–525.

Escher P, Lacazette E, Courtet M, Blindenbacher a, Landmann L, Bezakova G, Lloyd KC, Mueller U, Brenner HR (2005) Synapses form in skeletal muscles lacking neuregulin receptors. Science 308:1920–1923.

Fambrough DM, Hartzell HC (1972) Acetylcholine Receptors: Number and Distribution at Neuromuscular Junctions in Rat Diaphragm. Science (80-) 176:189–191.

Froehner SC, Adams ME, Peters MF, Gee SH (1997) Syntrophins: modular adapter proteins at the neuromuscular junction and the sarcolemma. Soc Gen Physiol Ser 52:197–207.

Fumagalli G, Balbi S, Cangiano A, Lømo T (1990) Regulation of turnover and number of acetylcholine receptors at neuromuscular junctions. Neuron 4:563–569.

Gautam M, Noakes PG, Mudd J, Nichol M, Chu GC, Sanes JR, Merlie JP (1995) Failure of postsynaptic specialization to develop at neuromuscular junctions of rapsyn-deficient mice. Nature 377:232–236.

Gee SH, Madhavan R, Levinson SR, Caldwell JH, Sealock R, Froehner SC (1998) Interaction of muscle and brain sodium channels with multiple members of the syntrophin family of dystrophin-associated proteins. J Neurosci 18:128–137.

Gilhus NE (2012) Myasthenia and the neuromuscular junction. Curr Opin Neurol 25:523–529.

Gokhale A, Larimore J, Werner E, So L, Moreno-De-Luca A, Lese-Martin C, Lupashin V V, Smith Y, Faundez V (2012) Quantitative proteomic and genetic analyses of the schizophrenia susceptibility factor dysbindin identify novel roles of the biogenesis of lysosome-related organelles complex 1. J Neurosci 32:3697–3711.

Goldman D, Brenner HR, Heinemann S (1988) Acetylcholine receptor alpha-, beta-, gamma-, and delta-subunit mRNA levels are regulated by muscle activity. Neuron 1:329–333.

Gottardi CJ, Peifer M (2008) Terminal regions of beta-catenin come into view. Structure 16:336–338.

Grady RM, Akaaboune M, Cohen AL, Maimone MM, Lichtman JW, Sanes JR (2003) Tyrosine-phosphorylated and nonphosphorylated isoforms of alpha-dystrobrevin: roles in skeletal muscle and its neuromuscular and myotendinous junctions. J Cell Biol 160:741–752.

Grady RM, Grange RW, Lau KS, Maimone MM, Nichol MC, Stull JT, Sanes JR (1999) Role for alpha-dystrobrevin in the pathogenesis of dystrophin-dependent muscular dystrophies. Nat Cell Biol 1:215–220.

Grady RM, Teng H, Nichol MC, Cunningham JC, Wilkinson RS, Sanes JR (1997) Skeletal and cardiac myopathies in mice lacking utrophin and dystrophin: a model for Duchenne muscular dystrophy. Cell 90:729–738.

Grady RM, Wozniak DF, Ohlemiller KK, Sanes JR (2006) Cerebellar synaptic defects and abnormal motor behavior in mice lacking alpha- and beta-dystrobrevin. J Neurosci 26:2841–2851.

Grady RM, Zhou H, Cunningham JM, Henry MD, Campbell KP, Sanes JR (2000) Maturation and maintenance of the neuromuscular synapse: genetic evidence for roles of the dystrophin--glycoprotein complex. Neuron 25:279–293.

Grewal PK, Holzfeind PJ, Bittner RE, Hewitt JE (2001) Mutant glycosyltransferase and altered glycosylation of alpha-dystroglycan in the myodystrophy mouse. Nat Genet 28:151–154.

Hack a a, Ly CT, Jiang F, Clendenin CJ, Sigrist KS, Wollmann RL, McNally EM (1998) Gamma-sarcoglycan deficiency leads to muscle membrane defects and apoptosis independent of dystrophin. J Cell Biol 142:1279–1287.

Hack AA, Groh ME, McNally EM (2000a) Sarcoglycans in muscular dystrophy. Microsc Res Tech 48:167–180.

Hack AA, Lam MY, Cordier L, Shoturma DI, Ly CT, Hadhazy M a, Hadhazy MR, Sweeney HL, McNally EM (2000b) Differential requirement for individual sarcoglycans and dystrophin in the assembly and function of the dystrophin-glycoprotein complex. J Cell Sci 113 (Pt 1:2535–2544.

Harris AJ (1981) Embryonic growth and innervation of rat skeletal muscles. III. Neural regulation of junctional and extra-junctional acetylcholine receptor clusters. Philos Trans R Soc Lond B Biol Sci 293:287–314.

Hartzell HC, Fambrough DM (1972) Acetylcholine receptors. Distribution and extrajunctional density in rat diaphragm after denervation correlated with acetylcholine sensitivity. J Gen Physiol 60:248–262.

Hu C-D, Chinenov Y, Kerppola TK (2002) Visualization of interactions among bZIP and Rel family proteins in living cells using bimolecular fluorescence complementation. Mol Cell 9:789–798.

Huganir RL, Miles K, Greengard P (1984) Phosphorylation of the nicotinic acetylcholine receptor by an endogenous tyrosine-specific protein kinase. Proc Natl Acad Sci U S A 81:6968–6972.

Huganir RL, Nicoll R a (2013) AMPARs and synaptic plasticity: the last 25 years. Neuron 80:704–717.

Huh K-H, Fuhrer C (2002) Clustering of nicotinic acetylcholine receptors: from the neuromuscular junction to interneuronal synapses. Mol Neurobiol 25:79–112.

Hyman C, Froehner SC (1983) Degradation of acetylcholine receptors in muscle cells: effect of leupeptin on turnover rate, intracellular pool sizes, and receptor properties. J Cell Biol 96:1316–1324.

Ibraghimov-Beskrovnaya O, Ervasti JM, Leveille CJ, Slaughter CA, Sernett SW, Campbell KP (1992) Primary structure of dystrophin-associated glycoproteins linking dystrophin to the extracellular matrix. Nature 355:696–702.

Iida T, Kobayashi E, Yoshida M, Sano H (1989) Calphostins, novel and specific inhibitors of protein kinase C. II. Chemical structures. J Antibiot (Tokyo) 42:1475–1481.

Jacobson C, Côté PD, Rossi SG, Rotundo RL, Carbonetto S (2001) The dystroglycan complex is necessary for stabilization of acetylcholine receptor clusters at neuromuscular junctions and formation of the synaptic basement membrane. J Cell Biol 152:435–450.

Jaworski A, Burden SJ (2006) Neuromuscular synapse formation in mice lacking motor neuron- and skeletal muscle-derived Neuregulin-1. J Neurosci 26:655–661.

Johannes FJ, Prestle J, Eis S, Oberhagemann P, Pfizenmaier K (1994) PKCu is a novel, atypical member of the protein kinase C family. J Biol Chem 269:6140–6148.

Jones G, Herczeg a, Ruegg M a, Lichtsteiner M, Kröger S, Brenner HR (1996) Substrate-bound agrin induces expression of acetylcholine receptor epsilon-subunit gene in cultured mammalian muscle cells. Proc Natl Acad Sci U S A 93:5985–5990.

Jones K., Compton a. ., Yang N, Mills M., Peters M., Mowat D, Kunkel L., Froehner S., North K. (2003) Deficiency of the syntrophins and α-dystrobrevin in patients with inherited myopathy. Neuromuscul Disord 13:456–467.

Kameya S, Miyagoe Y, Nonaka I, Ikemoto T, Endo M, Hanaoka K, Nabeshima Y, Takeda S (1999) Alpha1-Syntrophin Gene Disruption Results in the Absence of Neuronal-Type Nitric-Oxide Synthase At the Sarcolemma But Does Not Induce Muscle Degeneration. J Biol Chem 274:2193–2200.

Khurana TS, Watkins SC, Chafey P, Chelly J, Tomé FM, Fardeau M, Kaplan JC, Kunkel LM (1991) Immunolocalization and developmental expression of dystrophin related protein in skeletal muscle. Neuromuscul Disord 1:185–194.

Kim N, Burden SJ (2008) MuSK controls where motor axons grow and form synapses. Nat Neurosci 11:19–27.

Kobayashi E, Ando K, Nakano H, Iida T, Ohno H, Morimoto M, Tamaoki T (1989) Calphostins (UCN-1028), novel and specific inhibitors of protein kinase C. I. Fermentation, isolation, physico-chemical properties and biological activities. J Antibiot (Tokyo) 42:1470–1474.

Kramarcy NR, Sealock R (2000) Syntrophin isoforms at the neuromuscular junction: developmental time course and differential localization. Mol Cell Neurosci 15:262–274.

Kramarcy NR, Vidal a, Froehner SC, Sealock R (1994) Association of utrophin and multiple dystrophin short forms with the mammalian M(r) 58,000 dystrophin-associated protein (syntrophin). J Biol Chem 269:2870–2876.

Kumari S, Borroni V, Chaudhry A, Chanda B, Massol R, Mayor S, Barrantes FJ (2008) Nicotinic acetylcholine receptor is internalized via a Rac-dependent, dynamin-independent endocytic pathway. J Cell Biol 181:1179–1193.

Lacazette E, Le Calvez S, Gajendran N, Brenner HR (2003) A novel pathway for MuSK to induce key genes in neuromuscular synapse formation. J Cell Biol 161:727–736.

Lai K-O, Ip NY (2003) Central synapse and neuromuscular junction: same players, different roles. Trends Genet 19:395–402.

Lanuza MA, Besalduch N, González C, Santafé MM, Garcia N, Tomàs M, Nelson PG, Tomàs J (2010) Decreased phosphorylation of δ and ε subunits of the acetylcholine receptor coincides with delayed postsynaptic maturation in PKC θ deficient mouse. Exp Neurol 225:183–195.

Lanuza MA, Garcia N, Santafé M, González CM, Alonso I, Nelson PG, Tomàs J (2002) Pre- and postsynaptic maturation of the neuromuscular junction during neonatal synapse elimination depends on protein kinase C. J Neurosci Res 67:607–617.

Lanuza MA, Gizaw R, Viloria A, González CM, Besalduch N, Dunlap V, Tomàs J, Nelson PG (2006) Phosphorylation of the nicotinic acetylcholine receptor in myotube-cholinergic neuron cocultures. J Neurosci Res 83:1407–1414.

Lanuza MA, Li MX, Jia M, Kim S, Davenport R, Dunlap V, Nelson PG (2000) Protein kinase C-mediated changes in synaptic efficacy at the neuromuscular junction in vitro: the role of postsynaptic acetylcholine receptors. J Neurosci Res 61:616–625.

LaRochelle WJ, Froehner SC (1987) Comparison of the postsynaptic 43-kDa protein from muscle cells that differ in acetylcholine receptor clustering activity. J Biol Chem 262:8190–8195.

Lebakken CS, Venzke DP, Hrstka RF, Consolino CM, Faulkner J a, Williamson R a, Campbell KP (2000) Sarcospan-deficient mice maintain normal muscle function. Mol Cell Biol 20:1669–1677.

Lee TH, Linstedt AD (2000) Potential role for protein kinases in regulation of bidirectional endoplasmic reticulum-to-Golgi transport revealed by protein kinase inhibitor H89. Mol Biol Cell 11:2577–2590.

Lendvai B, Vizi ES (2008) Nonsynaptic chemical transmission through nicotinic acetylcholine receptors. Physiol Rev 88:333–349.

Li MX, Jia M, Jiang H, Dunlap V, Nelson PG (2001) Opposing actions of protein kinase A and C mediate Hebbian synaptic plasticity. Nat Neurosci 4:871–872.

Li W et al. (2003a) Hermansky-Pudlak syndrome type 7 (HPS-7) results from mutant dysbindin, a member of the biogenesis of lysosome-related organelles complex 1 (BLOC-1). Nat Genet 35:84–89.

Li X, Oghi KA, Zhang J, Krones A, Bush KT, Glass CK, Nigam SK, Aggarwal AK, Maas R, Rose DW, Rosenfeld MG (2003b) Eya protein phosphatase activity regulates Six1-Dach-Eya transcriptional effects in mammalian organogenesis. Nature 426:247–254.

Li X-M, Dong X-P, Luo S-W, Zhang B, Lee D-H, Ting AKL, Neiswender H, Kim C-H, Carpenter-Hyland E, Gao T-M, Xiong W-C, Mei L (2008) Retrograde regulation of motoneuron differentiation by muscle beta-catenin. Nat Neurosci 11:262–268.

Lichtman JW, Magrassi L, Purves D (1987) Visualization of neuromuscular junctions over periods of several months in living mice. J Neurosci 7:1215–1222.

Lin W, Burgess RW, Dominguez B, Pfaff SL, Sanes JR, Lee KF (2001) Distinct roles of nerve and muscle in postsynaptic differentiation of the neuromuscular synapse. Nature 410:1057–1064.

Liu Y, Sugiura Y, Wu F, Mi W, Taketo MM, Cannon S, Carroll T, Lin W (2012) β-Catenin stabilization in skeletal muscles, but not in motor neurons, leads to aberrant motor innervation of the muscle during neuromuscular development in mice. Dev Biol 366:255–267.

Livak KJ, Schmittgen TD (2001) Analysis of relative gene expression data using real-time quantitative PCR and the 2(-Delta Delta C(T)) Method. Methods 25:402–408.

Love DR, Hill DF, Dickson G, Spurr NK, Byth BC, Marsden RF, Walsh FS, Edwards YH, Davies KE (1989) An autosomal transcript in skeletal muscle with homology to dystrophin. Nature 339:55–58.

Lyons PR, Slater CR (1991) Structure and function of the neuromuscular junction in young adult mdx mice. J Neurocytol 20:969–981.

Mabb AM, Ehlers MD (2010) Ubiquitination in postsynaptic function and plasticity. Annu Rev Cell Dev Biol 26:179–210.

Marchand S, Devillers-Thiéry A, Pons S, Changeux J-P, Cartaud J (2002) Rapsyn escorts the nicotinic acetylcholine receptor along the exocytic pathway via association with lipid rafts. J Neurosci 22:8891–8901.

Marchand S, Stetzkowski-Marden F, Cartaud J (2001) Differential targeting of components of the dystrophin complex to the postsynaptic membrane. Eur J Neurosci 13:221–229.

Martinez-Pena y Valenzuela I, Mouslim C, Akaaboune M (2010) Calcium/calmodulin kinase II-dependent acetylcholine receptor cycling at the mammalian neuromuscular junction in vivo. J Neurosci 30:12455–12465.

Martinez-Pena y Valenzuela I, Mouslim C, Pires-Oliveira M, Adams ME, Froehner SC, Akaaboune M (2011) Nicotinic acetylcholine receptor stability at the NMJ deficient in α-syntrophin in vivo. J Neurosci 31:15586–15596.

Matsumura K, Ervasti JM, Ohlendieck K, Kahl SD, Campbell KP (1992) Association of dystrophin-related protein with dystrophin-associated proteins in mdx mouse muscle. Nature 360:588–591.

McCann CM, Tapia JC, Kim H, Coggan JS, Lichtman JW (2008) Rapid and modifiable neurotransmitter receptor dynamics at a neuronal synapse in vivo. Nat Neurosci 11:807–815.

Méjat A, Ramond F, Bassel-Duby R, Khochbin S, Olson EN, Schaeffer L (2005) Histone deacetylase 9 couples neuronal activity to muscle chromatin acetylation and gene expression. Nat Neurosci 8:313–321.

Merlie JP, Mudd J, Cheng TC, Olson EN (1994) Myogenin and acetylcholine receptor alpha gene promoters mediate transcriptional regulation in response to motor innervation. J Biol Chem 269:2461–2467.

Michele DE, Barresi R, Kanagawa M, Saito F, Cohn RD, Satz JS, Dollar J, Nishino I, Kelley RI, Somer H, Straub V, Mathews KD, Moore SA, Campbell KP (2002) Post-translational disruption of dystroglycan-ligand interactions in congenital muscular dystrophies. Nature 418:417–422.

Miles K, Anthony DT, Rubin LL, Greengard P, Huganir RL (1987) Regulation of nicotinic acetylcholine receptor phosphorylation in rat myotubes by forskolin and cAMP. Proc Natl Acad Sci U S A 84:6591–6595.

Miles K, Huganir RL (1988) Regulation of nicotinic acetylcholine receptors by protein phosphorylation. Mol Neurobiol 2:91–124.

Miles K, Wagner M (2003) Overexpression of nPKC theta is inhibitory for agrin-induced nicotinic acetylcholine receptor clustering in C2C12 myotubes. J Neurosci Res 71:188–195.

Miwa JM, Freedman R, Lester H a (2011) Neural systems governed by nicotinic acetylcholine receptors: emerging hypotheses. Neuron 70:20–33.

Mizuno Y, Thompson TG, Guyon JR, Lidov HG, Brosius M, Imamura M, Ozawa E, Watkins SC, Kunkel LM (2001) Desmuslin, an intermediate filament protein that interacts with alpha -dystrobrevin and desmin. Proc Natl Acad Sci U S A 98:6156–6161.

Mouslim C, Aittaleb M, Hume RI, Akaaboune M (2012) A role for the calmodulin kinase II-related anchoring protein (αkap) in maintaining the stability of nicotinic acetylcholine receptors. J Neurosci 32:5177–5185.

Musil LS, Carr C, Cohen JB, Merlie JP (1988) Acetylcholine receptor-associated 43K protein contains covalently bound myristate. J Cell Biol 107:1113–1121.

Nakano S, Shimohama S, Saitoh T, Akiguchi I, Kimura J (1992) Localization of protein kinase C in human skeletal muscle. Muscle Nerve 15:496–499.

Nawrotzki R, Loh NY, Ruegg MA, Davies KE, Blake DJ (1998) Characterisation of alpha-dystrobrevin in muscle. J Cell Sci 111 (Pt 1:2595–2605.

Neely JD, Amiry-Moghaddam M, Ottersen OP, Froehner SC, Agre P, Adams ME (2001) Syntrophin-dependent expression and localization of Aquaporin-4 water channel protein. Proc Natl Acad Sci U S A 98:14108–14113.

Nelson PG, Lanuza M a, Jia M, Li M-X, Tomas J (2003) Phosphorylation reactions in activity-dependent synapse modification at the neuromuscular junction during development. J Neurocytol 32:803–816.

Newey SE, Howman E V, Ponting CP, Benson M a, Nawrotzki R, Loh NY, Davies KE, Blake DJ (2001) Syncoilin, a novel member of the intermediate filament superfamily that interacts with alpha-dystrobrevin in skeletal muscle. J Biol Chem 276:6645–6655.

Newton AC (2001) Protein kinase C: structural and spatial regulation by phosphorylation, cofactors, and macromolecular interactions. Chem Rev 101:2353–2364.

Nimnual AS, Chang W, Chang NS, Ross AF, Gelman MS, Prives JM (1998) Identification of phosphorylation sites on AChR delta-subunit associated with dispersal of AChR clusters on the surface of muscle cells. Biochemistry 37:14823–14832.

Nishizuka Y (1992) Intracellular signaling by hydrolysis of phospholipids and activation of protein kinase C. Science 258:607–614.

Ohlendieck K, Ervasti JM, Matsumura K, Kahl SD, Leveille CJ, Campbell KP (1991) Dystrophin-related protein is localized to neuromuscular junctions of adult skeletal muscle. Neuron 7:499–508.

Ohno S, Akita Y, Hata A, Osada S, Kubo K, Konno Y, Akimoto K, Mizuno K, Saido T, Kuroki T (1991) Structural and functional diversities of a family of signal transducing protein kinases, protein kinase C family; two distinct classes of PKC, conventional cPKC and novel nPKC. Adv Enzyme Regul 31:287–303.

Ono F, Higashijima S, Shcherbatko a, Fetcho JR, Brehm P (2001) Paralytic zebrafish lacking acetylcholine receptors fail to localize rapsyn clusters to the synapse. J Neurosci 21:5439–5448.

Ono F, Mandel G, Brehm P (2004) Acetylcholine receptors direct rapsyn clusters to the neuromuscular synapse in zebrafish. J Neurosci 24:5475–5481.

Orozco IJ, Koppensteiner P, Ninan I, Arancio O (2013) The schizophrenia susceptibility gene DTNBP1 modulates AMPAR synaptic transmission and plasticity in the hippocampus of juvenile DBA/2J mice. Mol Cell Neurosci 58C:76–84.

Pacheco MA, Pastoor TE, Wecker L (2003) Phosphorylation of the alpha4 subunit of human alpha4beta2 nicotinic receptors: role of cAMP-dependent protein kinase (PKA) and protein kinase C (PKC). Brain Res Mol Brain Res 114:65–72.

Park M, Penick EC, Edwards JG, Kauer J a, Ehlers MD (2004) Recycling endosomes supply AMPA receptors for LTP. Science 305:1972–1975.

Pawlikowski BT, Maimone MM (2008) alpha-Dystrobrevin isoforms differ in their colocalization with and stabilization of agrin-induced acetylcholine receptor clusters. Neuroscience 154:582–594.

Perkins GA, Wang L, Huang LJ, Humphries K, Yao VJ, Martone M, Deerinck TJ, Barraclough DM, Violin JD, Smith D, Newton A, Scott JD, Taylor SS, Ellisman MH (2001) PKA, PKC, and AKAP localization in and around the neuromuscular junction. BMC Neurosci 2:17.

Peter AK, Marshall JL, Crosbie RH (2008) Sarcospan reduces dystrophic pathology: stabilization of the utrophin-glycoprotein complex. J Cell Biol 183:419–427.

Peter AK, Miller G, Crosbie RH (2007) Disrupted mechanical stability of the dystrophin-glycoprotein complex causes severe muscular dystrophy in sarcospan transgenic mice. J Cell Sci 120:996–1008.

Peters MF, Adams ME, Froehner SC (1997) Differential association of syntrophin pairs with the dystrophin complex. J Cell Biol 138:81–93.

Peters MF, Kramarcy NR, Sealock R, Froehner SC (1994) beta 2-Syntrophin: localization at the neuromuscular junction in skeletal muscle. Neuroreport 5:1577–1580.

Peters MF, Sadoulet-Puccio HM, Grady MR, Kramarcy NR, Kunkel LM, Sanes JR, Sealock R, Froehner SC (1998) Differential membrane localization and intermolecular associations of alpha-dystrobrevin isoforms in skeletal muscle. J Cell Biol 142:1269–1278.

Picciotto MR, Zoli M (2002) Nicotinic receptors in aging and dementia. J Neurobiol 53:641–655.

Piguet J, Schreiter C, Segura J-M, Vogel H, Hovius R (2011) Acetylcholine receptor organization in membrane domains in muscle cells: evidence for rapsyn-independent and rapsyn-dependent mechanisms. J Biol Chem 286:363–369.

Pilgram GSK, Potikanond S, Baines R a, Fradkin LG, Noordermeer JN (2010) The roles of the dystrophin-associated glycoprotein complex at the synapse. Mol Neurobiol 41:1–21.

Pires-Oliveira M, Moen D, Akaaboune M (2013) Dynamics of Nicotinic Acetylcholine Receptors and Receptor-Associated Proteins at the Vertebrate Neuromuscular Junction. Curr Alzheimer Res.

Qu ZC, Moritz E, Huganir RL (1990) Regulation of tyrosine phosphorylation of the nicotinic acetylcholine receptor at the rat neuromuscular junction. Neuron 4:367–378.

Quintero GC (2013) Role of nucleus accumbens glutamatergic plasticity in drug addiction. Neuropsychiatr Dis Treat 9:1499–1512.

Rees MLJ, Lien C-F, Górecki DC (2007) Dystrobrevins in muscle and non-muscle tissues. Neuromuscul Disord 17:123–134.

Rezvani K, Teng Y, De Biasi M (2010) The ubiquitin-proteasome system regulates the stability of neuronal nicotinic acetylcholine receptors. J Mol Neurosci 40:177–184.

Röder IV, Petersen Y, Choi KR, Witzemann V, Hammer J a, Rudolf R (2008) Role of Myosin Va in the plasticity of the vertebrate neuromuscular junction in vivo. PLoS One 3:e3871.

Röder I V, Choi K-R, Reischl M, Petersen Y, Diefenbacher ME, Zaccolo M, Pozzan T, Rudolf R (2010) Myosin Va cooperates with PKA RIalpha to mediate maintenance of the endplate in vivo. Proc Natl Acad Sci U S A 107:2031–2036.

Ross A, Rapuano M, Prives J (1988) Induction of phosphorylation and cell surface redistribution of acetylcholine receptors by phorbol ester and carbamylcholine in cultured chick muscle cells. J Cell Biol 107:1139–1145.

Rotzler S, Schramek H, Brenner HR (1991) Metabolic stabilization of endplate acetylcholine receptors regulated by Ca2+ influx associated with muscle activity. Nature 349:337–339.

Rudolf R, Bittins CM, Gerdes H-H (2011) The role of myosin V in exocytosis and synaptic plasticity. J Neurochem 116:177–191.

Sanes JR, Lichtman JW (1999) Development of the vertebrate neuromuscular junction. Annu Rev Neurosci 22:389–442.

Sanes JR, Lichtman JW (2001) Induction, assembly, maturation and maintenance of a postsynaptic apparatus. Nat Rev Neurosci 2:791–805.

Sava A, Barisone I, Di Mauro D, Fumagalli G, Sala C (2001) Modulation of nicotinic acetylcholine receptor turnover by tyrosine phosphorylation in rat myotubes. Neurosci Lett 313:37–40.

Schliebs R, Arendt T (2011) The cholinergic system in aging and neuronal degeneration. Behav Brain Res 221:555–563.

Schmidt N, Akaaboune M, Gajendran N, Martinez-Pena Y Valenzuela I, Wakefield S, Thurnheer R, Brenner HR (2011) Neuregulin/ErbB regulate neuromuscular junction development by phosphorylation of α-dystrobrevin. J Cell Biol 195:1171–1184.

Serdaroglu P, Askanas V, Engel WK (1992) Immunocytochemical localization of ubiquitin at human neuromuscular junctions. Neuropathol Appl Neurobiol 18:232–236.

Setou M, Seog D-H, Tanaka Y, Kanai Y, Takei Y, Kawagishi M, Hirokawa N (2002) Glutamate-receptor-interacting protein GRIP1 directly steers kinesin to dendrites. Nature 417:83–87.

Severance EG, Yolken RH (2007) Lack of RIC-3 congruence with beta2 subunit-containing nicotinic acetylcholine receptors in bipolar disorder. Neuroscience 148:454–460.

Shi L, Fu AKY, Ip NY (2012) Molecular mechanisms underlying maturation and maintenance of the vertebrate neuromuscular junction. Trends Neurosci:1–13.

Shi W, Chen Z, Schottenfeld J, Stahl RC, Kunkel LM, Chan Y-M (2004) Specific assembly pathway of sarcoglycans is dependent on beta- and delta-sarcoglycan. Muscle Nerve 29:409–419.

Shiao T, Fond A, Deng B, Wehling-Henricks M, Adams ME, Froehner SC, Tidball JG (2004) Defects in neuromuscular junction structure in dystrophic muscle are corrected by expression of a NOS transgene in dystrophin-deficient muscles, but not in muscles lacking alpha- and beta1-syntrophins. Hum Mol Genet 13:1873–1884.

Shyng SL, Xu R, Salpeter MM (1991) Cyclic AMP stabilizes the degradation of original junctional acetylcholine receptors in denervated muscle. Neuron 6:469–475.

Shyu YJ, Suarez CD, Hu C-D (2008) Visualization of ternary complexes in living cells by using a BiFC-based FRET assay. Nat Protoc 3:1693–1702.

Si J, Wang Q, Mei L (1999) Essential roles of c-JUN and c-JUN N-terminal kinase (JNK) in neuregulin-increased expression of the acetylcholine receptor epsilon-subunit. J Neurosci 19:8498–8508.

Smalheiser NR, Schwartz NB (1987) Cranin: a laminin-binding protein of cell membranes. Proc Natl Acad Sci U S A 84:6457–6461.

Straub RE, Jiang Y, MacLean CJ, Ma Y, Webb BT, Myakishev M V, Harris-Kerr C, Wormley B, Sadek H, Kadambi B, Cesare AJ, Gibberman A, Wang X, O'Neill FA, Walsh D, Kendler KS (2002) Genetic variation in the 6p22.3 gene DTNBP1, the human ortholog of the mouse dysbindin gene, is associated with schizophrenia. Am J Hum Genet 71:337–348.

Straub V, Campbell KP (1997) Muscular dystrophies and the dystrophin-glycoprotein complex. Curr Opin Neurol 10:168–175.

Stya M, Axelrod D (1983) Diffusely distributed acetylcholine receptors can participate in cluster formation on cultured rat myotubes. Proc Natl Acad Sci U S A 80:449–453.

Stya M, Axelrod D (1984) Mobility of extrajunctional acetylcholine receptors on denervated adult muscle fibers. J Neurosci 4:70–74.

Tang H, Goldman D (2006) Activity-dependent gene regulation in skeletal muscle is mediated by a histone deacetylase (HDAC)-Dach2-myogenin signal transduction cascade. Proc Natl Acad Sci U S A 103:16977–16982.

Tang H, Macpherson P, Marvin M, Meadows E, Klein WH, Yang X, Goldman D (2009) A histone deacetylase 4/myogenin positive feedback loop coordinates denervation-dependent gene induction and suppression. Mol Biol Cell 20:1120–1131.

Tansey MG, Chu GC, Merlie JP (1996) ARIA/HRG regulates AChR epsilon subunit gene expression at the neuromuscular synapse via activation of phosphatidylinositol 3-kinase and Ras/MAPK pathway. J Cell Biol 134:465–476.

Thomas GD, Shaul PW, Yuhanna IS, Froehner SC, Adams ME (2003) Vasomodulation by skeletal muscle-derived nitric oxide requires alpha-syntrophin-mediated sarcolemmal localization of neuronal Nitric oxide synthase. Circ Res 92:554–560.

Tommasi di Vignano A, Di Zenzo G, Sudol M, Cesareni G, Dente L (2000) Contribution of the different modules in the utrophin carboxy-terminal region to the formation and regulation of the DAP complex. FEBS Lett 471:229–234.

Torres LF, Duchen LW (1987) The mutant mdx: inherited myopathy in the mouse. Morphological studies of nerves, muscles and end-plates. Brain 110 (Pt 2:269–299.

Turney SG, Culican SM, Lichtman JW (1996) A quantitative fluorescence-imaging technique for studying acetylcholine receptor turnover at neuromuscular junctions in living animals. J Neurosci Methods 64:199–208.

Van Mier P, Lichtman JW (1994) Regenerating muscle fibers induce directional sprouting from nearby nerve terminals: studies in living mice. J Neurosci 14:5672–5686.

Wallace BG (1988) Regulation of agrin-induced acetylcholine receptor aggregation by Ca++ and phorbol ester. J Cell Biol 107:267–278.

Wang J, Ruan N-J, Qian L, Lei W -l., Chen F, Luo Z-G (2008a) Wnt/ -Catenin Signaling Suppresses Rapsyn Expression and Inhibits Acetylcholine Receptor Clustering at the Neuromuscular Junction. J Biol Chem 283:21668–21675.

Wang Z, Edwards JG, Riley N, Provance DW, Karcher R, Li X-D, Davison IG, Ikebe M, Mercer J a, Kauer J a, Ehlers MD (2008b) Myosin Vb mobilizes recycling endosomes and AMPA receptors for postsynaptic plasticity. Cell 135:535–548.

Watkins SC, Hoffman EP, Slayter HS, Kunkel LM (1988) Immunoelectron microscopic localization of dystrophin in myofibres. Nature 333:863–866.

Wiesner a, Fuhrer C (2006) Regulation of nicotinic acetylcholine receptors by tyrosine kinases in the peripheral and central nervous system: same players, different roles. Cell Mol Life Sci 63:2818–2828.

Williamson RA, Henry MD, Daniels KJ, Hrstka RF, Lee JC, Sunada Y, Ibraghimov-Beskrovnaya O, Campbell KP (1997) Dystroglycan is essential for early embryonic development: disruption of Reichert's membrane in Dag1-null mice. Hum Mol Genet 6:831–841.

Wu H, Lu Y, Barik A, Joseph A, Taketo MM, Xiong W-C, Mei L (2012) β-Catenin gain of function in muscles impairs neuromuscular junction formation. Development 139:2392–2404.

Wu H, Xiong WC, Mei L (2010) To build a synapse: signaling pathways in neuromuscular junction assembly. Development 137:1017–1033.

Xing Y, Takemaru K-I, Liu J, Berndt JD, Zheng JJ, Moon RT, Xu W (2008) Crystal structure of a full-length beta-catenin. Structure 16:478–487.

Xu R, Salpeter MM (1997) Acetylcholine receptors in innervated muscles of dystrophic mdx mice degrade as after denervation. J Neurosci 17:8194–8200.

Yamanouchi Y, Mizuno Y, Yamamoto H, Takemitsu M, Yoshida M, Nonaka I, Ozawa E (1994) Selective defect in dystrophin-associated glycoproteins 50DAG (A2) and 35DAG (A4) in the dystrophic hamster: an animal model for severe childhood autosomal recessive muscular dystrophy (SCARMD). Neuromuscul Disord 4:49–54.

Yang X, Arber S, William C, Li L, Tanabe Y, Jessell TM, Birchmeier C, Burden SJ (2001) Patterning of muscle acetylcholine receptor gene expression in the absence of motor innervation. Neuron 30:399–410.

Yoshida M, Hama H, Ishikawa-Sakurai M, Imamura M, Mizuno Y, Araishi K, Wakabayashi-Takai E, Noguchi S, Sasaoka T, Ozawa E (2000) Biochemical evidence for association of dystrobrevin with the sarcoglycan-sarcospan complex as a basis for understanding sarcoglycanopathy. Hum Mol Genet 9:1033–1040.

Yu X, Malenka RC (2003) Beta-catenin is critical for dendritic morphogenesis. Nat Neurosci 6:1169–1177.

Zaccaria ML, De Stefano ME, Gotti C, Petrucci TC, Paggi P (2000) Selective reduction in the nicotinic acetylcholine receptor and dystroglycan at the postsynaptic apparatus of mdx mouse superior cervical ganglion. J Neuropathol Exp Neurol 59:103–112.

Zhang B, Luo S, Dong X-P, Zhang X, Liu C, Luo Z, Xiong W-C, Mei L (2007) Beta-catenin regulates acetylcholine receptor clustering in muscle cells through interaction with rapsyn. J Neurosci 27:3968–3973.

Zhou X, Marks P a, Rifkind R a, Richon VM (2001) Cloning and characterization of a histone deacetylase, HDAC9. Proc Natl Acad Sci U S A 98:10572–10577.

Zubrzycka-Gaarn EE, Bulman DE, Karpati G, Burghes AH, Belfall B, Klamut HJ, Talbot J, Hodges RS, Ray PN, Worton RG (1988) The Duchenne muscular dystrophy gene product is localized in sarcolemma of human skeletal muscle. Nature 333:466–469.